University of Alberta

A study on the time-dependent kinetics of lidocaine

by

Leock Y. (Stella) Ngo ©

A thesis submitted to the Faculty of Graduate Studies and Research in partial fulfillment of
the requirements for the degree of Doctor of Philosophy
in
Pharmaceutical Sciences (Pharmacokinetics)
Faculty of Pharmacy and Pharmaceutical Sciences

Edmonton, Alberta
Spring 1997

National Library of Canada

Acquisitions and Bibliographic Services

395 Wellington Street
Ottawa ON K1A 0N4
Canada

Bibliothèque nationale du Canada

Acquisitions et services bibliographiques

395, rue Wellington
Ottawa ON K1A 0N4
Canada

Your file Votre référence

Our file Notre référence

The author has granted a non-exclusive licence allowing the National Library of Canada to reproduce, loan, distribute or sell copies of his/her thesis by any means and in any form or format, making this thesis available to interested persons.

The author retains ownership of the copyright in his/her thesis. Neither the thesis nor substantial extracts from it may be printed or otherwise reproduced with the author's permission.

L'auteur a accordé une licence non exclusive permettant à la Bibliothèque nationale du Canada de reproduire, prêter, distribuer ou vendre des copies de sa thèse de quelque manière et sous quelque forme que ce soit pour mettre des exemplaires de cette thèse à la disposition des personnes intéressées.

L'auteur conserve la propriété du droit d'auteur qui protège sa thèse. Ni la thèse ni des extraits substantiels de celle-ci ne doivent être imprimés ou autrement reproduits sans son autorisation.

0-612-21613-6

Canada

University of Alberta

Library Release Form

Name of Author: Leock Y. (Stella) Ngo

Title of Thesis: A study on the time-dependent kinetics of lidocaine

Degree: Doctor of Philosophy

Year this Degree Granted: 1997

Permission is hereby granted to the University of Alberta Library to reproduce single copies of this thesis and to lend or sell such copies for private, scholarly, or scientific research purposes only.

The author reserves all other publication and other rights in association with the copyright in the thesis, and except as hereinbefore provided, neither the thesis nor any substantial portion thereof may be printed or otherwise reproduced in any material form whatever without the author's prior written permission.

Ngo Leock Yee.

#1016 8510-111 St.,
Edmonton, Alberta
Canada T6G 1H7

Date: April 16, 1997

University of Alberta

Faculty of Graduate Studies and Research

The undersigned certify that they have read, and recommend to the Faculty of Graduate Studies and Research for acceptance, a thesis entitled "A study on the time-dependent kinetics of lidocaine" submitted by Leock Y. (Stella) Ngo in partial fulfillment of the requirements for the degree of Doctor of Philosophy in Pharmaceutical Sciences (Pharmacokinetics).

Dr. Y. K. Tam, Supervisor

RT Coutts
Dr. R. T. Coutts

Fak Jamali
Dr. F. Jamali

Dr. F. M. Pasutto

Dr. M. R. Gray

Fak Jamali
for Dr. D. Lalka, External Reader

Date: April 15, 97

DEDICATION

This thesis is dedicated to:

my father: Gian Ngo

my mother: Yin C. Lui

my brother: Benjamin B. Y. Ngo

my sister: Clara C. Y. Ngo

for your love, support and encouragement.

ABSTRACT

Time-dependent reduction in lidocaine (LD) clearance has been observed in humans and animals during a prolonged intravenous (i.v.) infusion (> 12 h). The current project is undertaken to explore potential mechanisms by evaluating potential alterations in hepatic blood flow, plasma protein binding, hepatic tissue binding and enzyme activities following LD administration.

In vivo studies were conducted using the chronic instrumented dog model. Liver functions and LD disposition kinetics were preserved after surgical instrumentation of dogs, which share similar pharmacokinetics of LD with humans. Identical i.v. doses were given on two separate occasions, separated by a 12-h i.v. infusion. During infusion, LD induced an increase in hepatic blood flow and a decline in hepatic intrinsic clearance (Cl_{int}); the latter effect persisted after cessation of infusion. Alterations in metabolic activities, but not plasma protein binding and hepatic tissue binding, probably play a major role. Cl_{int} is inversely related to cumulative dose of LD during infusion and a similar reduction in Cl_{int} could be achieved by a single oral dose.

As opposed to a close-to-unity value in i.v. studies, the blood-to-plasma concentration ratio (C_b/C_p) was unexpectedly large (up to ten-fold) and variable depending on time and site of sample collection after oral dosing. Results from a series of tests indicate that LD peak measured by our HPLC method was pure and thus C_b/C_p values were true. Slow efflux of drug from erythrocytes is implicated; however, the mechanism(s) is unknown.

Time-dependent kinetics of LD has been attributed to partial enzyme inactivation of the N-dealkylation pathway in previous isolated rat liver perfusion studies. In this

project, the effects of LD pretreatment on enzyme kinetics of N-dealkylation, aromatic ring hydroxylation and aryl methyl hydroxylation were assessed using rat liver microsomes. No difference in K_m and V_{max} between control and treatment groups could be detected. This discrepancy is not due to the use of different anesthetic agents, since brief exposure of rats to diethyl ether, methoxyflurane and sodium pentobarbital anesthesia did not have differential effects on LD metabolism, except for the minor pathway of MeOH-MEGX formation. The underlying reason for this discrepancy is not clear.

ACKNOWLEDGEMENTS

The author would like to express deep gratitude to Dr. Yun K. Tam for his expert and patient guidance through a most challenging project. His support and understanding through all these years is greatly appreciated. It was a privilege to work under his supervision.

The author sincerely thanks Dr. Ronald T. Coutts for his valuable interpretation of mass spectra and his help in editing manuscripts.

Sincere thanks are due to Dr. Soheir Tawfik for her surgical expertise and technical assistance and for her precious friendship; to Kevin Chan and Lakhu M. Keshvara for their contribution to the project; to SynPhar Laboratories, Edmonton, Alberta for the use of their photodiode array detector; to Dr. Takeo Sakuma at Perkin-Elmer Sciex Instruments, Concord, Ontario for LC/MS analysis; to Dr. Monica M. Palcic at the Department of Chemistry for the use of EnzymeKinetics software program; and, to Dr. Terry Taerum at the Computing and Network Services and Dr. Robert T. Hardin at the Faculty of Agriculture, Forestry, and Home Economics for their valuable advice in statistical analysis.

This work was supported in part by the Medical Research Council of Canada, the Alberta Heritage Foundation for Medical Research and the Alberta Heart and Stroke Foundation.

TABLE OF CONTENTS

1. INTRODUCTION 1

1.1 Nonlinear pharmacokinetics 1

1.2 Lidocaine 4

1.2.1 Therapeutic usage 4

1.2.2 Adverse reactions 5

1.2.3 Pharmacology 5

1.2.3.1 Local anesthetic action 5

1.2.3.2 Antiarrhythmic action 6

1.2.4 Pharmacokinetics 7

1.2.4.1 Absorption 7

1.2.4.2 Distribution 8

1.2.4.3 Elimination 10

1.2.4.3.1 Hepatic metabolism 10

1.2.4.3.2 Extrahepatic metabolism 14

1.2.4.3.3 Biliary excretion 14

1.2.4.3.4 Renal excretion 15

1.3 Lidocaine and nonlinear kinetics 16

1.3.1 Changes in hepatic blood flow 16

1.3.2 Changes in plasma protein binding 18

1.3.3 Changes in metabolic clearance 18

1.3.3.1 Saturation in hepatic metabolism 19

1.3.3.2 Product inhibition 20

1.3.3.3 Tissue binding in the liver 20

1.3.3.4 Enzyme inactivation 21

1.4 Rationale for choosing instrumented dog as an animal model 23

1.5 Rationale for choosing rats for *in vitro* studies 24

1.5.1 Potential influence of residual amounts of anesthetic agents on lidocaine biotransformation 25

1.6 Hypotheses 27

1.7 Objectives 28

2. EXPERIMENTAL SECTION 30

2.1 Materials and chemical reagents 30

2.2 *In vivo* studies in conscious dogs 31

2.2.1 Animals 31

2.2.2 Instrumentation 32

2.2.3 Surgical procedures, postoperative care and catheter maintenance 32

2.2.4 Intravenous studies 33

2.2.4.1 Non-instrumented dogs 34

2.2.4.2 Instrumented dogs 35

2.2.5 Oral studies in instrumented dogs 36

2.2.6 Plasma protein binding studies in canine plasma 37

2.2.7 Blood-to-plasma ratio studies 38

2.2.7.1 *In vitro* studies 38

2.2.7.1.1 General procedures 38

2.2.7.1.2 Time to reach equilibrium 39

2.2.7.1.3 Concentration dependency 39

2.2.7.1.4 Effect of lag time between sample collection and sample analysis 39

2.2.7.2 *In vivo* and *in vitro* comparison studies 39

2.2.7.3 Examination of the purity of lidocaine peak 40

2.3 *In vitro* studies using rat livers 42

2.3.1 Animals 42

2.3.2 Effects of anesthetic agents using the isolated rat liver perfusion technique ... 42

2.3.2.1 Treatment protocols 42

2.3.2.2 Isolated liver perfusion studies 43

2.3.3 Effects of lidocaine pretreatment on intrinsic clearance using rat liver microsomal preparations 44

2.3.3.1 Treatment protocols 44

2.3.3.2 Preparation of hepatic microsomes 44

2.3.3.3 Determination of microsomal protein content 45

2.3.3.4 Incubation studies 46

2.4 HPLC assay 47

2.4.1 Instrumentation and chromatographic conditions 47

2.4.2 Standard solutions 48

2.4.3 Sample preparation 49

2.4.3.1 Intravenous and oral studies in dogs 49

2.4.3.2 Isolated rat liver perfusion studies 50
    2.4.3.2.1 Measurement of unconjugated metabolites and lidocaine 50
    2.4.3.2.2 Acid hydrolysis 50
2.4.3.3 Rat liver microsomal studies 51
2.5 Radioactivity counting 51
2.6 Pharmacokinetic analysis 52
    2.6.1 lidocaine protein binding in canine plasma 52
    2.6.2 Intravenous studies in non-instrumented dogs 52
    2.6.3 Intravenous studies in instrumented dogs 53
    2.6.4 Oral studies in instrumented dogs 55
    2.6.5 Isolated rat liver perfusion studies 56
    2.6.6 Rat liver microsomal studies 57
2.7 Statistical analysis 57
    2.7.1 Intravenous and oral studies in dogs 57
    2.7.2 Isolated rat liver perfusion studies 58
    2.7.3 Rat liver microsomal studies 58

3. RESULTS 60

3.1 Intravenous studies in non-instrumented dogs 60
3.2 Intravenous studies in instrumented dogs 60
    3.2.1 Alterations in hepatic hemodynamics during lidocaine administration 61
    3.2.2 Binding of lidocaine to plasma proteins 62
    3.2.3 Tissue uptake of lidocaine and its metabolites by the liver 63

3.2.4 Alterations in hepatic elimination capacity 64

3.3 Oral studies in instrumented dogs 65

3.4 Blood-to-plasma ratio studies 67

3.4.1 *In vitro* studies 68

3.4.2 *In vivo* and *in vitro* comparison studies 69

3.4.3 Purity determination of lidocaine peak 70

3.5 Effects of anesthetic agents in the isolated rat liver perfusion studies 72

3.6 Effects of lidocaine pretreatment on intrinsic clearance using rat liver microsomes 74

4. DISCUSSION 117

4.1 Evaluation of chronic instrumented dogs for pharmacokinetic studies of lidocaine 117

4.2 Intravenous studies in dogs 119

4.2.1 Hepatic blood flow 120

4.2.2 Hepatic intrinsic clearance 121

4.2.2.1 Plasma protein binding 121

4.2.2.2 Hepatic tissue binding 122

4.2.2.3 Hepatic metabolism 123

4.2.2.4 Cumulative exposure 124

4.2.3 Implication 126

4.3 Oral studies in dogs 126

4.4 Nonlinear blood-to-plasma ratio 127

4.4.1 Implications of nonlinear drug distribution in blood on pharmacokinetic analysis 131

4.5 Effects of anesthetic regimens on lidocaine metabolism 132

4.6 Effect of pretreatment on lidocaine metabolism 135

5. SUMMARY AND CONCLUSIONS... 144

6. REFERENCES.. 148

LIST OF TABLES

Table 3.1 Summary of LD kinetic parameters after a single i.v. dose (2 mg/kg) administration in non-instrumented and instrumented dogs (n = 3). 80

Table 3.2 Effects of a 12-h continuous i.v. infusion of LD (76.3 ± 4.7 μg/min/kg) on various kinetic and physiological parameters in four instrumented dogs. 81

Table 3.3 Pairwise comparison of LD disposition kinetics following a single i.v. injection given before (day 1) and after (day 10) a 12-h i.v. infusion to four instrumented dogs. 82

Table 3.4 Comparison of AUC ratios of N-dealkylated metabolites and LD at the inlet and outlet of the liver on day 1 and day 10 in four instrumented dogs. 83

Table 3.5 Pairwise comparison of kinetic parameters of orally administered LD (10 mg/kg) before (day 1) and after (day 10) a 12-h i.v. infusion to four instrumented dogs. 84

Table 3.6 Summary of LD kinetic parameters obtained from the i.v. and oral studies in four instrumented dogs. 85

Table 3.7 *In vitro* distribution of LD in canine blood. 86

Table 3.8 Comparison of blood-to-plasma ratios based on LD concentration (HPLC) and peak area response of molecular ion (LC/MS). 87

Table 3.9 Effects of three anesthetic agents on LD disposition in a single-pass isolated rat liver perfusion study. 88

Table 3.10 Mean % of dose recovered as unchanged LD and its metabolites in effluent perfusate at steady state during a constant rate LD infusion for the three anesthetic treatment groups. 89

Table 3.11 Intra-day and inter-day precision of determination of enzymatic activities in rat liver microsomes. 90

Table 3.12 Kinetic parameters for LD metabolism in rat liver microsomes (n = 5 per group). 91

Table 3.13 Kinetic parameters for the formation of 3-OH-LD in rat liver microsomes. 92

LIST OF FIGURES

Figure 1.1 Schematic of lidocaine metabolism in humans and animals 29

Figure 2.1 Dosing regimens employed for i.v. studies in chronically instrumented dogs (n = 4). A similar protocol was adopted for oral studies except that a single dose of unlabeled LD (10 mg/kg) was given on day 1 and day 10 59

Figure 3.1 Mean plasma concentration *vs* time profiles of LD, MEGX and GX in the carotid artery after a single i.v. dose (2 mg LD/kg) administration in non-instrumented dogs (n = 4) 93

Figure 3.2 Mean (± SD) plasma concentration *vs* time profiles for LD and its N-dealkylated metabolites in the carotid artery during a constant rate i.v. infusion (75 µg/min/kg) in four instrumented dogs. 94

Figure 3.3 Mean (± SD) plasma concentration *vs* time profiles in the carotid artery after a single i.v. dose of LD (2 mg/kg) was infused over 5 min on day 1 and day 10 in four instrumented dogs: (a) LD, (b) MEGX, and (c) GX 95

Figure 3.4 Effect of a constant rate i.v. infusion of LD &75 µg/min/kg) on hepatic blood flows in four instrumented dogs. Each data point and its error bars are mean ± SD. Each solid line is drawn from a fit of the mean data using non-linear least squares regression analysis. 96

Figure 3.5 Concentration-dependency of unbound fraction (f_u) of LD in canine plasma, determined *in vitro* by ultrafiltration method. Data points are mean values (± SD) of triplicate determinations 97

Figure 3.6 Plasma protein binding of LD on day 1 and day 10 in instrumented dogs (n = 3). Free fractions (f_u) of LD were plotted against total LD concentration in plasma (four points per subject on each experimental day). Data for one dog are omitted because of a lack of plasma samples for protein binding determination. 98

Figure 3.7 Time courses of hepatic tissue uptake after a single i.v. dose of LD was infused over 5 min on day 1 and on day 10 in instrumented dogs. Data points are expressed as mean values (n = 4). Error bars are omitted for the sake of clarity. Amount of net uptake of LD and its metabolic products on each treatment day are estimated from the area under the ($flux_{in}$ - $flux_{out}$) curve. Early sampling time profiles (0 - 1 h) are expanded to reveal a rapid attainment of equilibrium in the hepatic tissue uptake process 99

Figure 3.8 Mean AUC values of LD and its metabolites in systemic circulation (CA) and at the outlet of the liver (HV) after a single i.v. dose administration of.......... 100

Figure 3.9 Mean plasma concentration *vs* time profiles of (a) LD, (b) MEGX and (c) GX after a single oral dosing of LD (10 mg/kg) on day 1 in the carotid artery (CA), the jugular (JV), portal (PV) and hepatic (HV) veins of four instrumented dogs. (For clarity, error bars are not shown). 101

Figure 3.10 Mean (± SD) plasma concentration *vs* time profiles in the carotid artery after a single oral LD dose (10 mg/kg) given on day 1 and day 10 in four instrumented dogs: (a) LD, (b) MEGX and (c) GX.......... 102

Figure 3.11 A plot of hepatic intrinsic clearance in instrumented dogs after single i.v. (2 mg/kg) and oral (10 mg/kg) dose administration on day 1 and day 10 and at the end of a 12-h i.v. infusion (75 µg/min/kg) on day 8 (n=4 per group). Cl_{int} values were estimated using plasma concentration and hepatic plasma flow. 103

Figure 3.12 Plots of blood-to-plasma concentration ratio *vs* plasma concentration of LD in the jugular (JV) and portal (PV) veins after (a & b) i.v. (2 mg/kg) and (c &d) oral (10 mg/kg) administration of LD to instrumented dogs (n = 4 per group).......... 104

Figure 3.13 Effect of increasing LD concentration on *in vitro* drug distribution in blank canine blood spiked with various amounts of LD. 105

Figure 3.14 Time courses of LD blood-to-plasma concentration ratio in the carotid artery (CA) and the jugular (JV), portal (PV) and hepatic (HV) veins as determined by HPLC assay and in the jugular and portal veins by ^{14}C radioactivity method after a single oral dose (10 mg/kg) administration to dog R113.......... 106

Figure 3.15 A typical diagram showing that UV spectrum (200 - 450 nm) of LD peak in a jugular venous blood sample (------) taken after a single oral dose of LD (10 mg/kg) is superimposable to that of authentic LD (----). These spectra are extracted at peak maxima.......... 107

Figure 3.16 A typical chromatogram of blank plasma spiked with authentic LD, MEGX, GX and internal standard (EMGX) with their corresponding UV spectra shown in the upper panel. 108

Figure 3.17 Representative mass spectra of (a) system control sample, (b) blank blood and (c) blood sample taken from the jugular vein at 60 min after administration of a single oral dose 10 mg/kg to dog T8. 109

Figure 3.18 (a) Mass spectrum of authentic LD showing molecular ion (MH$^+$) of *m/z* 235 and its fragmentation ion of *m/z* 86. (b) The (MH+16)$^+$ ion (*m/z* 251) in Figure 3.16c was selected for fragmentation, which yields the diagnostic ion of *m/z* 86 110

Figure 3.19 Representative concentration *vs* time profiles of LD and its metabolites in the effluent of isolated perfused rat livers. (a) Diethyl ether anesthesia (C_{in} = 17.3 μM, T_{ss} = 45 min); (b) methoxyflurane anesthesia (C_{in} = 14.9 μM, T_{ss} = 30 min); and (c) sodium pentobarbital anesthesia (C_{in} = 15.2 μM, T_{ss} = 30 min) 111

Figure 3.20 Time courses of *in vitro* LD metabolism in rat liver microsomes. The disappearance of LD and formation of its metabolites during incubation at substrate concentrations of (a) 3 μM, (b) 30 μM and (c) 300 μM are plotted against incubation time. Each data point represents mean value of two separate determinations 112

Figure 3.21 Effect of substrate concentration on the rates of N-dealkylation, 3-hydroxylation and arylmethyl hydroxylation of LD. LD (1 - 2500 μM) was incubated in the presence of NAPDH 1mM and rat liver microsomal protein 0.5 mg/mL in the final mixture. Inset shows rate of metabolite formation at low substrate concentrations (1 - 25 μM). Data represent mean (± SD) values for the control group (n = 5). Results for LD pretreated group are similarly described by Michaelis-Menten equation. The K$_m$ and V$_{max}$ values for each metabolic pathway for both control and LD pretreated groups are shown in Table 3.12 113

Figure 3.22 Representative Eadie-Hofstee plots of MEGX formation showing heterogeneity of N-dealkylase activities in rat liver microsomes. N-dealkylation of LD is catalyzed by two enzymes in some rat liver microsomes (as indicated by biphasic slope in panel a) and by one enzyme in other rat liver microsomes (linear slope in panel b). Data presented in the graph are obtained from two individual rat liver microsomal preparations in the control group 114

Figure 3.23 Deviation of 3-OH-LD formation rate (v) from linearity. The upward turn in the Lineweaver-Burk plot as LD concentration increases (that is as 1/S approaches zero) is indicative of high substrate inhibition . Representative data obtained from one rat liver microsome of the control group is shown here and Michaelis-Menten plot of this set of data is shown in Figure 3.24a. The same nonlinearity in enzyme kinetics is observed consistently in all microsomes for both control and LD pretreated groups 115

Figure 3.24 Michaelis-Menten plots of concentration dependency of formation rate of 3-OH-LD when rat liver microsomes were incubated with various substrate concentrations (1-2500 μM). Computer simulation curves are generated 116

Figure 4.1 Effect of increasing cumulative dose (calculated by: infusion rate × hours of infusion) on hepatic intrinsic clearance. Cl_{int} values after the 5-min infusion of LD (2 mg/kg, day 1) and at various time points of the 12-h i.v. infusion in our instrumented dogs (n = 4) were plotted against cumulative dose. Mean Cl_{int} values estimated from the study reported by LeLorier *et al.* (152) for both the 90-min infusion and 24-h infusion groups were plotted for comparison with our findings........ 141

Figure 4.2 A plot of hepatic intrinsic clearance vs cumulative hepatic influx in instrumented dogs after LD administration (i.v. single dose 2 mg/kg; oral single dose 10 mg/kg and a 12-h i.v. infusion 75 μg/min/kg) (n=4 per group). Cl_{int} and cumulative flux were calculated using plasma concentration and hepatic plasma flow. 142

Figure 4.3 Time courses of LD concentration in blood (C_b), plasma (C_p) and red blood cells (C_{rbc}) in (a) portal vein and (b) hepatic vein after a single oral dose (10 mg/kg) administration to one dog. 143

GLOSSARY OF ABBREVIATIONS AND SYMBOLS

α	probability of making a type I error
Å	Angstrom
°C	degree Celsius
″	inch(es)
$\int$	integral
%	percent
Σ	summation
AAG	alpha$_1$-acid glycoprotein
ACD	anticoagulant-citrate-dextrose
ACS	American Chemical Society
ALT	alanine aminotransferase
ANOVA	analysis of variance
APD	action potential duration
AST	aspartate aminotransferase
AUC	area under the plasma concentration *vs* time curve from time 0 to ∞
$AUC_{\Delta t_i}$	area under the plasma concentration curve within the ith time interval
$AUMC$	area under the first moment curve
C_b	LD concentration in whole blood
C_p	LD concentration in plasma
C_{rbc}	LD concentration in red blood cells
C_b/C_p	ratio of blood-to-plasma concentration
C_{CA}	plasma concentration in the carotid artery
C_{HV}	plasma concentration in the hepatic vein
C_{JV}	plasma concentration in the jugular vein
C_{in}	inlet concentration

C_{max}	peak concentration
C_{PV}	plasma concentration in the portal vein
C_{out}	outlet concentration
Cl_b	systemic clearance based on blood concentration-time profile
Cl_p	systemic clearance based on plasma concentration-time profile
Cl_p/F	oral clearance based on plasma concentration-time profile
Cl_H	hepatic clearance
Cl_H^p	hepatic clearance (calculated using plasma concentration and hepatic plasma flow)
$Cl_H\ (t_i^*)$	hepatic clearance at the mid-point of the ith time interval
Cl_{int}	hepatic intrinsic clearance
Cl_{int}^p	hepatic intrinsic clearance (calculated using plasma concentration and hepatic plasma flow)
CA	carotid artery
CV	coefficient of variation
CYP	cytochrome P450
dpm	disintegrations per minute
EDTA	disodium ethylenediaminetetraacetate
E_H	hepatic extraction ratio
E_H^p	hepatic extraction ratio (calculated using plasma concentration and hepatic plasma flow)
EMGX	N-ethyl-N-methylglycine-2,6-xylidide
EPR	effective refractory period
F	absolute bioavailability
F_H	hepatic availability
F_H^p	hepatic availability (calculated using plasma concentration and hepatic plasma flow)
f_u	free fraction in plasma
G	gauge

g	gram(s)
g	gravity
GX	glycine-2,6-xylidide
h	hour(s)
HCl	hydrochloride
Hct	hematocrit
HPLC	High performance liquid chromatography
HV	hepatic vein
I	inhibitor concentration
ICG	indocyanine green
id	inside diameter
IU	international unit(s)
i.v.	intravenous
JV	jugular vein
k_e	first-order elimination rate constant
kg	kilogram(s)
K_i	Inhibition constant
K_m	Michaelis constant
$\mathrm{K_p}$	plasma-to-erythrocyte partition coefficient
$\mathrm{K_s}$	dissociation constant
L	liter(s)
LC/MS	liquid chromatography/mass spectrometry
LD	lidocaine
M	molar(s)
μCi	microCurie
μg	microgram(s)
μL	microliter(s)

μM	micromolar
μmoles	micromoles
mCi	milliCurie
mg	milligram(s)
mL	milliter(s)
mm	millimeter(s)
mM	millimolar
mmol	millimole(s)
min	minute(s)
MEGX	N-monoethylglycine-2,6-xylidide
MeOH-LD	methylhydroxy-LD
MeOH-MEGX	methylhydroxy-MEGX
MS	mass spectrometry
MW	molecular weight
N	normality
n	number of observations
NADPH	β-nicotinamide adenine dinucleotide phosphate
NaOH	sodium hydroxide
nm	nanometer(s)
nmol	nanomole(s)
od	outside diameter
3-OH-LD	3-hydroxy-LD
4-OH-LD	4-hydroxy-LD
3-OH-MEGX	3-hydroxy-MEGX
4-OH-MEGX	4-hydroxy-MEGX
4-OH-XYL	4-hydroxy-XYL
p	probability of rejecting the null hypothesis when it is true

PDA	photodiode array
pH	negative logarithm of concentration of H^+ ions
pK_a	negative logarithm of equilibrium constant of acid
PV	portal vein
Q	perfusate flow rate
Q_H	total hepatic blood flow
Q_H^P	total hepatic plasma flow
Q_{HA}	hepatic artery blood flow
Q_{PV}	portal vein blood flow
r	coefficient of linear correlation
S	substrate concentration
SD	standard deviation
sec	second(s)
$\sin^{-1}$	arcsin
$t_{1/2}$	half life
T_{max}	time to maximum (peak) concentration
T_{ss}	time to reach steady state
USP	United States Pharmacopoeia
UV	ultra-violet
v	rate of metabolite formation
v/v	volume per volume
V_{dss}	volume of distribution at steady state
V_{max}	maximum velocity
w/v	weight per volume
XYL	2,6-xylidine

1. INTRODUCTION

1.1 Nonlinear pharmacokinetics

In pharmacokinetics, the body is regarded as an operator that transforms the input (dosage rate) into an output (plasma concentration) (1). After dose administration, the time course of drug concentration in the body is governed by absorption, distribution, biotransformation and renal elimination processes. To define these processes, mathematical equations are derived to obtain estimates of kinetic parameters such as the rate of absorption, bioavailability, volume of distribution, hepatic clearance and renal clearance. Regardless of which process, a basic assumption is that a drug follows first-order or linear kinetics.

Linearity is implicated when the law of superposition holds, meaning that concentration-time profiles for a given drug and individual are superimposable when normalized for time and size of dose. In other words, total and unbound drug concentrations in plasma and the amounts of drug and its metabolites recovered in urine should increase in direct proportion to dose when the drug is given in a single dose or multiple dose regimen. In the literature, however, there is ample evidence of drugs that do not conform to the principle of superposition, thus exhibiting nonlinear kinetics.

Nonlinearity may arise from many factors associated with absorption, distribution and elimination processes (2). Poor solubility, saturable carrier-mediated transport and saturable presystemic metabolism are common causes for nonlinear absorption after oral administration of drugs. Examples of drugs are phenytoin (3), amino-beta-lactam antibiotics (4) and verapamil (5). Saturable plasma protein binding is the most frequently encountered reason for nonlinear distribution of drugs such as valproic acid (6). Alterations in extravascular tissue binding could also contribute to nonlinear kinetics of a drug. However, this factor is less studied simply due to the difficulties in its assessment. Saturable uptake into erythrocytes and slow efflux from blood cells into plasma have been implicated in unusual disposition behavior of certain drugs such as chlorthalidone (7), acetazolamide (8), cyclosporin (9) and doxorubicin (10). Nonlinear drug metabolism could be attributed to saturation of metabolic enzymes (e.g. salicylate) (11), product inhibition (e.g. diltiazem) (12), autoinduction of enzyme activities (e.g. carbamazepine) (13), depletion of cofactors and formation of hepatotoxic metabolites (e.g. acetaminophen) (14).

A common feature underlying many drug transfer or transformation processes involves an interaction of drug molecules with biological molecules such as transport carriers, plasma proteins and enzymes. These biological systems usually have a finite capacity. It is conceivable that as drug concentration in the body approaches or becomes well above K_m, the concentration at which half of the maximum capacity is attained, first order kinetics no longer prevails. These capacity-limited processes have been described by Michaelis-Menten or concentration-dependent kinetics. Saturation of one or more of the absorption or disposition processes may occur as dose or dosing rate increases. The pharmacokinetics of such a drug is termed dose-dependent kinetics, which is reflected as a greater than or less than proportional increase in the area under the drug concentration-time curve with dose (15). Nonlinearity becomes apparent especially when the relative contribution of saturable pathway(s) to the overall processes is large.

Another type of nonlinearity is time-dependency, which is further subdivided into two types (16). The first type, chronopharmacokinetics, is associated with changes in kinetic parameters arising from diurnal variations in physiological functions (17). The second type is chemically-induced, which appears after the introduction of an exogenous substance, such as a drug, in the body and ultimately disappears after the removal of the causative agent. Time-dependent phenomenon involves actual physiological or biochemical changes in body tissues which are associated with nonlinear drug disposition processes. It could be distinguished from concentration- or dose- dependencies by the fact that pharmacokinetic parameters are altered with time while drug concentration or dose are invariant.

One of the manifestations of time-dependency is a change in drug elimination rate during infusion or repeated dose administration. Drugs could enhance or reduce their own clearance by inducing changes in various physiological functions. For instance, carbamazepine induces metabolic enzyme activities (18) whereas propranolol lowers cardiac output by 20 to 30% which is accompanied by a corresponding fall in hepatic blood flow (19). Time-dependent pharmacokinetics often limits the predictability of steady state concentration and the time to reach steady state based on single bolus dose data. Thus, recognition of nonlinear kinetics and understanding of the underlying mechanisms are warranted for planning a safe and efficacious dosage regimen. This is especially important for drugs which have a narrow therapeutic range and have metabolites which are pharmacologically active or toxic. This is exemplified by the nonlinear kinetics of lidocaine.

1.2 Lidocaine

Lidocaine (LD), 2-(diethylamino)-N-(2,6-dimethylphenyl)acetamide (Figure 1.1), is a weak base with a pK_a of 7.85 (20-23). It is a small, lipid soluble molecule (MW 234.34), which exists predominantly as the protonated form in physiological media (pH 7.4). First synthesized in 1943 by Löfgren (24), LD was introduced for clinical practice as a local anesthetic in 1948 (25) and later as an antiarrhythmic agent in the 1960s (26,27).

1.2.1 Therapeutic usage

To date, LD is still widely used as a local anesthetic agent for topical, epidural, infiltration and regional anesthesia (28). It is currently the drug of choice in the acute management of ventricular arrhythmias associated with myocardial infarctions or cardiac surgery (29,30). LD is usually well tolerated at therapeutic concentrations for antiarrhythmic effectiveness (6.4 to 21.3 μM, equivalent to 1.5 to 5 μg/mL) (30,31). It has a rapid onset of action when given intravenously (45 to 90 sec) (28) and its effects decline quickly upon termination of drug administration, thus permitting moment-to-moment titration of ventricular ectopic activity in patients (32). Standard dosage regimen consists of an intravenous (i.v.) loading dose of 1 - 2 mg/kg body weight given at a rate of 25 to 50 mg/min, followed by a continuous i.v. infusion of 20 - 50 μg/min/kg body weight (22,30). Clinical monitoring of plasma LD levels is essential not only because of its narrow therapeutic window, but also because of large intersubject variabilities in its disposition kinetics (30,33).

1.2.2 Adverse reactions

Frequently observed side effects of LD are associated with the central nervous system, such as drowsiness, dizziness, nausea and vomiting. At higher plasma levels (> 21.3 μM), severe adverse effects are slurred speech, confusion, muscle tremors and convulsions (34-37). Manifestation of drug toxicity is life-threatening, including respiratory depression, coma, seizures and cardiac arrest (38-40).

1.2.3 Pharmacology

1.2.3.1 Local anesthetic action

Local anesthetics are chemicals that reversibly block action potentials in excitable membranes. The generation and propagation of action potentials depend on the membrane potential, which is in turn regulated by the opening and closing of ion channels.

LD is an amide-type anesthetic agent with an intermediate duration of action (10 to 20 min). LD stabilizes neuronal membrane and prevents the transmission of nerve impulse by diminishing activities of sodium channels. Two general theories have been proposed to explain the action of local anesthetics (41). One mechanism involves a nonspecific perturbation of the bulk membrane structure by anesthetics, as implicated by a parallel relationship between anesthetic potency and hydrophobicity of drug molecules. The other hypothesis involves a direct binding of local anesthetic molecules to a specific receptor site on the sodium channels. Much evidence has accumulated to support the latter hypothesis (42). The binding site seems to be located on the inner surface of cell membranes (41,43,44). Both unionized and ionized forms of drug molecules are required to exert its action — uncharged form for diffusion across cell membrane to reach the site of action and charged form for binding to receptor. The anesthetic action is use- or voltage-dependent (45), since sodium channels at different states exhibit conformational changes and thus have different affinities for the drug (44). As a result of the binding, membrane permeability to sodium ions is greatly reduced (41,44), the threshold for excitation increases, impulse conduction slows, the rate of rise of the action potential decreases and the amplitude dampens. When the sodium current is progressively blocked over a critical length of the nerve, the ability to generate action potential is completely abolished and propagation across the blocked area is no longer possible.

1.2.3.2 Antiarrhythmic action

According to the Vaughan-Williams classification, LD is considered to be a class 1B antiarrhythmic agent, which is a membrane stabilizer that reduces refractory period. LD exerts most of its electrophysiological effects on the heart by a direct action in a concentration-dependent manner (46). LD interacts with cardiac sodium channel in activated and inactivated states whereas sodium channel in rested state has very low affinity for drug binding. Sites of action include normal Purkinje fibers, ventricular muscle fibers and ventricular ectopic foci. But sinoatrial node, atrioventricular node, atrial muscle fibers and atrial ectopic foci are unresponsive (32).

At therapeutic concentrations, automaticity is suppressed, conduction velocity is reduced, excitation threshold is elevated, and both the effective refractory period (ERP) and the action potential duration (APD) are shortened. However, the ratio of ERP/APD is increased so that the conduction tissue is refractory to a new depolarizing stimulus for a relatively longer period of time (47). These changes are caused by a slowing in the rate of phase 0 depolarization due to a decrease in the rate of the fast inward sodium current, an elevated outward potassium flux during phase 3 and a reduction in the rate of phase 4 (pacemaker) depolarization in the Purkinje fiber (47). The responsiveness of ischemic tissue to LD is markedly amplified when compared to normal myocardium (48,49).

1.2.4 Pharmacokinetics

1.2.4.1 Absorption

Following oral administration, LD is rapidly and extensively absorbed (50-52). Peak plasma concentration is usually achieved within 30 to 60 min after dosing (50,52,53). Approximately 84% of a single oral dose is recovered as unchanged drug and metabolites in urine (51). Oral bioavailability is poor due to high first-pass effect (50,53,54) and is highly variable among individuals (range 18 to 46%) (50,52). Bennett *et al.* (52) suggested a lack of dose dependency after a single dose administration (1.25 to 7 mg/kg body weight) in healthy volunteers, as indicated by a linear relationship between dose and the area under plasma concentration-time curve (AUC). Due to small quantities of dose reaching systemic circulation and high incidence of side effects caused by substantial production of toxic metabolites, oral dosing is not warranted for LD (50,55).

Intramuscular administration is an alternative approach for the attainment of rapid and reliable therapeutic concentrations (56-58). Near complete absorption (92% of dose) has been found in dogs (59). When LD is given as a local anesthetic, drug absorption may occur from extravascular sites to give appreciable plasma levels (21,60). The absorption rate varies with the vascularity of the site of injection (56,58) and whether or not epinephrine is co-administered (30,61).

1.2.4.2 Distribution

In healthy volunteers, there is a large intersubject variability in the extent of LD distribution in the body — a 7.5-fold difference has been observed in individuals in one study (52). Mean volume of distribution at steady state (V_{dss}) values obtained from different studies range from 0.65 to 2 L/kg (52,62-67), indicating extravascular distribution. Following a bolus i.v. injection, LD concentration-time profiles could be fitted to a two-compartment open model (50,62,66,68) with an initial rapidly declining phase (half-life of 5 to 10 min) (50,62,66,68,69) and a terminal linear phase (half-life of 80 to 108 min) (50,62,66-69). It has been proposed that LD is initially sequestered into the lungs, then to rapidly perfused organs such as the heart and the kidneys, followed by redistribution of the drug into skeletal muscle and adipose tissues (70). Tissue distribution studies have been performed using laboratory animals (70-74). *In vitro* measurement of tissue-to-plasma partition coefficients indicates that lung, kidney and spleen have the highest affinities for LD, followed in a descending order by adipose tissue > brain and heart > liver and skeletal muscle (70,71,74). At steady state in dogs, kidney tissue contained the highest content of LD compared to other tissues such as adipose tissue, liver, brain, muscle and heart (71). Extensive lung uptake has been observed shortly after i.v. injection in man (68,75,76) and in animals (74,77,78). Almost all of LD taken up seemed to be available for back-diffusion into systemic circulation, suggesting that lung elimination is insignificant (74,78,79).

Protein binding of LD in human plasma or serum is concentration-dependent (61,80,81) with considerable intersubject and intrasubject variabilities (82). At therapeutic concentrations, approximately 70% of LD is bound to plasma proteins (80,81). As total LD plasma concentration increases from 4.3 to 85.3 μM (1 to 20 μg/mL), there is an elevation of free fraction of LD from 30 to 70% (80). The major binding protein is alpha$_1$-acid glycoprotein (AAG), which accounts for 70% of the bound fraction at clinically relevant concentrations (82-88). The remaining 30% of bound drug is associated with serum albumin. This is because LD has a much higher affinity for AAG (K_a = 19.4 μM) than for serum albumin (K_a = 4.8 mM) (89,90). The binding of LD to AAG requires the presence of basic nitrogen center and an aromatic group, separated by approximately 7 Å (90). The xylidide portion of LD probably binds to a highly restricted site on AAG, whereas maximal binding occurs when the glycine nitrogen is a tertiary, rather than a primary or secondary amine (90). Protein binding of the two N-dealkylated metabolites that are present in both human and canine plasma, N-monoethylglycine-2,6-xylidide (MEGX) and glycine-2,6-xylidide (GX), are much lower than the parent drugs in patients with myocardial infarction (14.3 ± 3.0% and 5 ± 4% *vs* 55.4 ± 5.9% respectively) (91) and 30% or less in canine plasma (59). Furthermore, *in vitro* addition of MEGX, GX and hydroxylated metabolites of LD, such as 3-hydroxylidocaine (3-OH-LD) and 4-hydroxylidocaine (4-OH-LD), did not significantly increase LD free fraction in human serum (81). In view of the structural specificity and the lower affinities of binding proteins, competitive binding and subsequent displacement of LD from its binding sites by these metabolites are not anticipated.

LD partitions into erythrocytes (80) and equilibrium is achieved rapidly (< 30 sec) (92). At therapeutic concentrations, the ratio of blood-to-plasma concentrations (C_b/C_p) is 0.8 to 0.9 in normal volunteers (21,61,62,80,83,93,94). As drug concentration increases, the percentage of LD associated with the erythrocytes increases, resulting in an increase in C_b/C_p and a decrease in plasma-to-erythrocyte partition coefficient (K_p) value (80,84). Moreover, *in vitro* addition of AAG to blood is associated with a redistribution of LD out of erythrocytes into plasma, thus lowering C_b/C_p (84).

1.2.4.3 Elimination

LD is rapidly cleared from the body in humans and in animals. Mean systemic clearance values obtained from several studies in normal subjects range from 10.0 to 17.4 mL/min/kg (50,52,61-63,66-68,95,96). LD is predominantly eliminated by hepatic metabolism and < 10% of an i.v. dose is excreted unchanged in urine (20,51,67,91,97-99). Hepatic clearance contributes approximately 90% of the total systemic clearance (33). The hepatic extraction ratio in man is found to be in the range of 0.62 to 0.81 (61,100).

1.2.4.3.1 Hepatic metabolism

Hepatic metabolism of LD has been extensively studied in man (20,51,97-99,101,102) and in animals (51,102-113). A schematic diagram of metabolic pathways is depicted in Figure 1.1. Phase I metabolism takes place at the tertiary amine (N-dealkylation), at the para- or meta-positions of the aromatic ring (hydroxylation), at the arylmethyl group (hydroxylation) and at the amide linkage (hydrolysis) to form MEGX, 3- or 4-OH-LD, methylhydroxy-LD (MeOH-LD) and 2,6-xylidine (XYL) respectively. The glycine nitrogen is susceptible to N-oxidation by rat liver microsomes, although the contribution of this pathway has not been demonstrated *in vivo* (104). Primary metabolites undergo secondary N-dealkylation, ring hydroxylation, amide hydrolysis and conjugation. Conjugation reactions proceed mainly *via* glucuronidation and sulfation (51,105), whereas N-conjugation of the aromatic amine is negligible in rats, dogs and humans (51). In man, 74 to 80% of LD dose is recovered in urine as conjugates of XYL and 4-hydroxy-XYL (4-OH-XYL) (51,99). This indicates that N-dealkylation and cleavage of the amide bond of LD and its metabolites are predominant routes of LD biotransformation (97,114).

In man, MEGX and GX are the two metabolites detected in blood (52,91,115-120). Both metabolites possess antiarrhythmic properties, although they are less potent than the parent drug (~80% and 10 to 26% respectively) (121,122). MEGX is rapidly and predominantly eliminated by the liver and follows formation rate-limited kinetics. Mean elimination half-life of MEGX is 36 to 80 min after a single LD i.v. dose (52). Thomson *et al.* demonstrated a parallel decline in plasma levels of exogenously administered and of endogenously formed MEGX (123). Subsequent biotransformation of MEGX to GX *via* N-dealkylation is a minor pathway (107), but amide hydrolysis probably plays a more important role (114,124). Renal failure has no effect on MEGX elimination nor would it lead to its accumulation. On the other hand, GX follows elimination rate-limited kinetics, with a mean elimination half-life of 9.8 h and mean clearance of 168 mL/min after i.v. administration of GX in humans (121). Metabolism of GX to XYL could only account for 4.5% of the dose whereas approximately half of GX dose is excreted by the kidney (121). The fate of the remaining 40% to 50% of the dose is unknown.

In recent years, significant advances have been made with respect to the identification and characterization of enzyme systems responsible for drug biotransformation. To date, the cytochrome P450 (CYP) system is the most studied. In humans, N-deethylation of LD to MEGX is catalyzed by CYP3A4 (101,102). CYP3A4 constitutes approximately 28% of the total CYP content in an adult human liver and its hepatic level varies approximately 20-fold among individuals (125). A mean specific content in human livers of 0.345 ± 0.165 nmol/mg protein was reported by de Waziers *et al.* (126). CYP3A4 has a very broad substrate specificity (125,127-129) and is present in various extrahepatic tissues (126,130). The mucosal membrane of the gastrointestinal tract contains the second largest specific content of CYP3A4 with a heterogeneous distribution along the villus and along the gastrointestinal tract (duodenum > jejunum > ileum >> stomach, esophagus and colon) (126,131-133). Total CYP3A4 in small intestine is about 30 times lower than that in the liver (126). Gut metabolism of cyclosporin and midazolam, both substrates of CYP3A4, has been clearly established (134,135). In the literature, information about gut involvement in LD first-pass effect in humans is lacking, partly because oral administration is not a common practice in the clinics.

There is numerous documentation on species (51,102,110,129), strain (108), gender (110,136,137) and age (92,111) differences regarding LD hepatic metabolism. Comparison of dogs and rats to humans will be discussed in detail since these are the two animal models employed in this project.

Similar to humans, rats and dogs rapidly eliminated LD from the body with comparable terminal half-lives of less than 30 min and approximately 60 min respectively

(51,59,138,139). LD is extensively metabolized by the liver and exhibits a high extraction ratio in these two species (51). Thus, LD clearance is largely dependent on liver blood flow, as in the case for humans.

However, there exist some dissimilarities among the three species. First, N-dealkylation, followed by secondary N-dealkylation and amide hydrolysis, is the dominant pathway in humans and in dogs. In rats, there are two distinctly different catalytic sites competing for LD — the high affinity, low capacity one for 3-hydroxylation and the low affinity, high capacity one for N-dealkylation (110). At low substrate concentrations, LD metabolism favors the formation of 3-OH-LD rather than MEGX. At high concentrations, over 90% of total metabolites is found as MEGX. Second, substrate specificity of CYP3A overlaps with that of CYP2C in rats (129). For instance, CYP3A4 in man is responsible for catalysis of LD N-dealkylation and CYP2C for S-mephenytoin hydroxylation. This is reversed in rats — MEGX formation is mainly catalyzed by CYP2C11 and mephenytoin hydroxylation by CYP3A (129). Rat CYP3A2 has only a small contribution to N-dealkylase activities. Third, there exists a gender difference in the formation rates of LD metabolites (136), which arises from the preferential expression of CYP2C11 and CYP3A2 in the male rat, but not in the female population (129). On the contrary, no gender difference is seen in dogs and in humans (129). Fourth, position of ring hydroxylation of LD is dependent on species. In man, hydroxylation selectively occurs at the para-position; but in rats, it is at the meta-position.

In rats, multiforms of CYP are capable of mediating N-dealkylation of LD to MEGX, including CYP1A2 and CYP2B1 in addition to CYP2C11 and CYP3A2 mentioned in the above paragraph (102,107). Hydroxylation at the arylmethyl group is catalyzed by CYP2B2 purified from rat liver microsomes (102,107). 3-OH-LD is formed by both CYP1A2 (102,107) and 2D1/2 isozymes (106,108) in rats. Unfortunately, information regarding particular isozymes responsible for LD metabolic pathways in dogs is lacking.

1.2.4.3.2 Extrahepatic metabolism

Extrahepatic metabolism of LD might occur, as suggested by the observation of MEGX production in a liver-transplant patient whose liver was excised (140). The site of extrahepatic formation of MEGX in man is not clear. There is some *in vitro* evidence demonstrating extrahepatic production of MEGX in rabbit lung and small intestine homogenates (141) and in rat pulmonary microsomes (142). The CYP isozyme responsible for pulmonary N-dealkylase activity in rat is identified to be CYP2B1. Rat renal microsome is also capable of generating small quantities of 3-OH-LD and MEGX (142), although its contribution to phase I metabolism of LD is probably insignificant. On the other hand, *in vitro* studies using perfused human and rat kidneys and kidney slices revealed that an appreciable extent of conjugation reactions, particularly glucuronidation and sulfation, could occur in the renal cortex and medulla (131). The possibility of extrahepatic conjugation of hydroxylated metabolites of LD could not be excluded.

1.2.4.3.3 Biliary excretion

There is no evidence of biliary excretion of LD in humans (33,124). Virtually no LD is detected in bile both after i.v. bolus administration into rats (51) and at steady state in single-pass isolated rat liver perfusion studies (< 0.8%) (143,144). Most of the radioactivity measured in bile is associated with conjugates of hydroxylated metabolites (51,143).

1.2.4.3.4 Renal excretion

The renal clearance of LD is insignificant, accounting for less than 10% to the total systemic clearance in man (20,51,67,91,97-99). The recoveries of LD dose as parent drug in rats and in dogs are similar to that in humans (0.2%, 2.0% and 2.8% respectively) (51), although McMahon & Woods have reported a high value of 10 - 20% in dog urine (145). Species differences exist in terms of urinary recoveries of individual metabolites. In man, LD dose is recovered almost exclusively as conjugates of 4-OH-XYL (approximately 90% of total recoveries), whereas XYL conjugate, N-dealkylated and hydroxylated metabolites exist in < 4% of LD dose (51,99). Using acid and enzyme hydrolysis of conjugates, Tam *et al.* (146) showed that 4-OH-XYL existed exclusively as glucuronide. In dogs, 4-OH-XYL is also the most abundant metabolite found in urine but its level (35% of LD dose) is less than that in man. A larger % of LD dose is excreted as GX in dogs (12.6%) as compared to that in man (2.3%) (51). By contrast, conjugated forms of 3-OH-LD and 3-hydroxy-MEGX (3-OH-MEGX) are the predominant metabolites recovered in rat urine (31% and 37% of LD dose respectively) (51). Total urinary recoveries as LD and its known metabolites in humans and in animals could not account for all the dose administered, suggesting the existence of some unknown route(s) of LD removal.

1.3 Lidocaine and nonlinear kinetics

The kinetics of LD has been found to be time-dependent during a prolonged i.v. infusion. This phenomenon is first reported by Prescott *et al.* (116), who observed that plasma drug levels continued to rise during the infusions that lasted 36 to 46 h in patients with myocardial infarctions (116). These findings were confirmed by other investigators in cardiac patients (63,67,85,95,147-151). Tapering of dosing rate was required in an attempt to maintain LD plasma levels within the therapeutic range (63). Terminal half-lives of the drug after discontinuation of infusion were two- to three-fold longer than those measured after a bolus injection (63,95,148). This observation led some investigators to propose that the longer half-life observed at the end of an infusion could represent the distribution of LD to a deep tissue compartment which was not identified by bolus studies. However, a lack of change in the V_{dss} (63,148) did not support this view.

The increase in LD half-life during a prolonged infusion was accompanied by a similar magnitude of reduction in clearance (63,148,150,151). Alterations of one or more of the determinants of hepatic clearance, such as hepatic blood flow, plasma protein binding and intrinsic clearance of free drug, were examined in humans and in animals. Despite numerous efforts in the past years, the mechanisms responsible for this time-dependent phenomenon are not fully elucidated.

1.3.1 Changes in hepatic blood flow

LD is a high extraction ratio drug and its clearance is blood flow rate-limited. An inverse relationship between arterial LD blood level and cardiac index has been described

(100). A plausible explanation for the continuous rise in plasma concentration during prolonged infusion is a progressive fall in cardiac output and liver blood flow.

Systemic circulation is generally well preserved below toxic levels of LD (153,154). In the literature, there is evidence of a concentration-dependent increase in cardiac output and hepatic blood flow at clinically relevant plasma levels in humans and in animals (70,153,155). The stimulatory effect of LD on hepatic blood flow is thought to be secondary to a reduction in splanchnic vascular resistance (155) and is prominent even at low LD plasma level (4.7 μM; 1.1 μg/mL) when cardiac output is relatively stable (155). In contrast, a recent study (156) in rabbits have demonstrated that hepatic blood flow was significantly depressed by LD at steady state. This discrepancy might arise from the use of microsphere technique (70) and indocyanine green (ICG) clearance (155,156) to obtain a single-point, indirect estimate of cardiac output and hepatic blood flow. The validity of the latter method has been questioned by several investigators (157-159). Another potential source of variability is that some earlier studies were conducted using various anesthetic agents and under different depths of anesthesia (154,155,160-162). In addition, most hemodynamic studies were performed either shortly after a single dose injection (161-165) or during a short term infusion of LD (< 180 min) (155,160,166). It is not clear whether LD-induced changes in splanchnic hemodynamics are sustained during prolonged infusion. Thus, direct and continuous monitoring of hepatic blood flow in conscious subjects during a long term LD infusion is valuable to clarify the role of alteration in hepatic blood flow in LD time-dependent kinetics.

1.3.2 Changes in plasma protein binding

It is well known that plasma protein levels, including albumin and AAG, are altered in response to physiological stress, such as those associated with myocardial infarction and surgeries (167). For instance, AAG concentration falls significantly immediately after surgeries. This is followed by an increase in AAG level to approximately 1.7- to 2.3-fold of pre-operative values on day 5 post-operatively (167,168). A similar rise in AAG levels to approximately 1.4- to 2.8-fold of normal values (83,85,149,167) with peak values at day 4 to 5 was observed in patients with myocardial infarctions (169,170). The increase in AAG level has been linked to an increase in LD binding in plasma (83,85,149). Thus, the elevation in plasma AAG levels could explain the continuous rise of total LD concentrations in patients with myocardial infarctions (83,85,123,171). However, the inability to attain a steady state LD plasma level during prolonged infusion is also observed in normal subjects whose AAG levels were stable (63,123,150,151). Thus, alterations in plasma protein binding could not be the sole explanation of time-dependent kinetics of LD.

1.3.3 Changes in metabolic clearance

The effect of duration of LD infusion on its own disposition kinetics has been demonstrated in dogs. Terminal half-life was doubled and clearance was greatly reduced when the infusion was extended from 90 min to 24 h (152). These changes were accompanied by a decrease in hepatic extraction ratio during prolonged LD infusion. In addition, there was an upward displacement of steady state blood concentration during a low dose infusion when it was preceded by an initial high dose infusion (190). These findings suggested that there was a time-dependent and dose-dependent impairment in metabolic clearance of LD. However, the lack of metabolite data and hepatic blood flow measurement in these studies prohibits identification of the underlying mechanisms. Moreover, potential effects of the length of infusion time and dosing rate on LD disposition might be confounded by the influence of anesthesia and surgical operation.

It has been proposed that impairment of LD metabolism could be caused by saturation of enzymes (96,110,113), product inhibition (105,109,123,136), binding to hepatic tissue (136,172) and enzyme inactivation (144,173). These postulations have been explored using isolated perfused liver, isolated hepatocytes and liver microsomes harvested from rats.

1.3.3.1 Saturation in hepatic metabolism

In rats, the major routes of LD metabolism are aromatic ring hydroxylation and N-dealkylation (51). The ring hydroxylation pathway has a high affinity and low capacity (109,110) for LD and is saturable at outlet concentration (C_{out}) of > 2.3 μM in a single-pass isolated perfused rat liver (144). However, saturation of this pathway could not account for a significant reduction in hepatic extraction ratio, since its contribution to overall LD metabolism diminishes as LD concentration increases. N-Dealkylation, a low affinity and high capacity pathway, predominates at higher substrate concentrations (110,144). Linearity of this pathway has been demonstrated over a wide concentration range (up to C_{out} of 196 μM). Furthermore, a reduction in LD extraction ratio has been observed at similar drug concentrations following the administration of escalating doses and following repetitive administration of the same dose at different times (136). These findings further support that Michaelis-Menten kinetics play an insignificant role in nonlinear kinetics of LD.

1.3.3.2 Product inhibition

The effect of exogenous metabolites such as MEGX, GX, 3-OH-LD and XYL on LD disposition (136) have been evaluated using recirculating isolated rat liver perfusion preparation. Only MEGX, when added at a high dose, inhibits LD metabolism (136). One possible mechanism is competitive inhibition between MEGX and LD for the aromatic ring hydroxylation pathway (109,144). However, a 3-fold increase MEGX level only decreases LD extraction by 10% (144). Hence, it is unlikely that product inhibition is an important factor for the accumulation of LD during prolonged infusion.

1.3.3.3 Tissue binding in the liver

There is evidence that reversible and irreversible binding in the liver is responsible for time-related changes in clearance of a drug. An example is diltiazem, a tertiary amine drug with a pK_a similar to that of LD. The prolonged time to reach steady state in a single-pass isolated perfused rat liver is mainly caused by an extensive but reversible binding of diltiazem to hepatic tissue (174). Using isolated rat hepatocytes and labeled LD, Chen *et al.* found that a total of 87% of radioactivity was bound to cellular components and the remaining 13% existed as free form at low LD concentration (0.3 μM) (172). Of the bound fraction, 31% of the radioactivity was tightly bound to cell debris and 56% was readily displaced. Tissue binding is a capacity-limited process, as denoted by a reduction in the amount of total radioactivity bound in hepatocytes to 61% as LD concentration in the medium increased to 600.3 μM (172). Potential role of both reversible and irreversible binding to hepatic tissue was further evaluated by Tam and his collaborators (144,175,176). Studies in isolated rat liver perfused with LD solution at a constant rate consistently showed that LD and its metabolites reached steady state at 30 to 60 min (144), which was much longer than cellular uptake (within 3 min) (172). In addition, there was a characteristic "hump" in the MEGX level — that is, the MEGX level initially increased to a maximum within 5 min and then declined by as much as 40% to a plateau level. Liver models which incorporated tissue binding component were used to simulate time courses of LD and MEGX in a single-pass perfusion system (175,176). Results indicated that the effect of binding was to delay the time to reach steady state, which agreed with experimental observation. However, these models failed to predict the unusual behavior of MEGX level in effluent perfusate (175,176). In summary, although saturable tissue binding might lead to a slow rise of LD level to steady state, it alone could not account for the altered rate of MEGX formation in perfused rat liver.

1.3.3.4 Enzyme inactivation

Lennard *et al.* (136) found that, following the administration of a high LD dose, a low extraction ratio of LD was accompanied by a leftward shift in the liver binding curve. It was speculated that if hepatic binding and catalytic sites were the same, then it was possible that, with time, LD was converted to a metabolic intermediate which accumulated on these sites and thereby preventing further access of drug molecules to the enzymes. As a result, LD metabolism was impaired (136). Recently, Masubuchi *et al.* observed that

LD or its metabolic intermediates were irreversibly bound to rat liver microsomal pellet (106,177) and that metabolic activation was an essential requirement for irreversible binding to occur. This is supported by the fact that the extent of irreversible binding is diminished in the absence of oxygen and cofactor β-nicotinamide adenine dinucleotide phosphate (NADPH), in the presence of carbon monoxide, by heat denaturation of microsomal proteins and by coincubation with SKF 525A which is a potent inhibitor of CYP (106,177). However, whether LD metabolism is altered and, in particular, which specific CYP isozymes are impaired as a consequence of the irreversible binding is still unknown. More studies are needed to evaluate the role of irreversible binding of LD or its metabolic products in time-dependent reduction of LD clearance.

On the contrary, time-dependent changes in LD kinetics have been related to the N-dealkylation pathway (144). A plausible mechanism is inactivation of metabolic enzymes caused by the formation of a stable metabolic-intermediate complex with CYP isozymes (173). Complex formation has been observed with various drugs such as diphenhydramine (178,179), orphenadrine (179-181), tricyclic antidepressants (182) and macrolide antibiotics (183-185). Despite a vast difference in therapeutic use and pharmacological activities, these compounds all possess a secondary or tertiary amino group in their chemical structures and they are mainly metabolized in the liver by N-dealkylation. It has been proposed that subsequent N-oxygenation of the N-dealkylated metabolites leads to the formation of nitroso- and/or a nitroxide radical intermediates which interact with the heme moiety of CYP enzymes (180,184). Structure-activity analysis indicated that both lipophilicity and steric hindrance of the amine group govern the capability of a given drug to inactivate CYP (178,179,186). This phenomenon has been associated with the time-dependent kinetics of orphenadrine (187). LD is a basic lipophilic compound which contains a tertiary amine group. It is conceivable that LD is capable of impairing liver metabolic activities by enzyme inactivation. Gray *et al.* (176) and Saville *et al.* (175) have successfully developed and applied a mathematical model which includes an enzyme inactivation process to describe LD and MEGX time courses in isolated rat livers during a continuous single-pass perfusion. The characteristic initial rise of MEGX level to a maximum, followed by a gradual decline to a lower steady state level, is consistent with the theory of enzyme inactivation. However, a direct proof of the existence of complex formation during LD catalytic breakdown is still lacking.

1.4 Rationale for choosing instrumented dog as an animal model

There are a few reasons for choosing dog as an animal model for *in vivo* studies. First, time-dependent reduction in LD clearance during a long term i.v. infusion has been reproduced in dogs (152,190). Second, dogs and humans share similar disposition kinetics of LD. For instance, the drug is extensively metabolized with N-dealkylation being the major metabolic pathway in both species (51). As in humans, LD is approximately 70% bound in plasma and AAG is the major binding protein in dogs (139). Furthermore, there is a similar concentration-dependency of serum/plasma protein binding, ranging from 71% to 44% (59) or 87% to 59% (191) over a concentration range of 4.3 to 42.7 μM (1.0 to 10 μg/mL). Third, a chronically instrumented dog model has been developed and applied to investigate mechanisms underlying food and drug interaction

(188) and dose- or time-dependent bioavailability (189) in our laboratory. It is a powerful research tool and offers several advantages: 1) Liver, the major organ for LD elimination, remains intact in its natural environment. Organ functions with particular reference to metabolic capacity and hepatic circulation are likely to be preserved. 2) Direct measurements of physiological meaningful blood flow data could be continuously monitored throughout the entire duration of LD infusion in a conscious animal. This was not possible in the past. 3) In addition to hepatic hemodynamics, the instrumented dog model permits simultaneous measurement of time courses of drug concentrations in hepatic artery, portal and hepatic veins and, thereby, transhepatic fluxes of LD. Drug-induced changes in physiological and kinetic processes and their contribution to nonlinear kinetics of LD could be assessed *in vivo*.

1.5 Rationale for choosing rats for *in vitro* studies

Rats have been used to study the biotransformation of LD (51,102,104-109,111-113). A common feature shared by rats and humans is that LD is extensively metabolized by the liver in both species. Time-dependent kinetics of LD have previously been demonstrated in rats using isolated perfused livers. Evidence is provided by a concentration-independent reduction in the hepatic extraction ratio of LD upon repeated bolus dosing (136) and a gradual decline of MEGX levels with time of perfusion to a constant lower level at steady state (144,173,176,192). Interestingly, the latter time-effect disappeared when the animals were pretreated with a single dose of LD. Thus, rat is chosen as an animal model for *in vitro* studies in an attempt to further elucidate the mechanisms of time-dependent kinetics of LD.

Rat liver microsome is a convenient tool commonly used to quantify the relative contribution of individual pathways to overall metabolic processes. It also allows the researchers to explore the mechanism of drug-drug interaction and to identify metabolic intermediate enzyme complex formation. On the other hand, isolated perfused rat liver permits the study of kinetics and dynamics of transport, binding and metabolism of drugs. As opposed to isolated hepatocytes and subcellular preparations, isolated rat livers preserve the structural architecture, enzyme distribution, cell polarity and cell communication (193-196). A single-pass system allows one to perform a mechanistic investigation at steady state under a well-defined, controlled system. In our laboratory, this technique has been frequently employed to delineate the effect of enzyme inactivation and tissue binding on time-dependent kinetics of LD and diltiazem and to explore potential interactions among various tertiary amine drugs (174,197).

1.5.1 Potential influence of residual amounts of anesthetic agents on lidocaine biotransformation

As mentioned in earlier sections, previous findings from our group suggest that enzyme-metabolic intermediate complex formation is probably linked to the N-dealkylation pathway (144). On the contrary, Suzuki and his coworkers suggested that irreversible binding probably involved an arene oxide which was formed during the formation of 3-OH-LD (106,177). A possible explanation of this discrepancy is the difference in anesthetic agents used. There is ample evidence that systemic and regional hemodynamics (198-206), protein binding (207) and metabolic activities (208-219) are altered in man and animals under anesthesia. Both phase I and II metabolic pathways could be affected to various extents by different anesthetic agents. The effect of an acute exposure to anesthetic agents during surgical procedures, followed by perfusion of the isolated liver with a buffer, is not known. There exists a potential risk of drug-anesthetic interaction caused by trace amounts of anesthetic agent residing inside hepatocytes (220) or by persistent effects on enzyme systems even after the causative agents are removed (209). In this project, a single-pass isolated rat liver perfusion system is employed to verify whether the choice of anesthetic agents would influence metabolic studies of LD. The three anesthetic agents chosen were: diethyl ether (used in previous works in our laboratory), methoxyflurane (currently used in our laboratory) and sodium pentobarbital (used by Suzuki's group (106,177)).

1.6 Hypotheses

1. Time-dependent reduction in LD clearance could be partly attributed to a decline in hepatic blood flow during constant rate i.v. infusion.
2. Time-dependent kinetics of LD are related to an increase in plasma protein binding.
3. A saturable hepatic tissue binding process may contribute to time-dependent kinetics of LD.
4. The time-dependent reduction in LD clearance could be partially explained by a loss of metabolic activities, probably caused by a cumulative exposure-dependent enzyme inactivation process.

1.7 Objectives

1. To evaluate the potential effect of surgical instrumentation on LD disposition kinetics in dogs.
2. To quantify the contribution of hepatic blood flow, plasma protein binding, hepatic tissue uptake and intrinsic enzyme activities to the time-dependent phenomenon.
3. To study the relationship of cumulative exposure of the liver to LD intrinsic clearance.
4. To verify the observation of nonlinear distribution of LD into erythrocytes.
5. To evaluate potential residual effects of diethyl ether inhalation, methoxyflurane inhalation and sodium pentobarbital intraperitoneal injection on the rate and extent of LD metabolism.
6. To measure the effect of pretreatment with LD on enzyme activities of individual metabolic pathways.

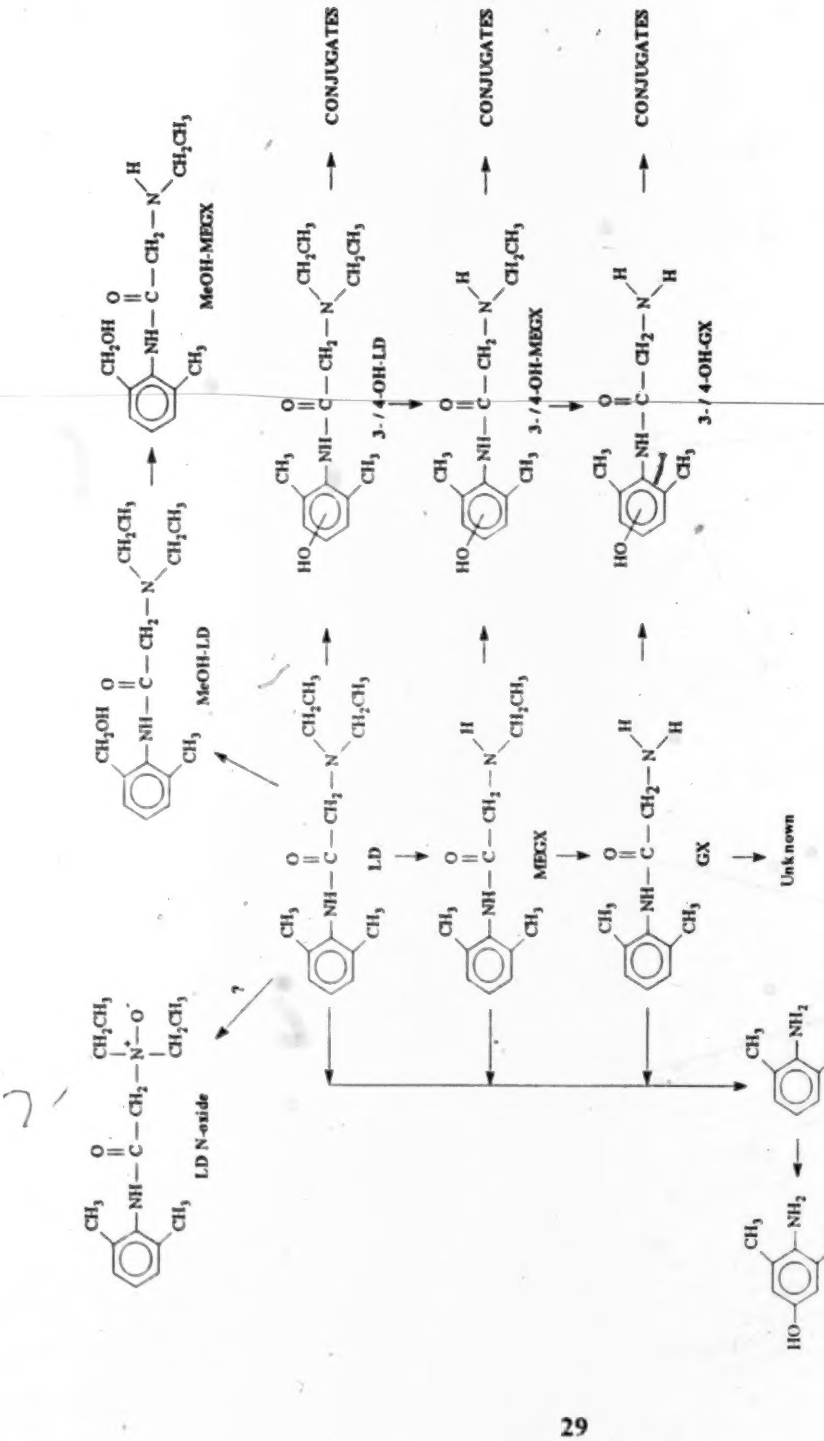
LD N-oxide
?
MeOH-LD
MeOH-MEGX
LD
MEGX
GX
Unknown
3-/4-OH-LD
3-/4-OH-MEGX
3-/4-OH-GX
CONJUGATES
CONJUGATES
CONJUGATES
XYL
CONJUGATES
4-OH-XYL
CONJUGATES

Figure 1.1 Schematic of LD metabolism in humans and animals.

2. EXPERIMENTAL SECTION[1]

2.1 Materials and chemical reagents

Xylocaine® 2% injection USP solution (Astra Pharmaceuticals Inc., Mississauga, Ontario, Canada) and LD hydrochloride (HCl) powder (Sigma Chemical Co., St. Louis, MO, USA) were used for dose administration for i.v. and oral studies in dogs respectively. [Carbonyl-^{14}C]-LD HCl (specific activity 51.7 mCi/mmol, purity >92%) was purchased from New England Nuclear (Mississauga, Ontario, Canada).

The same batch of LD HCl powder used for oral dosing was also used as the authentic compound in the HPLC assay. HCl salts of LD metabolites, MEGX, GX, 3-OH-LD and 3-OH-MEGX, and of the internal standard, N-ethyl-N-methylglycine-2,6-xylidide (EMGX), were kindly supplied by Astra Pharmaceuticals Inc. (Mississauga, Ontario, Canada). Other LD metabolites, MeOH-LD and methylhydroxy-MEGX (MeOH-MEGX), were synthesized based on the method of Nelson *et al.* (97). Solvents such as ethyl acetate (BDH Inc., Toronto, Ontario, Canada) and acetonitrile (Fisher Scientific, Nepean, Ontario, Canada) were HPLC grade and methylene chloride (BDH Inc., Toronto, Ontario, Canada) was analytical grade. Other reagents such as ortho-phosphoric acid, potassium dihydrogen phosphate and potassium bicarbonate (all supplied by BDH Inc., Toronto, Ontario, Canada) were ACS grade. Sodium salt of 1-heptanesulfonic acid was purchased from Sigma Chemical Co. (St. Louis, MO, USA).

---

[1] A version of this and subsequent chapters has been published/submitted for publication. Ngo, L. Y., Tam, Y. K. and Coutts R. T. Lack of residual effects of diethyl ether, methoxyflurane, and sodium pentobarbital on lidocaine metabolism in a single-pass isolated rat liver perfusion system. *Drug Metabolism and Disposition* 23(4): 525-528, 1995. Ngo, L. Y., Tam, Y. K., Tawfik, S., Coutts, R. T. and Gray, M. R. Effects of intravenous infusion of lidocaine on its pharmacokinetics in conscious instrumented dogs. *Journal of Pharmaceutical Sciences*, submitted.

Most ingredients of potassium phosphate buffer and Kreb's bicarbonate buffer (supplied by BDH Inc., Toronto, Ontario, Canada) were ACS grade, except for magnesium sulfate and sodium citrate (Fisher certified grade, Fisher Scientific, Nepean, Ontario, Canada). Glycerol (>99%) and a reduced form of NADPH and disodium ethylenediaminetetraacetate (EDTA) were purchased from Sigma Chemical Co. (St. Louis, MO, USA). Bio-rad reagent was supplied by Bio-Rad Laboratories (Richmond, CA, USA), sodium heparin solution by LEO Laboratories Canada Ltd. (Alax, Ontario, Canada) and saline by Baxter Co. (Toronto, Ontario, Canada).

2.2 *In vivo* studies in conscious dogs

2.2.1 Animals

Surgical and experimental protocols were approved by the Health Sciences and Animal Welfare Committee at the University of Alberta. Random source, healthy female mongrel dogs (total n = 8) were supplied by Biosciences Animal Services, University of Alberta. Dogs were housed in facilities with controlled temperature (22 °C) and a 12-h light/dark cycle. Diet, composed of Tuffy's chunk (Star Kist Foods, Willowdale, Canada) and Dr. Ballard canned meat (Friskies Pet Care, Don Mills, Canada), was given once daily. Dogs were allowed to have free access to water.

2.2.2 Instrumentation

Transit-time ultrasonic perivascular flow probes and a flowmeter (Model T201D, Transonic Systems, Ithaca, NY, USA) were employed for blood flow measurements. Readings were recorded on an IBM-compatible PC using P-Option software (Transonic Systems, Ithaca, NY, USA). Flow probes were tested and calibrated by the manufacturer. In addition, calibrations for accuracy and precision of flow readings were performed in our laboratory before surgical implantation into and after removal from the dogs. Calibration ranges were 0 - 400 mL/min for the 4R series (hepatic artery) and 0 - 1000 mL/min for the 8R series (portal vein). Flow probes gave an accuracy within 15% of the expected reading. A moving average of 10 sec was used for blood flow measurements (221).

2.2.3 Surgical procedures, postoperative care and catheter maintenance

After an overnight fast, a dog was anesthetized under 2% halothane in oxygen for surgical implantation of four Silastic® catheters (0.062″ id × 0.125″ od, medical grade, Dow Corning Co., Midland, MI, USA) into the carotid artery, the jugular, portal and hepatic veins and one flow probe each around the hepatic artery and portal vein. Details of surgical procedures, postoperative care and catheter maintenance as outlined in a previous publication (222) were followed with some modifications. The surgery was performed on two separate occasions, at least one week apart. The carotid artery and the jugular vein catheters were inserted during the first occasion. Cannulation of the portal and hepatic veins and the placement of the two flow probes were completed on the second occasion. For non-instrumented dog studies, dogs received only the jugular vein and carotid artery cannulation.

All dogs were allowed to recover for at least two weeks before experiments were initiated. Physiological parameters such as body weight, body temperature, white blood cell count, red blood cell count, hemoglobin content and hematocrit were monitored (Coulter Counter M 430, Coulter Electronics Inc., FL, USA) in all dogs weekly throughout the investigation periods. The catheters were flushed every two days and kept in heparin lock (1,000 IU/mL during first five days and 10,000 IU/mL thereafter) to maintain patency. ACD solution, which consisted of 0.4% anhydrous citric acid, 1.32% sodium citrate (dihydrate), 1.47% dextrose (monohydrate), and 1.5% of 37% formaldehyde, was used to sterilize the lumen of each catheter. When skin surfaces around the catheter sites and flow probe sites were infected, the wounds were disinfected with hydrogen peroxide 3% w/v and sprayed with gentamicin sulfate solution 1.1 mg/mL (Gentocin®, Schering Canada Inc., Point-Claire, Quebec, Canada).

2.2.4 Intravenous studies

On the day of experiment, each dog was transferred from its cage to the laboratory at least 1.5 h before an experiment, in order to let the subject get accustomed to the environment and to establish baseline blood flows. The animal was placed in a sling frame, which provided both restraint and support to the dog. Food was restricted until the end of experiment. A 20G Teflon® venous catheter (Quik-Cath®, Baxter Healthcare Corporation, Deerfield, IL, USA) was used for drug administration, which was initiated at approximately 10:30 a.m. to minimize experimental error due to diurnal variations. Dose solution was prepared from Xylocaine® 2% solution (Astra Pharmaceuticals Inc., Mississauga, Ontario, Canada) and appropriate dilution with saline was made to achieve desired concentrations under sterile conditions.

2.2.4.1 Non-instrumented dogs

Four female dogs (18.0 - 23.0 kg) were used for this study. A single i.v. dose of LD (2.19 ± 0.18 mg/kg body weight) was administered over 5 min *via* the left cephalic vein using a Harvard pump (Model 940, Harvard Apparatus, South Natick, MASS, USA). Blood samples (3 mL) were drawn simultaneously from the carotid artery and jugular vein catheters into polypropylene tubes (Sarstedt Inc., St-Laurent, Quebec, Canada) before dose administration and at 2.5, 5, 7.5, 10, 15, 30, 45, 60, 90, 120, 180, 240, 360 and 480 min after initiation of the 5-min infusion. Saline (5 mL) was used to flush blood residing in the lumen of the catheters back into bloodstream. Heparin lock (10 IU/mL in saline) was then used to maintain the patency of the catheters. Before a blood sample was taken, the heparin solution in the catheters was removed. A 0.1 M EDTA solution (25 µL/mL blood) was used as the anticoagulant. Plasma samples were obtained after centrifugation at 2,500 × *g* (Dynac centrifuge, Clay Adams, USA) for 20 min and stored at -20°C until analysis.

2.2.4.2 Instrumented dogs

Four instrumented female dogs (19.0 - 23.5 kg) were recruited and a sequential design (Figure 2.1) was employed for this study. On day 1, a single i.v. dose of a mixture of unlabeled LD (2.02 ± 0.13 mg/kg body weight) and ^{14}C-labeled LD (24.7 ± 3.1 μCi) was administered over 5 min *via* the left cephalic vein using a Harvard pump (Model 940, Harvard Apparatus, South Natick, MASS, USA). On day 8, each dog received a constant rate i.v. infusion of unlabeled LD (76.3 ± 4.7 μg/min/kg body weight) *via* the left saphenous vein for 12 hours, with the use of an IMED volumetric infusion pump (Model 960, IMED Corporation, San Diego, CA, USA). Thirty-six hours after the termination of infusion (day 10), each dog was challenged with the same dosing regimen as on day 1 (2.08 ± 0.11 mg/kg body weight unlabeled LD and 24.6 ± 4.3 μCi ^{14}C-labeled LD) *via* the left cephalic vein.

Blood flow rates through the hepatic artery and portal vein were recorded for approximately 30 min before dose administration and then continuously until the end of an experiment. For the 5-min infusion studies (days 1 and 10), blood samples (3 mL) were collected simultaneously from all four catheters before dose administration and at the same time intervals as in section *2.2.4.1*. Additional blood samples (2 mL) from the jugular vein were also taken at 0, 30, 60 and 90 min for the determination of C_b/C_p. During the 12-h infusion (day 8), blood samples were taken from all four blood vessels at 0, 4, 6, 8, 10 and 12 h. An aliquot of drug solution (1 mL) was simultaneously withdrawn from the infusion line to monitor infusion rate. Plasma samples were prepared by centrifugation (see section

2.2.4.1). Total amount of blood withdrawn was limited to less than 10% of the dog's total blood volume. Except for an aliquot of plasma samples (300 μL) used immediately for radioactivity counting, all samples were stored at -20 °C until analysis.

2.2.5 Oral studies in instrumented dogs

A similar design to that described in section *2.2.4.2* was adopted for this study, except that a single oral LD dose of 10.2 ± 0.1 mg/kg body weight was given to each dog (n = 4, 20 - 25 kg) on days 1 and 10. Appropriate amount of LD HCl salt was weighed and given to the animal in a gelatin capsule, immediately followed by flushing of the buccal cavity with 30 mL of water. On day 8, LD i.v. solution was prepared and was infused at a constant rate (74.9 ± 2.9 μg/min/kg body weight) to the animals for 12 h in the same manner as that described in section *2.2.4.2*.

Blood samples were simultaneously collected from all four catheters both after oral administration and during i.v. infusion and drug solution were withdrawn on day 8 as outlined in section *2.2.4.2* with two modifications. First, sampling time intervals following oral administration were 0, 5, 10, 15, 30, 45, 60, 75, 90, 120, 150, 180, 240, 360 and 480 min. Second, blood samples were also collected from the portal vein in addition to the jugular vein for the determination of C_b/C_p. Plasma samples were obtained using the method described in section *2.2.4.1*. All samples were stored at -20 °C until analysis.

2.2.6 Plasma protein binding studies in canine plasma

Protein binding studies in canine plasma were performed in three sets of samples using the Amicon Micropartition MPS-1 Ultrafiltration System equipped with YMT membrane (Amicon, Danvers, MA, USA):

1. To determine concentration dependency of LD protein binding, preliminary *in vitro* studies were done using blank canine plasma spiked with different amounts of unlabeled LD. Concentration range encompassed 4.3 to 85 μM (1 to 20 μg/mL).
2. Plasma samples collected from the carotid artery and the portal vein 2.5 to 10 min after single i.v. administration to instrumented dogs (n = 3) on day 1 and day 10 (four samples per subject per experiment).
3. Plasma samples taken from the jugular and portal veins at 30, 60 and 90 min after a single oral dose was given to an instrumented dog (n = 4, four to five samples per subject per experiment).

Plasma samples (550 μL) were added to microcentrifuge tubes (Brinkmann Instruments Inc., Westbury, NY, USA), which were coated with 0.01 μCi ^{14}C-labeled LD (corresponding to 0.18 nmoles). pH of plasma samples was adjusted to 7.4 with orthophosphoric acid 1% (v/v) and samples were allowed to equilibrate at 37 °C for one hour prior to centrifugation (5 min, 500 × *g*, Dynac centrifuge, Clay Adams, USA). The volume of ultrafiltrate was within 10 - 15% of total plasma volume such that disturbance in protein binding equilibrium was minimized. ^{14}C radioactivity in aliquots (50 μL) of ultrafiltrate and plasma was measured. Adsorption of LD to the ultrafiltration device and to the YMT membrane was negligible, if any (94,139,191).

2.2.7 Blood-to-plasma ratio studies

2.2.7.1 In vitro studies

2.2.7.1.1 General procedures

3 μL of ^{14}C-labeled LD solution (specific activity 51.7 mCi/mmol; 0.1 mCi/ mL methanol) was diluted in 1.5 mL methanol. An aliquot (50 μL; 22,200 dpm) of the diluted solution was transferred into a polypropylene tube (Sarstedt Inc., St-Laurent, Quebec, Canada) and dried under a gentle stream of nitrogen gas. Xylocaine® 2% solution (Astra Pharmaceuticals Inc., Mississauga, Ontario, Canada) was diluted with saline to prepare stock solutions at various concentrations, ranging from 0.11 to 4.3 mM. An aliquot (50 μL) of an appropriate stock solution was added to fresh drug-free canine blood (final volume of 2.5 mL) in a ^{14}C-LD coated polypropylene tube. Spiked blood samples were gently mixed using a Labquake® rotary mixer (Labindustries Clinical and Research Instruments, Berkeley, CA, USA). At the end of an equilibration period, an aliquot of blood sample (200 μL) were transferred into a polypropylene vial for sample treatment prior to counting. The rest of the blood was centrifuged at 2,500 × *g* (Dynac centrifuge, Clay Adams, USA) for 20 min to obtain plasma. An aliquot of 50 μL of each plasma sample was counted for radioactivity. These handling procedures were applied to sections *2.2.7.1.2* to *2.2.7.1.4*.

2.2.7.1.2 *Time to reach equilibrium*

Spiked blood samples (initial concentrations of 4.3 and 42.7 µM) were allowed to mix gently at 37 °C and at room temperature for 0, 5, 30, 60 and 180 min.

2.2.7.1.3 *Concentration dependency*

Effect of total LD concentration on C_b/C_p was examined at 2.1, 4.3, 10.7, 21.3 42.7 and 85.3 µM (equivalent to 0.5, 1, 2.5, 5, 10 and 20 µg/mL respectively). Spiked blood samples were equilibrated for one hour at 37 °C prior to sample analysis.

2.2.7.1.4 *Effect of lag time between sample collection and sample analysis*

Spiked blood samples (final concentrations of 4.3 and 42.7 µM) were equilibrated at 37 °C for one hour, then allowed to stand on bench top at room temperature for 0, 5, 30, 60 min, 3 h and 24 h prior to sample analysis.

2.2.7.2 *In vivo and in vitro comparison studies*

An oral dose of unlabeled LD (10 mg/kg) was administered to one dog (R113) on a single occasion separated from the oral studies. Carotid arterial, jugular, portal and hepatic venous blood samples (2 mL) were simultaneously collected at 0, 7.5, 18.5, 30, 45, 60, 75, 90, 120, 150, 180, 240, 360 and 480 min into polypropylene tubes which contained 0.1 M EDTA solution (25 µL/mL blood) as anticoagulant. Polypropylene tubes used for collection of the jugular and portal venous samples were previously coated with a fixed amount of ^{14}C-labeled LD (approximately 22,200 dpm). After equilibration at room temperature for one hour, samples were treated according to the procedures described in section *2.2.7.1.1*. C_b/C_p of LD were determined using both the HPLC and ^{14}C-radioactivity counting methods for *in vivo* and *in vitro* values respectively.

2.2.7.3 Examination of the purity of lidocaine peak

The purity of LD peak on the HPLC chromatogram was examined for possible interference from unknown compounds. Canine blood and plasma samples collected from the carotid artery at 0 and 60 min on day 1 and day 10 and at 12 h during an infusion on day 8 for both i.v. and oral studies (see sections *2.2.4.2* and *2.2.5*) were analyzed. In addition, portal venous blood and plasma samples (0 and 60 min) obtained during oral studies were also analyzed. These samples were extracted, together with a system control, which contained equal volume of distilled, deionized water, and blood and plasma samples spiked with authentic LD HCl, in the same manner (see section *2.4.3.1*) prior to analysis using the following methods:

1. HPLC equipped with UV detection using different elution conditions

   Instrumentation of the HPLC system and mobile phase composition were outlined in section *2.4.1*. Elution of samples were carried out at various proportions of aqueous buffer solution and acetonitrile, in an attempt to separate potential interference peaks under the LD peak.

2. HPLC equipped with photodiode array detection (PDA) method

   The HPLC system (Waters Instruments, Mississauga, Ontario, Canada) was equipped with a model 600 pump, a model 717 Plus automatic injector, a model 996 photodiode array detector and a IBM-compatible PC computer system equipped with Millennium chromatographic software program, v. 2.1. Mobile phase composition and type of the HPLC column were identical to that used in section *2.4.1*. The mobile phase composition was a mixture of aqueous buffer solution and acetonitrile (90:10 v/v). Analytes were eluted under isocratic condition at 1.0 mL/min.

3. Liquid chromatography / Mass spectrometry (LC/MS)

LD was given as a single 5-min injection (2 mg/kg), a 12-h i.v. infusion and a single oral dose (10 mg/kg) to one dog (T8) on three separate occasions. Arterial blood and plasma samples taken at 0 and 60 min from this dog, in addition to those samples mentioned in the first paragraph in section *2.2.7.3.*, were extracted and eluted using the HPLC method described in section *2.4.3.1*. The mobile phase that eluted during the time interval at half of maximum peak height of LD before and after the peak maxima was collected. Constituents were extracted with 4 mL ethyl acetate, which was then evaporated to complete dryness using a vacuum drying system (Savant Speedvac system, Model SC 100, Savant Instruments Inc., Farmingdale, NY, USA). Residues were stored at -20 °C until LC/MS analysis.

The LC/MS system consisted of a PE Series 200 autosampler, a Shimadzu LC-10A pump with a SCL-10A controller, a single quadrupole mass spectrometer (model API 100, Perkin-Elmer Sciex Instruments Co., Concord, Ontario, Canada).

The mobile phase composition was a mixture of methanol, water and formic acid (50:50:0.1 v/v). Samples were reconstituted in 1 mL of the mobile phase and an aliquot of 3 - 10 μL were injected. Flow rate was 20 μL/min. Vacuum was maintained at 1.1×10^{-5} torr. System control samples and authentic compounds were run alongside with canine samples.

2.3 *In vitro* studies using rat livers

2.3.1 Animals

Male Sprague-Dawley rats (200 - 250 g) were supplied by Biosciences Animal Services, University of Alberta, Alberta, Canada. Before the day of experiment or surgery, the rats were housed for at least 72 hours under a 12-hour light and dark cycle. Water and rat chow (Wayne Rodent Plox 8604-00, Continental Grain Company, Chicago, IL, USA) were given *ad libitum*.

2.3.2 Effects of anesthetic agents using the isolated rat liver perfusion technique

2.3.2.1 Treatment protocols

A completely randomized design was employed in this study. The animals (body weight = 221 ± 13 g, liver weight = 9.21 ± 1.06 g) were randomly assigned to one of the three anesthetic regimens: 1) diethyl ether (BDH Inc., Toronto, Ontario, Canada) inhalation (n = 6); 2) methoxyflurane (Metofane®, Pitman-Moore Ltd., Mississauga, Ontario, Canada) inhalation (n = 6); and, 3) intraperitoneal sodium pentobarbital injection

(Somnotol®, MTC Pharmaceuticals, Cambridge, Ontario, Canada) (n = 6) at a dose of 67 - 120 mg/kg body weight. Induction of anesthesia occurred rapidly and surgical plane of anesthesia was achieved within 10 min and at 20 - 30 min for volatile anesthetics and sodium pentobarbital, respectively.

2.3.2.2 Isolated liver perfusion studies

Details of the surgical procedures for isolated rat liver perfusion were as reported previously (144,174,223). The viability of the liver was evaluated by monitoring oxygen consumption, intrahepatic pressure, levels of aspartate (AST) and alanine (ALT) aminotransferases in the effluent perfusate and the physical appearance of the liver before and after drug infusion. Both AST and ALT levels were determined using a Dri-Stat diagnostic kit (Beckman Instrumentation Inc., Carlsbad, CA, USA). Further evidence of liver viability was provided by stable outlet concentrations of LD and its metabolites at steady state during constant rate infusion of LD.

The excised liver was allowed to acclimatize inside the perfusion chamber at 37 °C for 20 min. LD solution (17.32 ± 1.53 μM) was infused *via* the portal vein at a constant flow rate of 3.47 ± 0.37 mL/min/g liver. Samples were taken from the inlet at 0, 10, 20, 40 and 60 min to monitor the infusion rate. Perfusate samples were collected at the outlet at 0, 1, 3, 5, 7, 10, 13, 16, 20 min and every 5 min until 60 min for measurement of unchanged LD and its metabolites. Samples were stored at -20°C until analysis. Upon cessation of infusion, the liver was removed from the chamber, blotted dry and weighed.

2.3.3 Effects of lidocaine pretreatment on intrinsic clearance using rat liver microsomal preparations

2.3.3.1 Treatment protocols

A completely randomized block design with day as the block was used for this study. Rats (n = 5 per group) were randomly assigned to either control or treatment group. All rats were subjected to jugular vein cannulation under methoxyflurane anesthesia and were allowed to recover from surgery for two days. To maintain the patency of the catheter, the catheter was flushed daily and kept in a heparin lock (20 IU/mL). LD (10 mg/kg body weight) was administered via the catheter 24 h prior to harvesting the livers for microsomal preparation. Control animals were given the same volume of saline. Blood tests such as white blood cell count, red blood cell count, hemoglobin and hematocrit and liver function tests such as AST and ALT were performed on the day of liver harvest.

2.3.3.2 Preparation of hepatic microsomes

Liver microsomes were prepared according to the method of Omura and Sato (224) with some modifications. Rats (body weight = 260.7 ± 11.3 g) were anesthetized with methoxyflurane and the abdominal cavity was opened for portal vein cannulation. The livers were perfused *in situ* with ice-cold isotonic (1.15%) potassium chloride solution for 2 to 3 min and then excised. The following steps were performed at 4°C. The livers were finely minced and homogenized in three volumes of the same solution using a glass homogenizer equipped with a glass pestle (Glas-Col® , Cole-Parmer Instrument Co., Terre Hautein, IN, USA). The homogenate was centrifuged at 10,000 × *g* for 30 min using a Model IEC B-20A centrifuge equipped with a No. 870 rotor (International Equipment Company, Boston, MASS, USA). The supernatant was evenly distributed into polycarbonate tubes (Ultratube®, 13 × 64 mm, Nalge Company, Rochester, NY, USA) and was centrifuged at 105,000 × *g* for 60 min in a Model L8-55 ultracentrifuge (Beckman® Instruments Inc., Palo Alto, CA, USA; rotor type 503 Ti). After the supernatant was discarded, the microsomal pellet was washed and resuspended in 100 mM potassium phosphate buffer (pH 7.4). After re-centrifugation (105,000 × *g*, 60 min), the microsomal pellet was resuspended in a volume of 100 mM potassium phosphate buffer containing 1 mM EDTA and 20% v/v glycerol (Sigma Chemical Co., St. Louis, MO, USA) equivalent to original liver weight and stored at -80°C in 1 mL aliquots.

2.3.3.3 Determination of microsomal protein content

Microsomal protein was quantified using the Bradford method (225). Standard curve was prepared using bovine serum albumin (Sigma Diagnostic, St. Louis, MO, USA). Bovine serum albumin powder was reconstituted with an appropriate volume of water to give a stock solution of 400 μg/mL. Aliquots of the stock solution (0, 2, 4, 6, 8, 10 and 12 μL) were added in triplicates to the wells of a microtitre plate (Cell Wells™ 96 well plate, Corning Laboratory Sciences Co., Richmond Hill, Ontario, Canada). Sufficient volumes of the Bio-rad reagent (Bio-Rad Laboratories, Richmond, CA, USA) were added such that a final volume in each well was 200 μL. For the determination of protein concentration of liver microsomes, the original sample was diluted by a factor of 1/25 to 1/500. Aliquots (10 μL) of each diluted samples in triplicates were mixed with 190 μL of the Bio-rad reagent. Absorbance readings were taken at 590 nm using Molecular Devices MAXline microtitre plate reader.

2.3.3.4 Incubation studies

A microsomal reaction mixture (final volume, 500 μL) containing microsomal protein (0.5 mg/mL), 5 mM $MgCl_2$, 5 μM $MnCl_2$, 1 mM NADPH in 100 mM potassium phosphate buffer (pH 7.4) was pre-incubated at 37 °C for 5 min. The reaction was initiated by adding aliquots (50 μL) of various pre-warmed LD stock solutions to the mixture and carried out in air in microcentrifuge tubes (Brinkmann Instruments Inc., Westbury, NY, USA) at 37 °C. Substrate concentrations in incubation mixtures ranging from 1 - 2500 μM were studied in duplicates. Based on data obtained in a preliminary study, incubation time was determined to be 1, 2, 4 and 10 min at substrate concentrations of 1 to 2.5, 5 to 25, 50 to 250 and 500 to 2500 μM respectively. Choice of incubation time was restricted to the period when: 1) less than 20% of the total substrate consumption had occurred; 2) the rate of product formation or substrate utilization was still linear; and, 3) generation of secondary metabolites had not occurred. The reaction was terminated by the addition of 1 N NaOH (50 μL). All samples were quickly frozen in dry ice-acetone bath and stored at -20°C until analysis.

To evaluate inter-and intra-day variability in incubation procedures, same batch of liver microsome, prepared from an untreated rat, was incubated with LD at 30 μM in triplicates on four separate occasions.

2.4 HPLC assay

2.4.1 Instrumentation and chromatographic conditions

The HPLC system (Waters Instruments, Mississauga, Ontario, Canada) was equipped with two model 501 pumps, a WISP model 712 automatic injector, a model 441 UV detector set at 214 nm and a IBM-compatible PC computer system equipped with Baseline software program. Chromatographic resolution of LD and its metabolites was achieved using a reversed-phase LiChrospher® 60 RP-Select B column (5 μm, 125 mm x 4 mm, Merck, Darmstadt, F. R., Germany).

An isocratic elution method was used for the quantification of LD and two N-dealkylated metabolites in canine blood and plasma samples. The mobile phase composition was a mixture of an aqueous buffer solution and acetonitrile (84:16 v/v). The aqueous buffer solution (pH 3.5) contained 6.66 g potassium dihydrogen phosphate, 150 μL orthophosphoric acid, and 0.005 M sodium salt of 1-heptanesulfonic acid as ion pairing agent. Distilled, deionized water was added to make up the final volume to 1 L. Flow rate was 1.0 mL/min.

A gradient elution method at a constant flow rate of 1.6 mL/min was developed for good resolution of the analytes, especially 3-OH-LD and MeOH-LD, in rat liver perfusate and microsomal samples. The mobile phase composition was initially maintained at aqueous buffer solution: acetonitrile (91:9 v/v) from 0 to 5 min, then changed linearly over ten minutes to 81:19 v/v and was maintained at 81:19 v/v from 15 to 26.5 min before returning to the initial conditions within one minute. The column was then allowed to equilibrate for 7.5 min before the next run. The total run time was 35 min.

2.4.2 Standard solutions

Standard stock solutions of LD and its metabolites were prepared separately in deionized water to a final concentration of 1 mg/mL base equivalent. New stock solutions for LD and its metabolites, except for MeOH-LD and MeOH-MEGX, were prepared every three months and stored at -20°C. Stock solutions of the two methylhydroxylated metabolites were prepared every month due to degradation during long term storage. On the day of analysis, a working stock solution was prepared by mixing appropriate aliquots of individual stock solutions of LD and its metabolites in deionized water. Serial dilution with the appropriate drug-free matrix (canine plasma, rat liver perfusate or microsomal mixture) was then made to give various concentrations for the calibration curves. For quantification of conjugated metabolites in isolated rat liver perfusate samples, calibration curves for LD, MEGX, GX, 3-OH-LD and 3-OH-MEGX were prepared by spiking known amounts of these compounds in blank perfusate. The mixtures were subjected to acid hydrolysis procedures as described in section *2.4.3.2.2*.

Calibration curves were linear over a range of 0.025 - 50 μg/mL for LD (r>0.999), 0.010 - 10 μg/mL for MEGX, MeOH-LD and GX (r>0.999) and 0.020 - 5 μg/mL for 3-

OH-LD ($r>0.996$) when ethyl acetate-0.1 N HCl extraction method was used. For single-step extraction method using methylene chloride, linearity of calibration curves was established over a range of 0.025 - 5.0 μg/mL for LD and most of its metabolites and of 0.025 - 0.50 μg/mL for MeOH-LD and MeOH-MEGX ($r>0.998$). Assay procedures were validated by comparing results with quality control samples prepared by other colleagues in the laboratory. Triplicates of three different concentrations were prepared and analyzed together with standard and unknown samples. The intra- and inter-day coefficients of variation for accuracy and precision of all analytes were < 15%.

2.4.3 Sample preparation

2.4.3.1 Intravenous and oral studies in dogs

For the quantification of LD, MEGX and GX, 50 μL EMGX solution (25 μg/mL) and 50 μL 0.1 N NaOH were added to a 500 μL plasma or blood sample in glass tubes (16 × 100 mm, Kimax®, Kimble, IL, USA). Blood cells were lysed by the addition of an equal volume of water prior to alkalization. Each sample was extracted with 4 mL of ethyl acetate by shaking for 10 min using a vortex shaker (IKA-VIBRAX-VXR, Terochem Laboratories Ltd., USA) and centrifuged at 1,800 × *g* (Dynac centrifuge, Clay Adams, USA) for 10 min. The organic layer was transferred into clean glass tubes (13 × 100 mm, Kimax®, Kimble, IL, USA) and extracted with 350 μL of 0.1 N HCl. The samples were vortexed for 10 min and centrifuged for 10 min. The aqueous layer was separated from the organic layer using the quick freeze method in a dry ice-acetone bath and was then dried using the Savant Speedvac centrifugal vacuum evaporation system (Model SC 100, Savant Instruments Inc., Farmingdale, NY, USA). The residues were reconstituted with 300 μL of 0.01N HCl (pH 2.2). 150 μL of the solution was injected into the HPLC system.

2.4.3.2 Isolated rat liver perfusion studies

2.4.3.2.1 Measurement of unconjugated metabolites and lidocaine

100 μL of EMGX solution (25 μg/mL) was added to a 1 mL aliquot of rat liver perfusate samples. Potassium bicarbonate (~1 g) was added to adjust pH of the sample to 8.5. Each sample was extracted with 8 mL of methylene chloride by vortexing for 10 min on a vortex shaker. After centrifugation at 1,800 × *g*, the organic phase was separated and evaporated to dryness under a gentle stream of nitrogen. The residue was reconstituted in 300 μL of 0.01N HCl and 150 μL was injected onto the HPLC column.

2.4.3.2.2 Acid hydrolysis

To 0.5 mL of liver perfusate sample collected at steady state was added an equal volume of 6 N HCl and 0.1 mL of internal standard solution. After incubation at 100 °C for one hour, each sample was adjusted to pH 7.0 by adding an equimolar volume of 6 N NaOH. The samples were then treated and analyzed according to the procedures described in section *2.4.3.2.1*. Control samples were prepared by adding 0.5 mL of 0.1 M potassium phosphate buffer (pH 7.4) to liver perfusate samples prior to and after incubation at 100 °C for one hour. LD and its metabolites, except for MeOH-LD and

MeOH-MEGX, were stable when subjected to acid and heat treatment. The two methyl-hydroxylated analytes were degraded in acidic solution. Hence, conjugates of these two metabolites could not be measured by acid hydrolysis. Attempts to hydrolyze conjugates enzymatically failed to demonstrate the existence of glucuronide and sulfate forms of both metabolites.

2.4.3.3 Rat liver microsomal studies

400 μL of incubation mixture was transferred from a microcentrifuge tube (Brinkmann Instruments Inc., Westbury, NY, USA) to a glass tube (16 mm × 100 mm, Kimax®, Kimble, IL, USA), in which 50 μL of EMGX (100 μg/mL) was added as internal standard. LD and its primary metabolites (MEGX, 3-OH-LD and MeOH-LD) were extracted with 4 mL of ethyl acetate and then with 350 μL of 0.1 N HCl solution according to the procedures described in section *2.4.3.1*.

2.5 Radioactivity counting

Aliquots (300 μL) of plasma samples collected from all four catheters for i.v. studies and of plasma (50 μL) and ultrafiltrate (50 μL) samples for protein binding studies were dissolved in 5 mL EcoLite+™ liquid scintillation cocktail (ICN, Costa Mesa, CA, USA). ^{14}C radioactivity were counted using a Wallac Model 1410 liquid scintillation counter (Wallac Oy, Turku, Finland). Counting efficiencies for ^{14}C-isotope were high (90 - 95%).

For counting radioactivity in blood samples, red blood cells were solubilized using the wet oxidation method. To each aliquot of whole blood (50 μL) was added 50 μL of perchloric acid (70% v/v) and 100 μL hydrogen peroxide (30% w/v). The mixture was heated in a water bath set at 70 to 80 °C until tissue was completely digested. 5 mL EcoLite+™ liquid scintillation cocktail (ICN, Costa Mesa, CA, USA) was then added to each sample. The mixtures were left overnight in the dark at room temperature to reduce chemiluminescence prior to ^{14}C counting.

2.6 Pharmacokinetic analysis

2.6.1 Lidocaine protein binding in canine plasma

Free fraction (f_u) was calculated (94) as follows:

$$f_u = \frac{dpm\ per\ 50\ \mu L\ ultrafiltrate}{dpm\ per\ 50\ \mu L\ plasma} \tag{2.1}$$

2.6.2 Intravenous studies in non-instrumented dogs

Pharmacokinetic parameters were estimated using established non-compartmental analysis (226). The area under the LD plasma concentration *vs* time curve (AUC) and the area under the first moment curve (AUMC) were approximated using LAGRAN® (227). Elimination rate constant (k_e) was calculated from the slope of the terminal phase. Half-life ($t_{½}$), plasma clearance (Cl_p), volume of distribution at steady state (V_{dss}) were computed according to equations 2.2 to 2.4:

$$t_{1/2} = \frac{ln\,2}{k_e} \tag{2.2}$$

$$Cl_p = \frac{F \times Dose}{AUC} \tag{2.3}$$

$$V_{d_{ss}} = \frac{F \times Dose \times AUMC}{AUC^2} \tag{2.4}$$

F, the absolute bioavailability, is assumed to be equal to unity for i.v. administration of LD.

2.6.3 Intravenous studies in instrumented dogs

Plasma concentration-time profile in the carotid artery was used to estimate conventional kinetic parameters according to equations 2.2 to 2.4. Blood clearance (Cl_b) was the product of Cl_p and C_p/C_b. Plasma profiles in individual blood vessels, combined with electronically measured hepatic arterial and portal venous blood flows, were used to quantify transhepatic fluxes. Parameters such as hepatic extraction ratio (E_H), hepatic availability (F_H) and hepatic clearance (Cl_H) were estimated by integrating the area under the flux-time curves as follows:

$$F_H = 1 - E_H \tag{2.5}$$

$$E_H = \frac{\int_{t_1}^{t_2} flux_{in}dt - \int_{t_1}^{t_2} flux_{out}dt}{\int_{t_1}^{t_2} flux_{in}dt} \tag{2.6}$$

where $flux_{in}$ and $flux_{out}$ at each time point were calculated based on equations 2.7 and 2.8:

$$flux_{in} = Q_{HA}^t \times C_{CA}^t + Q_{PV}^t \times C_{PV}^t \tag{2.7}$$

$$flux_{out} = Q_H^t \times C_{HV}^t \tag{2.8}$$

Q_{HA}^{t} and Q_{PV}^{t} are hepatic arterial and portal venous blood flow rates at time t respectively. Q_{H}^{t}, the total hepatic blood flow at time t, is the sum of Q_{HA}^{t} and Q_{PV}^{t}. C_{CA}^{t}, C_{PV}^{t} and C_{HV}^{t} are plasma LD concentrations in the carotid artery, portal and hepatic veins at time t respectively.

Average hepatic clearance (Cl_H) was computed according to equation 2.9:

$$Cl_H = \frac{\int_{t_1}^{t_2} Cl_H(t) \times C(t)dt}{AUC} \tag{2.9}$$

$$\approx \frac{\sum_{i=1}^{n}[Cl_H(t_i^{*}) \times AUC_{\Delta t_i}]}{AUC}$$

where the product $AUC_{\Delta t_i}$ is the area under the plasma LD concentration curve within the ith time interval between two sampling time points t_{i-1} and t_i and AUC is the area under plasma concentration *vs* time curve from 0 min to ∞. $Cl_H(t_i^{*})$ is the hepatic clearance at the mid-point of the ith time interval as computed in the following:

$$Cl_H(t_i^{*}) = \frac{Cl_H^{t_{i-1}} + Cl_H^{t_i}}{2} \tag{2.10}$$

$$Cl_H^{t} = Q_H^{t} \times E_H^{t} \tag{2.11}$$

E_H^{t}, the hepatic extraction ratio at time t, was computed using equation 2.6. Hepatic intrinsic clearance (Cl_{int}) was estimated based on the well-stirred model (228) using equation 2.12:

$$Cl_{int} = \frac{Cl_H}{1 - E_H} \tag{2.12}$$

Well-stirred model is used because it has been shown that this model gives a better fit of LD kinetic data than the parallel-tube model (228).

During the 12-h i.v. infusion, E_H, Cl_H and Cl_{int} values were calculated according to equations 2.6, 2.11 and 2.12 at each sampling time point.

The hepatic tissue uptake process was evaluated using ^{14}C-labeled LD as a tracer dose. Net amount of ^{14}C radioactivity (dpm) bound in the liver was estimated by the difference in the areas under the *flux*$_{in}$ and *flux*$_{out}$ *vs* time curves, as computed using equations 2.7 and 2.8 where C'_{CA}, C'_{PV} and C'_{HV} are in terms of total ^{14}C radioactivity (dpm/mL) in plasma. To express the extent of hepatic tissue uptake process in term of percent of LD dose, net amount of ^{14}C dpm retained in the liver is divided by the product of 2.22×10^{-6} dpm/μCi, specific activity (51.7 μCi/μmoles LD) and the ratio of ^{14}C-labeled LD to unlabeled LD in dose solution, then the ratio of the amount of LD dose equivalent (μmoles) retained by the liver to total dose administered (μmoles) is multiplied by 100%. We recognize that total radioactivity in plasma samples arise not only from ^{14}C-labeled LD, but also from its metabolic products that retain the carbonyl group. Nevertheless, the total amount of unlabeled and ^{14}C-labeled LD and its metabolites (μmoles) bound in the liver could be estimated by multiplying the net ^{14}C dpm by the ratio of unlabeled LD to ^{14}C-labeled LD in dose solution.

2.6.4 Oral studies in instrumented dogs

Oral clearance (Cl_p/F) and volume of distribution ($V_{d\,ss}/F$) were estimated using equations 2.3 and 2.4. Peak concentration, C_{max} and its corresponding time, T_{max} in the four blood vessels were read from the concentration-time profiles. Elimination parameters such as E_H, F_H, Cl_H and Cl_{int} values were assessed as that described in section *2.6.3*, with one exception. Plasma flow rates, obtained by multiplying blood flow rates with (1 - hematocrit), was used to calculate Cl_H. The hematocrit (Hct) of individual dog was measured on each day of an experiment. For the oral study in which both blood and plasma samples were collected for the whole time course, LD concentration in red blood cells (C_{rbc}) is estimated using equation 2.13:

$$C_{rbc} = \frac{C_b - C_p(1 - Hct)}{Hct} \tag{2.13}$$

2.6.5 Isolated rat liver perfusion studies

The time to reach steady state (T_{ss}) was determined statistically using the procedure reported by Saville *et al.* (173). The mean steady-state concentrations of LD and its metabolites were calculated by averaging the concentration data from the time to reach steady state to the end of infusion. The efficiency of the isolated liver to remove LD was estimated by Cl_{int}, E_H and Cl_H using equations 2.12, 2.14 and 2.15 respectively.

$$E_H = \frac{C_{in} - C_{out}}{C_{in}} \tag{2.14}$$

$$Cl_H = Q \times E_H \tag{2.15}$$

where Q is the perfusate flow rate (mL/min), C_{in} (μM) is the inlet LD concentration and C_{out} (μM) is the outlet LD concentration.

The percent of dose recovered as unchanged LD and as metabolites were computed by multiplying the molar ratio of steady state effluent LD or metabolite *concentrations before and after acid hydrolysis to inlet* LD concentration with 100. The percent of dose recovered as conjugated forms of metabolites was estimated by the difference between the percent of dose recovered as metabolites after acid treatment and those of unconjugated metabolites. In addition, the mass balance at steady state was determined by summing the percent recoveries of LD and all of its metabolites at the outlet.

2.6.6 Rat liver microsomal studies

Enzyme kinetic parameters were determined by nonlinear least squares regression of unweighted data using WinNonlin (229) and by linear regression of transformed data using EnzymeKinetics (230).

2.7 Statistical analysis

2.7.1 Intravenous and oral studies in dogs

To test the effects of instrumentation on LD disposition kinetics, non-parametric Wilcoxon signed-rank test was performed. For the i.v. and oral studies in instrumented dogs, all parameters were subjected to the Wilcoxon matched pairs signed-rank test for pairwise comparison of values obtained following single dose administration on day 1 and day 10. To test our hypothesis that hepatic blood flow, intrinsic enzyme activities and net hepatic tissue uptake were reduced after exposure to a 12-h i.v. infusion of LD, one-tailed test was applied for parameters such as Cl_b, Cl_H, Q_H, E_H, F_H, Cl_{int} and the amount of LD and its metabolites retained in the liver. Differences in the mean values on day 1 and day

10 for other parameters such as AUCs for LD and its metabolites and their ratios were tested using two-tailed test. Non-parametric Kruskal-Wallis one-way analysis of variance (ANOVA) was performed to detect any significant changes in parameters at various time intervals during a 12-h i.v. infusion on day 8 of both the i.v. and oral studies. All tests were conducted at a significance (α) level of 0.05. Data are reported as mean ± SD.

2.7.2 Isolated rat liver perfusion studies

ANOVA was used to detect differences in all kinetic parameters among diethyl ether, methoxyflurane and pentobarbital treatment groups. Percentage data were analyzed using the arcsin ($\sin^{-1}(\sqrt{Y})$) transformation prior to ANOVA (231). Conclusions based on ANOVA of original data and of transformed data agree with each other and plots of residuals show similar patterns of distribution of variance in corresponding sets of data. Therefore, results of analysis of original data are presented in Table 3.10. When significant F values are obtained ($p < 0.05$), the Student-Newman-Keuls test is used to compare the means among the three groups. All tests are conducted at the 0.05 level of significance. Values are reported as mean ± SD.

2.7.3 Rat liver microsomal studies

Data were subjected to non-parametric two independent sample Mann-Whitney U Rank Sum test ($\alpha = 0.05$) for statistical comparison between mean values of control and LD pretreatment groups.

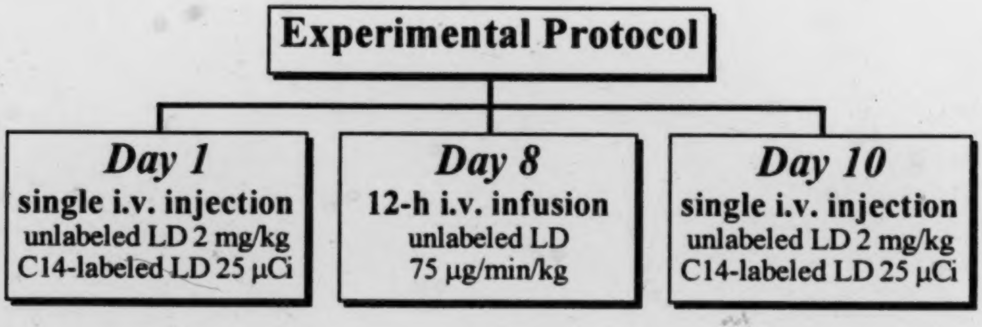
Experimental Protocol
Day 1
single i.v. injection
unlabeled LD 2 mg/kg
C14-labeled LD 25 μCi
Day 8
12-h i.v. infusion
unlabeled LD
75 μg/min/kg
Day 10
single i.v. injection
unlabeled LD 2 mg/kg
C14-labeled LD 25 μCi

Figure 2.1 Dosing regimens employed for i.v. studies in chronically instrumented dogs (n = 4). A similar protocol was adopted for oral studies except that a single dose of unlabeled LD (10 mg/kg) was given on day 1 and on day 10.

3. RESULTS

3.1 Intravenous studies in non-instrumented dogs

Mean plasma concentration *vs* time profiles of LD and its metabolites in the carotid artery are depicted in Figure 3.1. Following a single i.v. dose, time course of LD plasma levels showed an initial rapidly declining phase, followed by a linear terminal phase. Our results showed that half-life, systemic plasma clearance, volume of distribution at steady state and AUC value of LD were not different between non-instrumented and instrumented dogs ($n = 3$; $p > 0.05$) (Table 3.1). Data for dog #2 were excluded in the calculation of mean values because this dog had a major blood loss between the two studies. Consistent with previously reported findings (59,232,233), primary and secondary products of the N-dealkylation pathway, namely MEGX and GX, were the principal metabolites detected in canine plasma. MEGX kinetics is formation-limited after LD injection, as reflected by a similar $t_{½}$ (68.8 ± 16.5 min) as that of the parent drug (Table 3.1).

3.2 Intravenous studies in instrumented dogs

Therapeutic concentrations of LD were achieved at the dosing rate employed in our i.v. infusion studies (Table 3.2). All animals tolerated the drug well with nausea and emesis being the only symptoms of adverse reaction observed. Emesis usually occurred three to six times beginning at three to four hours after initiation of infusion in all dogs.

C_b/C_p ratios of LD were found to be similar on day 1 (0.91 ± 0.13) and day 10 (0.94 ± 0.12) ($p = 0.715$). These values were used to estimate Cl_b from Cl_p.

Time courses of plasma concentration of LD and its metabolites in the carotid artery during the 12-h continuous i.v. infusion of LD are depicted in Figure 3.2. We did not observe a continuous rise in plasma level of the parent drug, as indicated by a lack of significant difference in mean C_p values at various time of infusion (Table 3.2). Cl_H of LD by the liver remained unchanged at different time of infusion (Table 3.2). Plasma concentration *vs* time profiles of LD after single i.v. doses before and after the 12-h infusion were superimposable to each other (Figure 3.3a). Pairwise comparison of values of disposition parameters such as $t_{½}$, V_{dss} and Cl_b (Table 3.3) failed to reveal any significant differences.

3.2.1 Alterations in hepatic hemodynamics during lidocaine administration

In the present study, we have successfully employed transit time flow probes to obtain direct and reliable measurements of hepatic blood flow rates in an intact animal throughout the whole duration of LD infusion. Q_H in three out of the four dogs was elevated between three to eight hours after initiation of LD infusion (Figure 3.4). In the remaining dog, the rise in Q_H was delayed (from seventh hour until the end of infusion). The magnitude of change varied from 11% to 79% (n = 4), but no significant differences could be detected among the mean values at various time of infusion due to a small sample size and large variabilities (Table 3.2). The elevation in mean Q_H values was mainly attributed to a significant increase in Q_{HA} values ($p = 0.004$), with a variability ranging from 1.6- to 9.2-fold in individual dogs (n = 4). Q_{PV}, however, remained constant in all dogs throughout the 12 h period ($p = 0.736$) (Figure 3.4).

Interestingly, single i.v. LD doses did not exhibit any effect on splanchnic hemodynamics, as indicated by stable values of Q_{HA}, Q_{PV} and Q_H. Mean Q_H values on day 1 and day 10 were similar (Table 3.3). Our dogs are similar to humans in this regard, as evident by findings of a lack of change in hepatic blood flow (96) and cardiac output (165) in man when therapeutic doses of LD are given as bolus injection.

3.2.2 Binding of lidocaine to plasma proteins

Consistent with the literature (61,80,94,139,191), our data reveal that binding of LD to plasma proteins is concentration-dependent. *In vitro* determinations of LD protein binding in canine plasma showed that f_u increased proportionally from 0.18 ± 0.02 to 0.34 ± 0.01 at total LD concentrations ranging from 4.3 to 21.3 μM and then became quite stable at ~0.42 to 0.45 when LD concentration were between 42.7 to 85.3 μM (Figure 3.5). Early dog plasma samples, collected from the carotid artery and the portal vein 2.5 to 10 min after the 5-min infusion of LD, were analyzed for protein binding. The total (free and bound) LD concentration in these samples ranged from 5.5 to 20.1 μM for day 1 and from 6.0 to 20.0 μM for day 10. f_u values were found to vary between 0.22 to 0.37 for day 1 and between 0.20 to 0.39 for day 10 samples (Figure 3.6). These values agreed with those obtained from *in vitro* determination and were similar between day 1 and day 10 in individual dogs. The scattering of data points was mainly due to intersubject variability. Linear regression analysis was performed for individual plots of free fraction *vs* total LD concentration (Figure 3.6). Statistical test results indicated that the slopes of regression lines were not different between day 1 and day 10 ($p = 0.285$).

3.2.3 Tissue uptake of lidocaine and its metabolites by the liver

In vivo uptake of LD and/or its metabolites into hepatic tissue in instrumented dogs was evaluated using ^{14}C-labeled LD as a tracer of transhepatic fluxes of LD and its metabolites. Time courses of $flux_{in}$, $flux_{out}$ and their difference ($flux_{in} - flux_{out}$) across the liver are depicted in Figure 3.7. A net tissue uptake process occurred rapidly and was near completion within 15 minutes after injection. There was a lack of back diffusion of LD and its metabolic products into systemic circulation, suggesting that hepatic uptake of these compounds probably involves tight binding. When the first dose was given on day 1, the total amount of LD and its metabolites retained by liver tissue was estimated to be equivalent to 39.7 ± 14.5 µmoles (that is, 20.6 ± 6.2% of LD dose given). Based on the assumption that the liver weight in dogs is approximately 32 g/kg body weight (234), the mean total amount of LD and its metabolites taken up by hepatic tissue was estimated to be 56.5 ± 20.6 nmol/g liver.

When challenged with the 5-min infusion of identical dose of ^{14}C-labeled and unlabeled LD 36 h after the discontinuation of the 12-h i.v. infusion, the extent of net uptake of LD and its metabolites was equivalent to 30.1 ± 15.1 µmoles of LD (that is, 15.8 ± 7.6% of LD dose given or 43.9 ± 21.9 nmol/g liver). The difference in mean values of net amount uptake (in µmoles of LD) of day 1 and day 10 did not reach statistical significance ($p = 0.072$) because of the great intersubject variability in the magnitude of changes (+3.4% to -65.3%).

3.2.4 Alterations in hepatic elimination capacity

LD underwent extensive hepatic elimination in dogs and a high extraction ratio, ranging from 0.95 to 0.99 on day 1, was observed in our instrumented dogs. Cl_H values comprised about 81% of Cl_b (Day 1, Table 3.3). During 4 to 12 h of constant rate i.v. infusion, mean Cl_H values remained constant despite a continuous fall in mean E_H values (Table 3.2). This was because of a compensatory effect caused by an elevation of Q_H values. On the other hand, there was a progressive decline in Cl_{int} values with time to 15 to 60% of the corresponding values at 4 h by the end of infusion in three dogs. In the remaining dog, there was no consistent pattern in the change of Cl_{int} values. No statistically significant differences could be detected among the mean values (Table 3.2).

When data obtained during the 12-h i.v. infusion were compared to baseline values (day 1), mean values of E_H at 4, 6, 8, 10 and 12 h during infusion were significantly lower ($p = 0.019$), and F_H values were consistently higher than their corresponding values on day 1 ($p = 0.019$). Mean Cl_{int} values during i.v. infusion were also significantly less than that on day 1 ($p = 0.016$). These trends were consistently observed in all dogs. Before the animals were challenged with an identical dose of LD 36 h after the termination of i.v. infusion, levels of LD and its metabolites in plasma were below the detection limit of the HPLC assay. The mean Cl_{int} value on day 10, however, was significantly less than that on day 1 ($p = 0.034$) (Table 3.3). The extent of reduction in Cl_{int} values varied among dogs, day 10 values being 9 - 75% of the corresponding values on day 1.

Shown in Figure 3.8 are AUCs for LD and its N-dealkylated metabolites at the inlet and outlet of the liver. AUC values of LD in hepatic vein, but not in carotid artery, were elevated in all dogs on day 10 by 1.29- to 8.86-fold, with the mean values on day 1 and day 10 being 15 ± 9 nmol×min/mL *vs* 35 ± 22 nmol×min/mL respectively ($p = 0.068$). This increase was accompanied by an increase in mean AUC values of MEGX in the carotid artery (day 1: 79 ± 36 nmol×min/mL *vs* day 10: 134 ± 40 nmol×min/mL; $p = 0.068$) and in the hepatic vein (day 1: 66 ± 31 nmol×min/mL *vs* day 10: 126 ± 41 nmol×min/mL; $p = 0.068$) (Figure 3.8). On the contrary, mean AUC values of GX tended to decrease in the hepatic vein (day 1: 408 ± 191 nmol×min/mL *vs* day 10: 284 ± 136 nmol×min/mL; $p = 0.068$) in all dogs (Figure 3.8). The AUC ratios of the parent drug and its metabolites are listed in Table 3.4. At the outlet of the liver, the AUC ratio of GX to MEGX was significantly reduced on day 10 whereas that of MEGX to LD remained constant throughout the experiment.

3.3 Oral studies in instrumented dogs

Mean plasma concentration *vs* time profiles of LD and its metabolites obtained from the four blood vessels on day 1 are depicted in Figure 3.9. Absorption process peaked at approximately one hour after oral administration (Table 3.5). This is consistent with reported values of 45 min (138) and 60 min (50,235) in dogs. Concentrations of MEGX and GX were highest in the hepatic vein (Figure 3.9), indicating that the liver was the major site of their formation. MEGX concentrations in the portal vein were slightly higher than the corresponding values in the carotid artery throughout the time course, suggesting that N-dealkylation might also occur in the gut. Disposition kinetics of orally administered LD was probably unaffected by previous infusion of the drug, as evident by the superposability of arterial plasma concentration-time profiles of LD (Figure 3.10) and a lack of difference in mean values of oral clearance and volume of distribution on day 1 and day 10 (Table 3.5). Unlike the findings in the i.v. studies, there was no change in plasma profile of MEGX when the second oral dose was given (Figure 3.10).

Assessment of hepatic elimination processes following oral administration is complicated by nonlinear and changing C_b/C_p, which is inconsistent with the close-to-unity value in the i.v. studies. Conversely, blood-to-plasma concentration ratios of MEGX and GX were constant during a course of i.v. infusion and upon both i.v. and oral administration. Nonlinearity in blood distribution has never been documented for LD and will be further addressed in section *3.4*. At present, kinetic analysis was carried out using hepatic plasma flow. Mean values of F^p_H, Q^p_H, E^p_H, Cl^p_H and Cl^p_{int} are summarized in Table 3.6. No significant difference was found between any pairs of mean values on day 1 and day 10 in the oral studies (Table 3.6). Mean Cl_{int} value of LD (day 1) was much lower when single dose of LD was given orally than when given i.v. (Table 3.6). Moreover, the large intersubject variability in Cl_{int} observed following the first i.v. injection for 5 min (Figure 3.11a, day 1) disappeared when the drug was given as a single oral dose on day 1 (Figure 3.11b). Pretreatment of dogs with a 12-h infusion did not further reduce Cl_{int} value after oral administration (day 1 *vs* day 10, $p = 0.273$) (Table

3.6). Plasma protein binding of LD was not altered upon repetitive oral administration, as indicated by similar f_u values obtained on day 1 and day 10 in each dog.

3.4 Blood-to-plasma ratio studies

When LD was given orally, we found that values of C_b/C_p were unexpectedly high and variable, ranging from 0.88 to 10.3. The ratio seems to depend on the site and time of sample collection. For instance, samples taken from the portal vein generally exhibited a close-to-unity C_b/C_p, despite a wide range of plasma concentrations (Figures 3.12c and 3.12d). By contrast, those samples collected from the jugular vein displayed an approximately 10-fold difference in their C_b/C_p values (Figures 3.12c and 3.12d). There is a tendency of an increase in C_b/C_p as time after dose administration progresses or as plasma concentration declines in all samples. The same pattern was consistently observed in all dogs on both experimental days; that is, before and after a 12-h infusion. In addition, a marked difference in C_b/C_p values existed between jugular venous samples that were obtained after single i.v. injection and those after oral doses, despite similar plasma LD concentrations (Figures 3.12a *vs* 3.12c and Figures 3.12b *vs* 3.12d). Thus, this phenomenon could not be explained simply based on concentration-dependency. Moreover, values of the free fraction of LD in the jugular venous plasma samples obtained either after single i.v. dosing or oral dosing were similar to each other. It is unlikely that plasma protein binding could play a role in the remarkably high C_b/C_p values occurred only after oral dose administration.

We have performed a series of preliminary experiments in an effort to explore the possibilities of artifacts arising from sample handling and analysis and of co-elution of an unknown substance or metabolite which exists in substantial quantity only after extensive first-pass metabolism of LD when given orally.

3.4.1 *In vitro* studies

Equilibrium of LD distribution into erythrocytes was attained rapidly (within 5 min) (Table 3.7). No further increase in the extent of LD accumulation in erythrocytes was observed when sample mixing was allowed for up to three hours. Temperature at which equilibration process took place did not influence LD distribution in blood. Evidence is provided by mean C_b/C_p values of 0.71 ± 0.02 and 0.71 ± 0.06 when spiked blood samples (final concentration of 4.3 μM) were equilibrated at room temperature and at 37 °C respectively. Moreover, C_b/C_p values remained relatively constant in *in vitro* samples despite a delay in centrifugal separation of erythrocytes from plasma for up to 3 h (Table 3.7) or even 24 h (data not shown). There was a good agreement between data determined using ^{14}C radioisotope counting and HPLC methods (Table 3.7).

Distribution of LD into erythrocytes is dependent on blood LD concentration, as evident by an increase in C_b/C_p values from 0.70 ± 0.03 at 2.1 μM to 1.10 ± 0.15 at 85.3 μM (Figure 3.13). The concentration range is chosen to encompass portal venous blood concentrations which might be greater than the therapeutic range. Our data are consistent with those reported in the literature (80). As LD concentration increases, plasma protein binding becomes saturated (Figure 3.5). An increase in plasma free fraction may shift the distribution equilibrium towards red blood cells (80,84). However, the effect of blood concentration on C_b/C_p is modest, as oppose to much greater values in samples obtained from *in vivo* studies. The concentration range we studied encompasses the highest concentration observed in portal vein samples collected after oral dosing of LD. Therefore, other factors besides concentration effects and artifacts due to sample handling procedures should be considered.

3.4.2 *In vivo* and *in vitro* comparison studies

After oral administration of 10 mg/kg LD to dog R113, complete blood and plasma concentration-time profiles in the four blood vessels were obtained. Time courses of LD C_b/C_p at these four sampling sites are depicted in Figure 3.14. Similar values of C_b/C_p, as determined by HPLC assay, were found in the carotid artery, jugular and portal veins with a maximum value of approximately 2.0 to 2.5. On the other hand, C_b/C_p ratio showed a markedly different pattern in hepatic vein with a peak value of 8.7 in the post-absorption phase. There was a delayed rise in C_b/C_p values for this particular experiment. Generally, a trend of increasing C_b/C_p values was quite obvious by 30 to 60 min. Blood samples collected from the jugular and portal veins were equilibrated *in vitro* with ^{14}C-labeled LD previously added to sample collection tubes. C_b/C_p values based on ^{14}C radioactivity were much lower than the corresponding values determined by HPLC (Figure 3.14). This discrepancy is unlikely to be caused by the techniques employed, since application of these methods to spiked blood samples resulted in data which agreed closely with each other (Table 3.7). One possible reason could be the presence of some co-eluting compounds underneath the LD peak at our chromatographic conditions.

3.4.3 Purity determination of lidocaine peak

Three approaches were employed in an effort to verify the purity of the LD peak on our HPLC column. The first approach utilizes difference in polarity by varying acetonitrile to buffer composition of the mobile phase. Both isocratic and gradient methods were run. In spite of a wide difference in retention time of LD (9.7 min and 26.5 min respectively), no extra peak could be detected. Second, analysis using photodiode array detection (PDA) method demonstrates that the UV spectrum (200 to 400 nm) of LD peak of a blood sample were superimposable with authentic LD (Figure 3.15). Further, superposability of UV spectra extracted before, after and at peak maxima, as well as purity test results, suggested that LD peak is homogenous. On the other hand, modification at sites far away from the chromophore, such as the tertiary amine group, might not result in a significant change in UV spectrum (see Figure 3.16 for illustration). It is possible that the unknown compound(s) might contain a similar chromophore to LD. To confirm identity of LD peak, LC/MS analysis was performed as the third approach.

Major findings of LC/MS analysis are summarized in the following: 1) LD HCl (Sigma Co., St. Louis, MO, USA), which was used for preparation of oral dose and of calibration curve of HPLC assay, is very pure. 2) Representative mass spectra of a system control sample (that is, deionized water subjected to the same extraction procedures together with dog samples), blank blood and a blood sample collected 60 min after LD oral administration to dog T8 are shown in Figure 3.17. The corresponding C_b/C_p value for the particular 60-min blood and plasma samples was 28. The presence of ions such as *m/z* 117, 130, 161, 225, 241, 257, and clusters of ions around 353 and around 430, 683 and 711 in blood samples are also detected in system control sample. Thus, the possibility of the presence of endogenous compounds in blood as a cause for the higher than expected C_b/C_p ratio could be ruled out. 3) Fragmentation of molecular ion (MH^+, *m/z* 235) at low electron volt gives rise to *m/z* 86 ion, which is selected as a tracer for any LD related compounds (Figure 3.18a). A *m/z* 251 ion, which was absent in the system control sample and in authentic LD HCl powder, was detected in mass spectra of blood and plasma samples taken after a 5-min i.v. injection, single oral dosing and at the end of a 12-h infusion. Using the selected ion monitoring mode, this *m/z* 251 ion is shown to fragment and give the *m/z* 86 ion (Figure 3.18b). This strongly suggests that *m/z* 251 ion might be structurally related to LD. A difference in 16 amu suggests the addition of an oxygen atom to LD. Although the source of this ion is unclear, the presence of this ion could not explain for the high C_b/C_p ratio for two reasons. First, this ion is also detected in blank blood and plasma spiked with authentic LD. Second, the relative abundance of this ion to MH^+ is similar in blood and plasma samples obtained after oral and i.v. administration of LD. Only when this ion is present in excessively abundant quantities in blood samples would it accounts for the greater-than-unity C_b/C_p values. 4) Ratio of peak area response of *m/z* 235 ion in blood to that in plasma samples were in close agreement with the corresponding values determined by HPLC assay (Table 3.8). Hence, we have verified the measured C_b/C_p values of LD using our HPLC chromatographic conditions are not artifactual.

3.5 Effects of anesthetic agents in the isolated rat liver perfusion studies

The livers used in this study were viable, as indicated by a constant oxygen uptake over the entire duration of perfusion. Overall mean values of oxygen consumption of the livers at time 0, 20, 40 and 60 min were 3.34 ± 0.76, 3.55 ± 0.69, 3.67 ± 0.52 and 3.62 ± 0.48 mL oxygen/hr per g liver respectively. These mean values were not significantly different from each other and were comparable to values reported previously, ranging from 2.95 ± 0.25 mL oxygen/hr per g liver weight (196) to 4.41 ± 0.11 mL oxygen/hr per g liver (236). Moreover, mean AST concentrations were 6.4 ± 1.5 IU/L and 7.0 ± 2.4 IU/L and mean ALT levels were 3.6 ± 1.3 IU/L and 5.1 ± 2.1 IU/L at the start and at the end of perfusion respectively. These values agreed with the findings of Schmidt *et al.* (237) who detected 18 IU/L of AST and 7 IU/L of ALT in the medium after 4 hours of perfusion using hemoglobin-free Kreb's bicarbonate buffer.

The concentration time courses of LD and its metabolites during LD infusion at constant rate are shown in Figure 3.19. The profiles shared a common pattern for rats treated with diethyl ether, methoxyflurane and sodium pentobarbital anesthesia. There were no significant differences among the mean times for LD to reach steady state (T_{ss}) for the three groups, which were 44.2 ± 5.8 min, 33.3 ± 11.7 min and 37.5 ± 10.4 min respectively. Consistent with previous findings (144), the level of MEGX showed a characteristic increase to a maximum at 5 - 10 min and gradually declined to steady state level. The time course of 3-OH-LD was parallel to that of the parent drug whereas that of MeOH-LD reached steady state rapidly. Effluent concentrations of MeOH-MEGX which are below the quantitation limit are assigned a value of zero.

There were no significant differences in the steady state mean values of C_{out}, E_H, and Cl_{int} of LD among the three treatment groups (Table 3.9). The latter was reflected by a similar mean % of dose recovered as unchanged drug in the perfusate (Table 3.10). Examination of individual metabolite levels showed that major pathways of LD biotransformation was not differentially affected by the type of anesthetics used. Steady state % of LD dose recovered as N-dealkylated and 3-hydroxylated metabolites were comparable among the three groups (Table 3.10). Although there was a trend towards higher MeOH-LD and MeOH-MEGX recoveries in the pentobarbital treated group, only that of MeOH-MEGX reached a significant level ($p = 0.04$). Acid hydrolysis study revealed that 3-hydroxylated metabolites were further conjugated in the isolated rat liver preparation. The % recoveries of 3-OH-MEGX and of 3-OH-LD increased approximately six fold and two fold respectively after acid hydrolysis. Based on preliminary results from enzyme hydrolysis study, approximately 10 to 16% of total 3-OH-MEGX conjugates was released as free metabolite after β-glucuronidase treatment whereas only 1 to 5% exists as sulfate. The nature of the remaining 3-OH-MEGX conjugate was not known. On the other hand, 3-OH-LD conjugates existed mainly as glucuronide (70 - 90%); only trace amount of sulfate (less than 2%) was found. Nevertheless, statistical analysis of mean % of LD dose recovered as conjugated forms of 3-OH-MEGX and 3-OH-LD were not different among the three anesthetic regimens (Table 3.10). Lastly, total mean % of LD dose recovered at steady state were similar despite different anesthetic agents were used (Table 3.10).

3.6 Effects of lidocaine pretreatment on intrinsic clearance using rat liver microsomes

After surgery and catheterization, all the rats were in good health as indicated by the facts that hematological test results were within normal range and that there was no apparent loss in their body weight (control group: 259 ± 14 g *vs* 255 ± 11 g; LD pretreatment group: 254 ± 10 g *vs* 254 ± 17 g before surgery and at sacrifice respectively). Livers looked healthy with a uniform pale pinkish color. Liver function test values were within normal range and no difference was observed between the two groups (AST: 44.4 ± 6.7 IU/L *vs* 45.4 IU/L and ALT: 70.0 ± 9.5 IU/L *vs* 73.8 ± 13.6 IU/L for control and LD pretreatment groups respectively). Similarly, liver mass (12.3 ± 1.4 g *vs* 11.2 ± 0.6 g) and total hepatic protein content (13.3 ± 1.0 mg protein/g liver *vs* 13.0 ± 1.1 mg protein/g liver for control and treatment groups respectively) were not altered by a single LD pretreatment at a dose of 10 mg/kg.

LD has a half-life of approximately 30 min in rats (51). At 120 min after the administration of a single i.v. LD dose (10 mg/kg), most of the dose was eliminated and blood LD and unconjugated metabolite concentrations have declined to a low level (less than 0.5 μM) (105). Data from preliminary studies have shown that no detectable amounts of LD and its metabolites could be measured in hepatic microsomes which were prepared at 2, 12 and 24 h after the pretreatment dose.

Representative time courses of LD metabolism in rat liver microsomes at low, medium and high substrate concentrations are depicted in Figure 3.20. The formation of primary metabolites was linear with time of incubation and started to deviate as their conversion to secondary metabolites became significant. Time of microsomal incubation was decided within the linearity phase in order to obtain initial reaction rates. Reproducibility of initial reaction rate determination during microsomal incubation procedures were validated by quality control samples. Except for 3-hydroxylation pathway, overall intra-day and inter-day precision were within 10% (Table 3.11). In general, the formation of 3-OH-LD tends to exihibit a larger variability than the other two pathways.

The effect of substrate concentration on LD metabolism is illustrated in Figure 3.21. The rate of formation of 3-OH-LD was higher than that of MEGX at low substrate concentrations (Figure 3.21). But the formation of MEGX became the predominant pathway with increasing LD concentrations (> 10 μM). Similar patterns are observed in liver microsomes obtained from control and LD pretreated rats.

Formation of MEGX. N-dealkylation of LD to MEGX has a large capacity, since it becomes saturable at very high substrate concentration (> 2.5 mM) (Figure 3.21). Eadee-Hofstee analysis reveals that there are two distinct enzymes responsible for MEGX formation in approximately half of the rat liver microsomes in both control and treatment groups. This is graphically demonstrated by the biphasic decline in Figure 3.22a. Kinetic parameters for MEGX formation in these liver microsomes were estimated by fitting an Michaelis-Menten equation which has two saturable processes to our data points using nonlinear regression analysis. Comparison of K_{m1} and K_{m2} values in these rat liver microsomes (Table 3.12) suggests that LD dealkylation might be preferentially metabolized by the high-affinity, low-capacity component of N-dealkylase at clinically relevant drug concentrations. For the rest of rat liver microsomes, LD N-dealkylation is catalyzed by one microsomal enzyme as suggested by the linearity of the Eadie-Hofstee plot (Figure 3.22b). This enzyme has similar values of K_m and V_{max} to the low-affinity, high-capacity component of N-dealkylase in the two-component system; thus they were grouped together as K_{m2} and V_{max2} in Table 3.12. Since both biphasic and monophasic kinetics were found in both control and LD pretreated rats with approximately equal probability, it is unlikely that the loss of the high-affinity, low-capacity enzyme activity is related to *in vivo* pretreatment with LD.

Formation of 3-OH-LD. The effect of increasing LD concentration on ring hydroxylation is shown in Figure 3.23. Formation rate of 3-OH-LD reached a maximum and then declined rapidly to a stable level as substrate concentration increased. This is consistently observed in all rat liver microsomes of both control and LD pretreated groups. Lineweaver-Burk plot is nonlinear, showing a sudden upward turn as 1/[S] approaches zero (Figure 3.23). This is implicative of high substrate inhibition (238).

Initial data analysis was performed to define substrate concentration range at which linear kinetics is obeyed. This involves point-by-point deletion of data points, starting from the highest substrate concentrations, until linear regression analysis of Lineweaver-Burk plot yields estimates of K_m and V_{max} which are within acceptable limits of deviation (< 10%) between two consecutive steps. Usually this occurred at substrate concentration of 10 μM. Then estimates of K_{m1} and V_{max1} were obtained by nonlinear regression analysis using Michaelis-Menten equation (Table 3.12).

Subsequent computer simulation studies shows that deviation of 3-OH-LD formation from linearity could not be explained by the postulation that LD acts as its own inhibitor. According to equation 3.1, the rate of 3-hydroxylation would eventually decline to zero as substrate concentration increases to infinity. Thus, high substrate inhibition (equation 3.1) fails to predict the plateau phase which was observed at high LD concentrations.

$$v = \frac{V_{max} \times S}{K_m + S(1 + \frac{S}{K_i})} \tag{3.1}$$

where v is the rate of metabolite formation, S is the initial substrate (LD) concentration in microsomal incubation mixture, and K_i is the inhibition constant.

The possibility of product inhibition secondary to high substrate concentration is explored. It is likely that MEGX, rather than MeOH-LD, acts as an inhibitor in rat liver microsomal incubation mixtures for several reasons. First, it is clearly shown that MEGX is the dominant product of LD metabolism, especially at high substrate concentrations. Second, there is evidence in the literature that MEGX competes with the parent drug for ring hydroxylation pathway (109,110,144). Initial computer simulation analysis based on the assumption of competitive inhibition (equation 3.2) failed to predict our data (Figure 3.24).

$$v = \frac{V_{max} \times S}{K_m(1 + \frac{I}{K_i}) + S} \tag{3.2}$$

where I is the concentration of inhibitor (MEGX). This can be explained by the fact that parent drug is always present in excessive quantities relative to MEGX in the incubation mixtures. On the contrary, product inhibition by MEGX could be described by non-competitive inhibition, a special case of linear mixed inhibition when *Ki* equals to Ki' (equation 3.3):

$$\mathrm{v} = \frac{V_{max} \times S}{K_m(1 + \frac{I}{K_i}) + S(1 + \frac{I}{K_i'})} \qquad (3.3)$$

A good fit of simulation curve to our data points suggests a strong likelihood of product inhibition (Figure 3.24). This is further supported by the close agreement of K_m and V_{max} values determined by nonlinear regression analysis based on simple Michaelis-Menten equation at low substrate concentrations (1 - 10 μM) and those based on non-competitive product inhibition equation (1 - 1000 μM). Values for each rat liver microsomes in the control group are listed in Table 3.13 for illustration. Same findings are observed for the LD pretreated group. It is possible that mechanisms other than product inhibition may also play a role, but further investigation requires a series of inhibition studies which is beyond the scope of this project.

Formation of MeOH-LD. Lineweaver-Burk analysis shows that MeOH-LD formation is linear within substrate concentration from 10 to 250 μM. Measurement of formation rate of this metabolite at low substrate concentrations (1 - 5 μM) is not feasible because its amount was below our quantitation limit. Our results show that arylmethylhydroxylation has the lowest metabolic capacity (V_{max}) and thus it has a minor contribution to LD metabolism.

The ratio of V_{max}/K_m, a measure of hepatic metabolic clearance, for each metabolic pathway is provided in Table 3.12. The efficiency of these pathways is ranked in the descending order: 3-OH-LD > MEGX > MeOH-LD for both control and LD pretreated groups. No statistically significant difference could be detected between mean values of all kinetic parameters for the control and LD pretreated groups.

Table 3.1 **Summary of LD kinetic parameters[a] after a single i.v. dose (2 mg/kg) administration in non-instrumented and instrumented dogs (n = 3).[b]**

Dog	Non-instrumented dogs			
	$t_{1/2}$ (min)	V_{dss} (L/kg)	Cl_p (mL/min/kg)	AUC (nmol×min/mL)
#3	51.4	1.59	26.8	343
#4	45.2	0.92	21.7	423
#5	63.9	1.62	27.5	308
Mean	53.5	1.38	25.3	358
SD	9.5	0.40	3.2	59

Dog	Instrumented Dogs			
	$t_{1/2}$ (min)	V_{dss} (L/kg)	Cl_p (mL/min/kg)	AUC (nmol×min/mL)
#1	75.3	1.49	26.9	327
#5	54.5	1.38	28.6	304
#7	64.3	1.33	23.1	396
Mean	64.7	1.40	26.2	343
SD	10.4	0.08	2.8	48

[a] Values are estimated using carotid arterial plasma concentration profiles.

[b] Data for dog #2 are omitted because this dog had a major blood loss between the two studies.

Table 3.2 **Effects of a 12-h continuous i.v. infusion of LD (76.3 ± 4.7 μg/min/kg) on various kinetic and physiological parameters in four instrumented dogs.**[a]

	Time of infusion						p value[b]
	0 h	4 h	6 h	8 h	10 h	12 h	
C_p[c] (μM)	0	11.1 ± 2.0	10.7 ± 2.7	10.3 ± 2.6	9.7 ± 2.1	9.8 ± 2.2	0.408
Q_H (mL/min/kg)	26.4 ± 2.7	28.1 ± 2.9	28.6 ± 5.4	33.3 ± 7.7	35.1 ± 7.5	35.5 ± 6.0	0.201
E_H	-	0.83 ± 0.10	0.79 ± 0.10	0.72 ± 0.08	0.67 ± 0.09	0.66 ± 0.16	0.230
F_H	-	0.17 ± 0.10	0.21 ± 0.10	0.28 ± 0.08	0.33 ± 0.09	0.34 ± 0.16	0.230
Cl_H (mL/min/kg)	-	23.0 ± 1.6	22.4 ± 2.7	23.6 ± 2.9	23.1 ± 3.8	22.7 ± 2.1	0.876
Cl_{int} (mL/min/kg)	-	174 ± 101	123 ± 40	89 ± 18	75 ± 32	83 ± 48	0.191

[a] Values are reported as mean ± SD (n = 4).

[b] p values from the Kruskal-Wallis one-way ANOVA.

[c] Mean plasma concentrations in the carotid artery.

Table 3.3 Pairwise comparison of LD disposition kinetics following a single i.v. injection given before (day 1) and after (day 10) a 12-h i.v. infusion to four instrumented dogs.[a]

	Day 1	Day 10	*p* value[b]
AUC (nmol×min/mL)[c]	356 ± 48	350 ± 36	0.788
$t_{½}$ (min)[c]	68.1 ± 10.9	57.7 ± 2.4	0.144
V_{dss} (L/kg)[c]	1.38 ± 0.08	1.36 ± 0.17	0.715
Cl_b (mL/min/kg)[c]	27.5 ± 6.0	27.5 ± 3.5	0.500
Q_H (mL/min/kg)	24.7 ± 3.3	22.1 ± 3.4	0.233
E_H	0.97 ± 0.018	0.92 ± 0.046	0.034
F_H	0.027 ± 0.018	0.084 ± 0.046	0.034
Cl_H (mL/min/kg)	22.3 ± 3.7	20.4 ± 3.2	0.233
Cl_{int} (mL/min/kg)	1224 ± 859	285 ± 104	0.034

[a] Values are reported as mean ± SD (n = 4).

[b] *p* values from the Wilcoxon matched-pairs signed-rank test.

[c] Values are calculated based on plasma LD concentrations in the carotid artery.

Table 3.4 **Comparison of AUC ratios of N-dealkylated metabolites and LD at the inlet[a] and outlet of the liver on day 1 and day 10 in four instrumented dogs.[b]**

Ratios of AUC	Carotid artery			Hepatic vein		
	Day 1	Day 10	*p* value[b]	Day 1	Day 10	*p* value[b]
$\frac{MEGX}{LD}$	0.22 ± 0.08	0.39 ± 0.14	0.068	5.51 ± 2.52	4.71 ± 2.91	0.715
$\frac{GX}{MEGX}$	6.07 ± 3.93	2.76 ± 1.79	0.068	6.95 ± 3.89	2.57 ± 1.93	0.068

[a] The values obtained in the portal vein are the same as those in the carotid artery on both day 1 and day 10. Thus, only the values for the carotid artery are reported here to represent the AUC ratios at the inlet of the liver.

[b] Values are reported as mean ± SD (n = 4).

[c] *p* values from the Wilcoxon matched pairs signed-rank test.

Table 3.5 Pairwise comparison of kinetic parameters of orally administered LD (10 mg/kg) before (day 1) and after (day 10) a 12-h i.v. infusion to four instrumented dogs.[a]

	Day 1	Day 10	*p* value[b]
$C_{max,\,CA}$ (μM)	2.6 ± 1.0	1.9 ± 0.7	0.144
$T_{max,\,CA}$ (min)	51 ± 19	30 ± 12	0.109
$C_{max,\,PV}$ (μM)	36.9 ± 19.5	41.8 ± 35.8	0.715
$T_{max,\,PV}$ (min)	45 ± 17	44 ± 27	0.715
AUC (nmol×min/mL)[c]	54.9 ± 11.9	51.1 ± 28.4	1.00
Cl_p/F (mL/min/kg)[c]	192 ± 40	251 ± 130	0.465
V_{dss}/F (L/kg)[c]	24.1 ± 6.1	33.1 ± 10.1	0.465

[a] Values are reported as mean ± SD.

[b] *p* values from the Wilcoxon matched pairs signed-rank test.

[c] Values were calculated using carotid arterial plasma concentrations.

Table 3.6 Summary of LD kinetic parameters obtained from the i.v. and oral studies in four instrumented dogs.[a]

	i.v. studies[b]			Oral studies		
	Day 1	Day 10	p value[c]	Day 1	Day 10	p value[c]
F_H^p	0.027 ± 0.018	0.084 ± 0.046	0.034	0.099 ± 0.054	0.071 ± 0.020	0.233
Q_H^p (mL/min/kg)	14.7 ± 1.3	14.2 ± 2.9	0.715	14.1 ± 1.9	14.0 ± 1.4	0.715
E_H^p	0.97 ± 0.02	0.92 ± 0.05	0.034	0.90 ± 0.05	0.93 ± 0.02	0.233
Cl_H^p (mL/min/kg)	13.3 ± 1.7	13.2 ± 2.7	0.500	12.7 ± 1.9	13.0 ± 1.5	0.137
Cl_{int}^p (mL/min/kg)	734 ± 506	180 ± 59	0.034	161 ± 91	196 ± 64	0.137

[a] Values are reported as mean ± SD.

[b] Data are recalculated using hepatic plasma flow.

[c] p values from the Wilcoxon matched pairs signed-rank test.

Table 3.7 ***In vitro* distribution of LD in canine blood.**

Time	Effect of time of equilibration		Effect of lag time before centrifugation	
	$C_p = 4.3\ \mu M$	$C_p = 42.6\ \mu M$	$C_p = 4.3\ \mu M$	$C_p = 42.6\ \mu M$
(min)	C_b/C_p	C_b/C_p	C_b/C_p	C_b/C_p
0	0.75[a] (0.80)[b]	1.00 (1.00)	-	-
5	0.72 (0.74)	0.92 (0.91)	0.70 (0.68)	0.93 (1.05)
30	0.66 (0.73)	0.95 (0.95)	0.76 (0.69)	0.84 (1.06)
60	0.64 (0.76)	1.01 (0.97)	0.73 (0.71)	1.00 (0.93)
180	0.79 (0.79)	0.94 (1.02)	0.67 (0.64)	0.99 (0.93)
Mean	0.71 (0.76)	0.96 (0.97)	0.72 (0.68)	0.94 (0.99)
SD	0.06 (0.03)	0.04 (0.04)	0.04 (0.03)	0.07 (0.07)

[a] Values are measured by ^{14}C radioactivity counting method.

[b] Values in bracket are determined by HPLC analysis of the corresponding samples following extraction procedures as outlined in section *2.4.3.1*.

Table 3.8 Comparison of blood-to-plasma ratios based on LD concentration (HPLC) and peak area response of molecular ion (LC/MS).[a]

Route of LD administration	Sampling site	LD concentration (μM)		Blood-to-plasma ratio	
		Blood	Plasma	HPLC	LC/MS
i.v.	CA	1.29	1.40	0.92	0.86
oral	CA	2.29	0.31	7.29	8.26
oral	PV	16.06	14.19	1.13	1.17
i.v. infusion	CA	12.36	9.16	1.35	1.19

[a] Blood and plasma samples are collected at 60 min following single i.v. and oral dose administration and at 12 h after initiation of an i.v. infusion given on separate occasions to one dog.

Table 3.9 Effects of three anesthetic agents on LD disposition in a single-pass isolated rat liver perfusion study.[a]

Kinetic Parameters	Diethyl Ether	Methoxyflurane	Pentobarbital	p value[b]
Q (mL/min/g liver weight)	3.56 ± 0.26	3.25 ± 0.43	3.64 ± 0.35	0.17
C_{in} (μM)	17.8 ± 0.5	17.2 ± 1.4	16.8 ± 2.1	0.50
C_{out} (μM)	1.8 ± 0.7	1.9 ± 0.7	1.4 ± 0.4	0.45
E_H	0.90 ± 0.04	0.89 ± 0.04	0.91 ± 0.02	0.51
Cl_H (mL/min)	28.9 ± 1.9	28.0 ± 1.5	29.0 ± 1.6	0.52
Cl_{int} (mL/min)	352 ± 191	295 ± 132	374 ± 153	0.68

[a] Values are mean ± SD (n = 6 per group).

[b] p values from the one-way ANOVA.

Table 3.10 Mean % of dose recovered as unchanged LD and its metabolites in effluent perfusate at steady state during a constant rate LD infusion for the three anesthetic treatment groups.[a]

Compound	Diethyl Ether	Methoxyflurane	Pentobarbital	p value[b]
LD	9.7 ± 3.9	11.1 ± 4.2	8.6 ± 2.3	0.50
MEGX	16.1 ± 4.0	18.3 ± 2.5	16.1 ± 2.6	0.38
GX	2.6 ± 1.3	1.8 ± 0.7	2.4 ± 0.8	0.40
unconjugated 3-OH-LD	6.6 ± 1.9	6.6 ± 1.7	7.4 ± 1.6	0.66
conjugated 3-OH-LD	11.1 ± 5.1	11.2 ± 5.3[c]	13.5 ± 5.4	0.69
unconjugated 3-OH-MEGX	2.3 ± 0.9	2.8 ± 0.7	2.5 ± 0.9	0.66
conjugated 3-OH-MEGX	11.3 ± 2.2	14.6 ± 3.4[c]	12.3 ± 7.0	0.52
MeOH-LD	1.6 ± 0.6	1.8 ± 0.4	2.3 ± 0.9	0.21
MeOH-MEGX	0.29 ± 0.26	0.14 ± 0.21	0.68 ± 0.48[d]	0.04
Total	58.1 ± 6.2	67.0 ± 7.8	60.8 ±11.9	0.29

[a] Values are mean ± SD (n = 6 per group).

[b] p values from the one-way ANOVA.

[c] Values are mean ± SD (n = 5 per group).

[d] Value significantly different from methoxyflurane treated group at $p < 0.05$.

Table 3.11 Intra-day and inter-day precision of determination of enzymatic activities in rat liver microsomes.

	Rate of metabolite formation (nmol/min/mg protein)		
Day	3-OH-LD	MeOH-LD	MEGX
1	0.697 ± 0.059 (8.4%)[a]	0.147 ± 0.010 (6.7%)	1.180 ± 0.009 (0.8%)
2	0.837 ± 0.012 (1.4%)	0.148 ± 0.009 (6.3%)	1.087 ± 0.032 (3.0%)
3	0.498 ± 0.005 (1.1%)	0.138 ± 0.009 (6.7%)	1.120 ± 0.039 (3.4%)
4	0.645 ± 0.029 (4.5%)	0.124 ± 0.007 (5.7%)	1.059 ± 0.045 (4.2%)
Mean	0.669	0.139	1.112
SD	0.140	0.011	0.052
CV[b]	20.9 %	7.9 %	4.7 %

[a] Values are mean ± SD of triplicate determination. Intra-day precision (CV) is given in bracket.

[b] Inter-day precision (n = 4).

Table 3.12 Kinetic parameters[a] for LD metabolism in rat liver microsomes (n = 5 per group).

	N-dealkylation						3-Hydroxylation			Arylmethyl hydroxylation		
	V_{max1}	K_{m1}	V_{max1}/K_{m1}	V_{max2}	K_{m2}	V_{max2}/K_{m2}	V_{max}	K_m	V_{max}/K_m	V_{max}	K_m	V_{max}/K_m
Control	3.71	31.45	0.13	10.79	125.6	0.088	0.83	1.04	0.79	0.15	10.52	0.020
	± 0.70[b]	± 12.16[b]	± 0.05[b]	± 1.71	± 21.7	± 0.020	± 0.23	± 0.16	± 0.15	± 0.08	± 3.23	± 0.020
LD-treated	2.74[c]	21.74[c]	0.13[c]	10.91	114.6	0.098	0.70	0.93	0.89	0.16	12.52	0.014
				± 0.66	± 20.0	± 0.020	± 0.19	± 0.43	± 0.49	± 0.05	± 3.44	± 0.006

[a] V_{max}, K_m and V_{max}/K_m are expressed as nmol/mL/mg protein, μM and mL/min/mg protein respectively.

[b] Values are mean ± SD (n = 3). The high-affinity, low capacity enzyme is not evident in liver microsomes harvested from the remaining two rats.

[c] Mean values obtained from two rat liver microsomes. The high-affinity, low capacity enzyme is not evident in the other three rat liver microsomal preparations.

Table 3.13 Kinetic parameters for the formation of 3-OH-LD in rat liver microsomes.[a]

(A) Simple Michaelis-Menten equation[a]**:**

	Rat liver microsomes				
	#1	#2	#3	#4	#5
$V_{max}{}^{b}$ (nmol/min/mg protein)	0.92 ± 0.04	1.02 ± 0.05	1.04 ± 0.02	0.56 ± 0.02	0.62 ± 0.01
$K_m{}^{b}$ (μM)	1.23 ± 0.19	1.03 ± 0.21	1.16 ± 0.10	0.87 ± 0.11	0.90 ± 0.07
r	0.992	0.987	0.998	0.994	0.998

[a] Nonlinear regression analysis (substrate concentrations range from 1 - 10 μM).

[b] Values are mean ± asymptotic standard error.

(B) Product Inhibition[c]**:**

	Rat liver microsomes				
	#1	#2	#3	#4	#5
$V_{max}{}^{d}$ (nmol/min/mg protein)	0.86 ± 0.03	0.97 ± 0.02	0.92 ± 0.04	0.54 ± 0.01	0.55 ± 0.02
$K_m{}^{d}$ (μM)	1.00 ± 0.19	0.85 ± 0.12	0.78 ± 0.20	0.77 ± 0.07	0.58 ± 0.12
$K_i{}^{d,e}$ (μM)	76.9 ± 10.4	107.5 ± 14.1	105.8 ± 23.3	102.8 ± 8.0	296.0 ± 94.1
r	0.975	0.970	0.917	0.987	0.909

[c] Nonlinear regression analysis (substrate concentrations range from 1 - 2500 μM).

[d] Values are mean ± asymptotic standard error.

[e] Initial estimate of K_i for each rat liver microsomal study is obtained from the corresponding K_{m2} of MEGX formation.

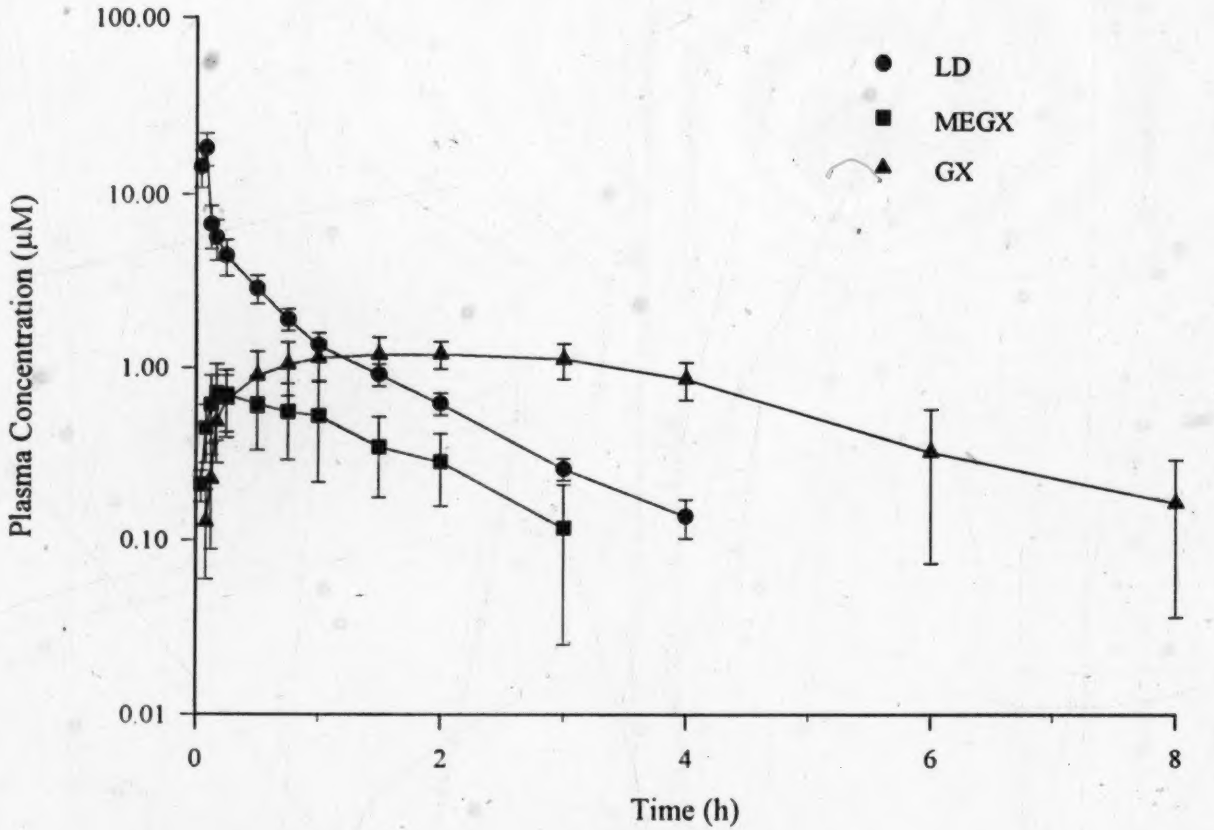

Figure 3.1 Mean plasma concentration *vs* time profiles of LD, MEGX and GX in the carotid artery after a single i.v. dose (2 mg LD/kg) administration in non-instrumented dogs (n = 4).

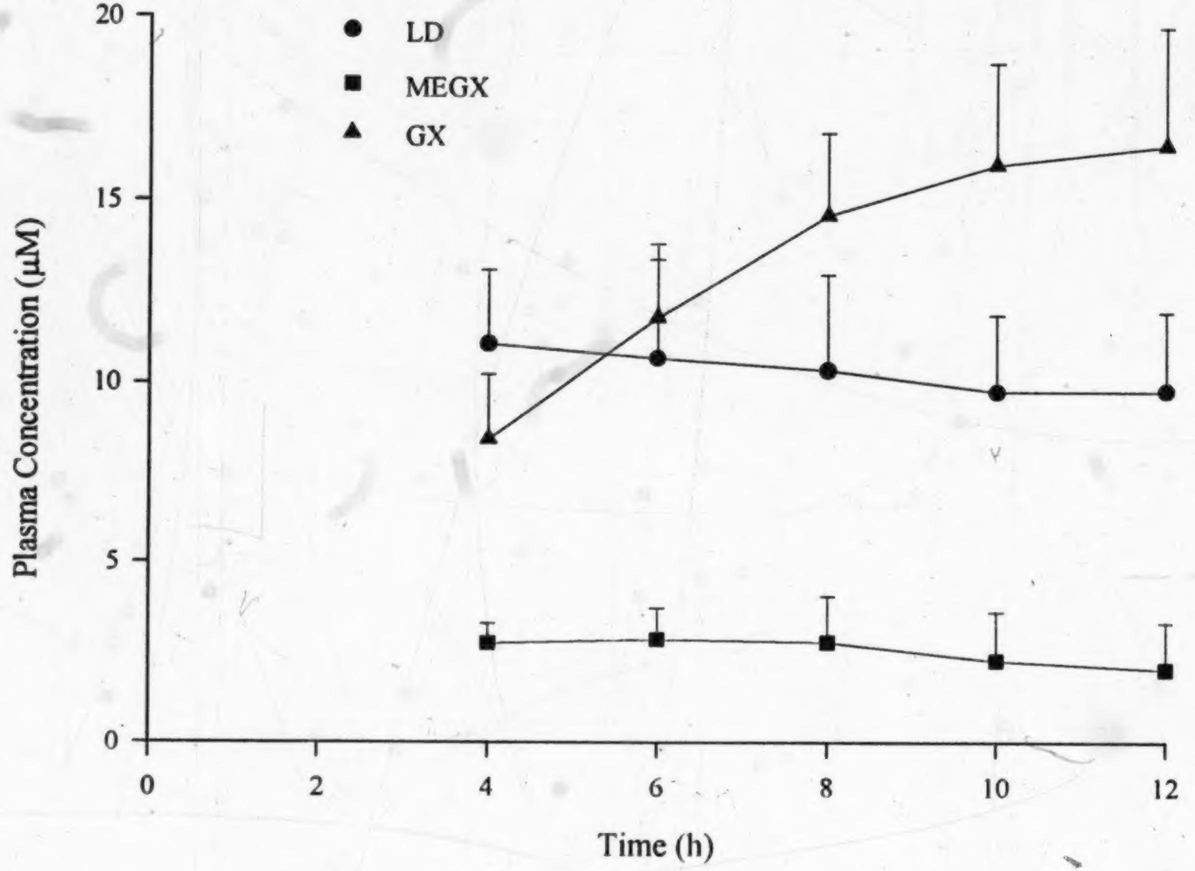

Figure 3.2 Mean (± SD) plasma concentration *vs* time profiles for LD and its N-dealkylated metabolites in the carotid artery during a constant rate i.v. infusion (75 µg/min/kg) in four instrumented dogs.

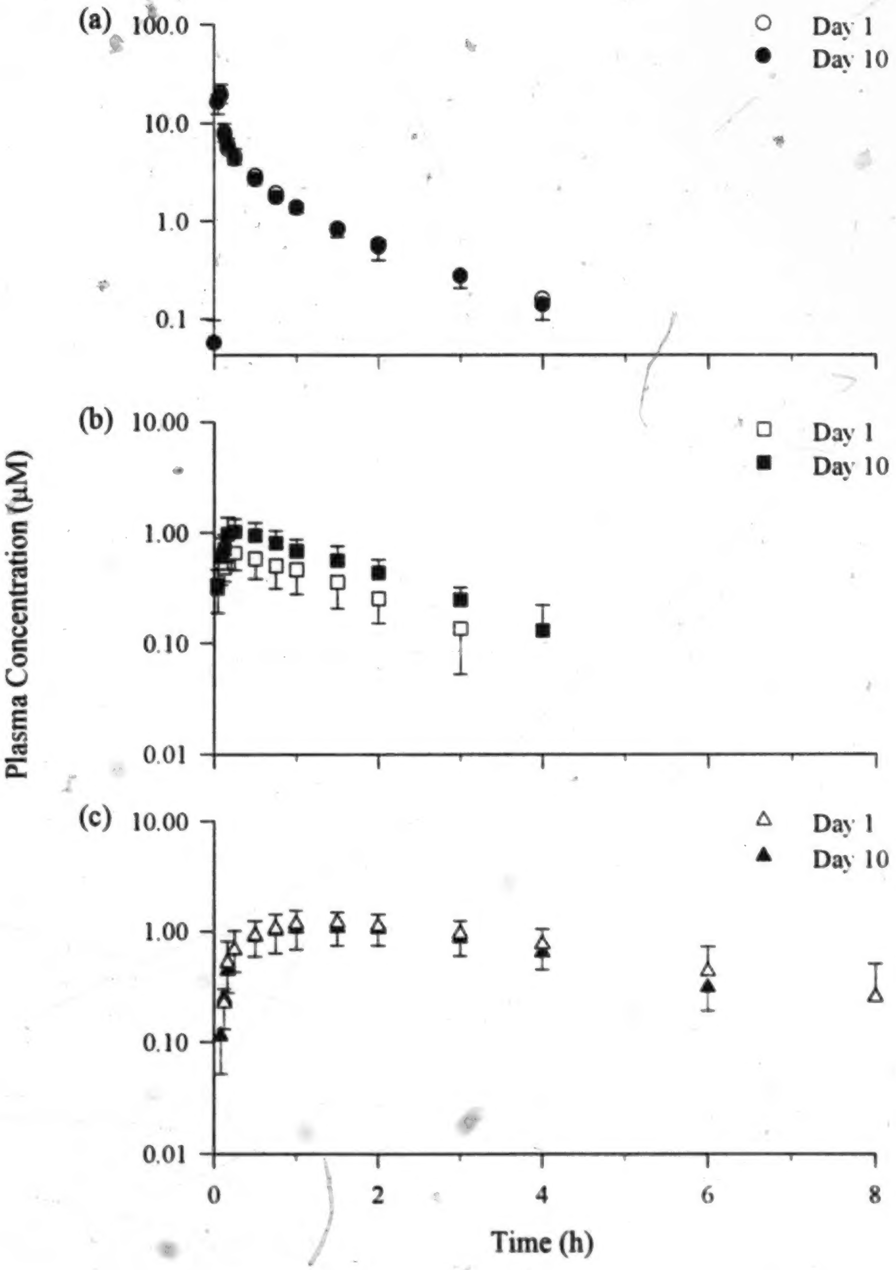

Figure 3.3 Mean (± SD) plasma concentration *vs* time profiles in the carotid artery after a single i.v. dose of LD (2 mg/kg) was infused over 5 min on day 1 and day 10 in four instrumented dogs: (a) LD, (b) MEGX, and (c) GX.

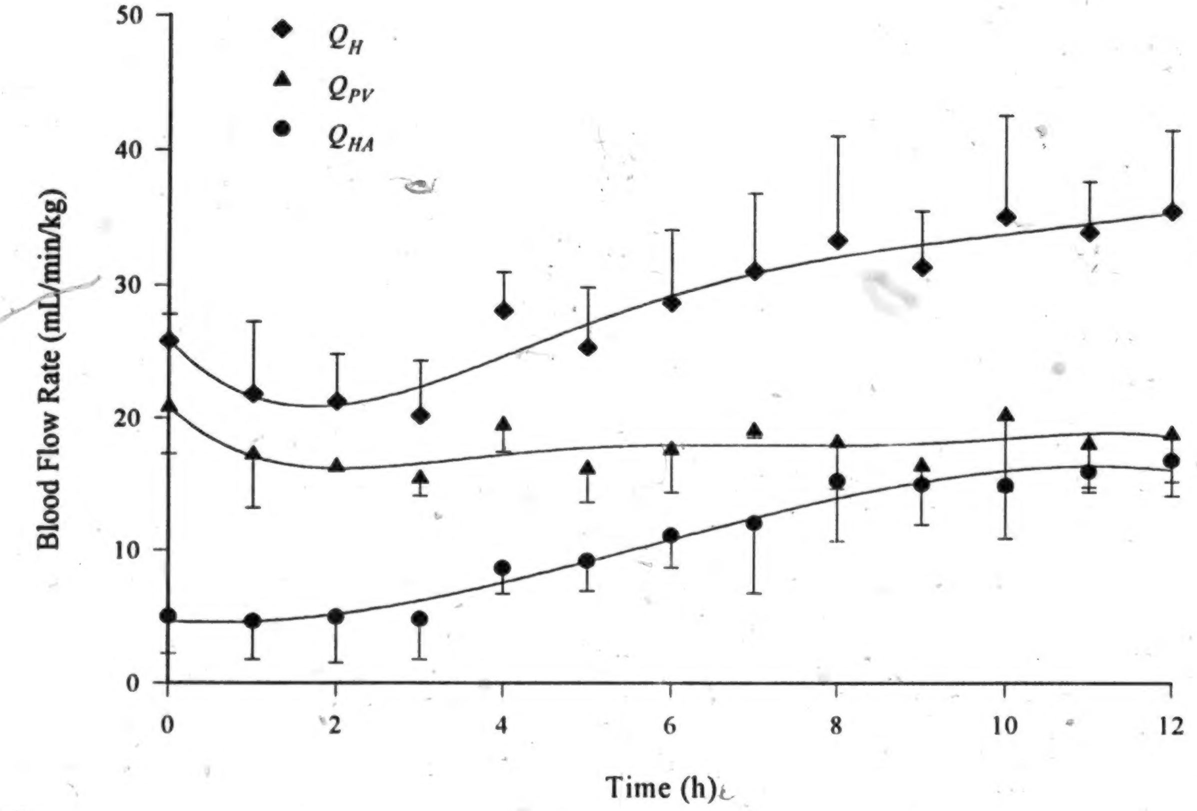

Figure 3.4 Effect of a constant rate i.v. infusion of LD (75 μg/min/kg) on hepatic blood flows in four instrumented dogs. Each data point and its error bars are mean ± SD. Each solid line is drawn from a fit of the mean data using non-linear least squares regression analysis.

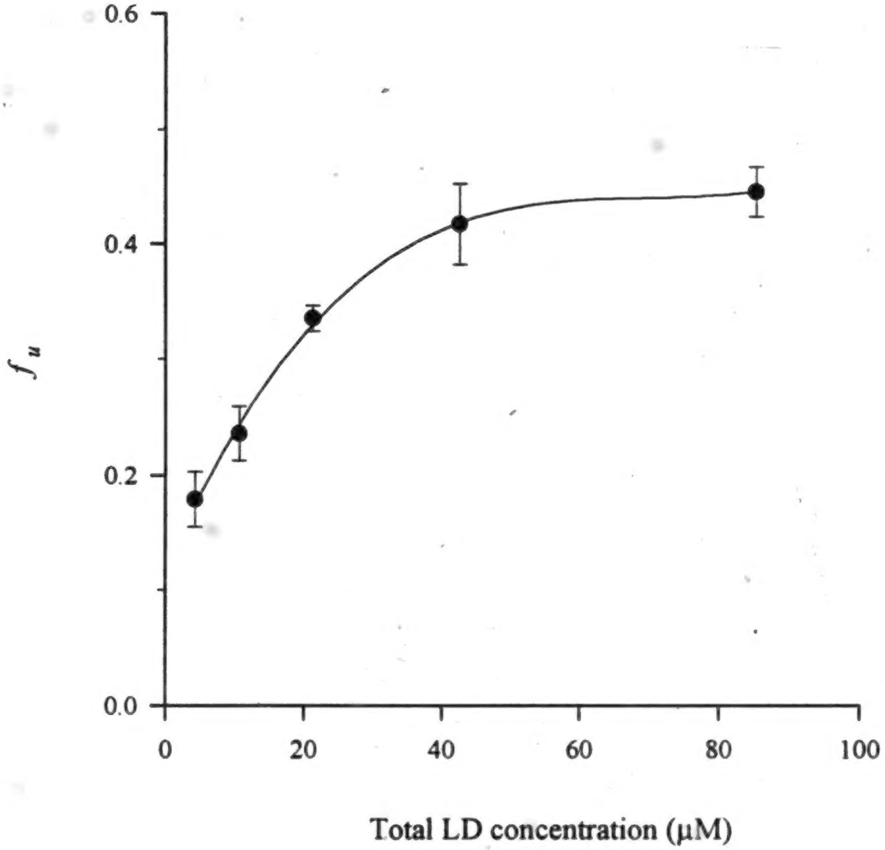

Figure 3.5 **Concentration-dependency of unbound fraction (*f_u*) of LD in canine plasma, determined *in vitro* by ultrafiltration method. Data points are mean values (± SD) of triplicate determinations.**

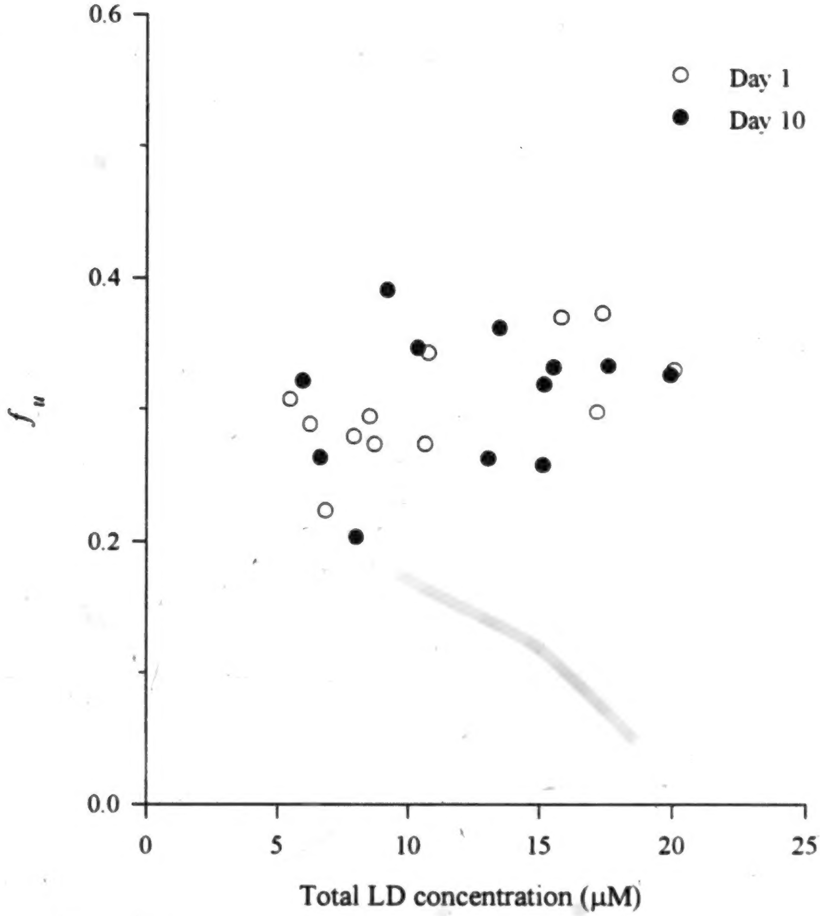

Figure 3.6 Plasma protein binding of LD on day 1 and day 10 in instrumented dogs (n = 3). Free fractions (f_u) of LD were plotted against total LD concentration in plasma (four points per subject on each experimental day). Data for one dog are omitted because of a lack of plasma samples for protein binding determination.

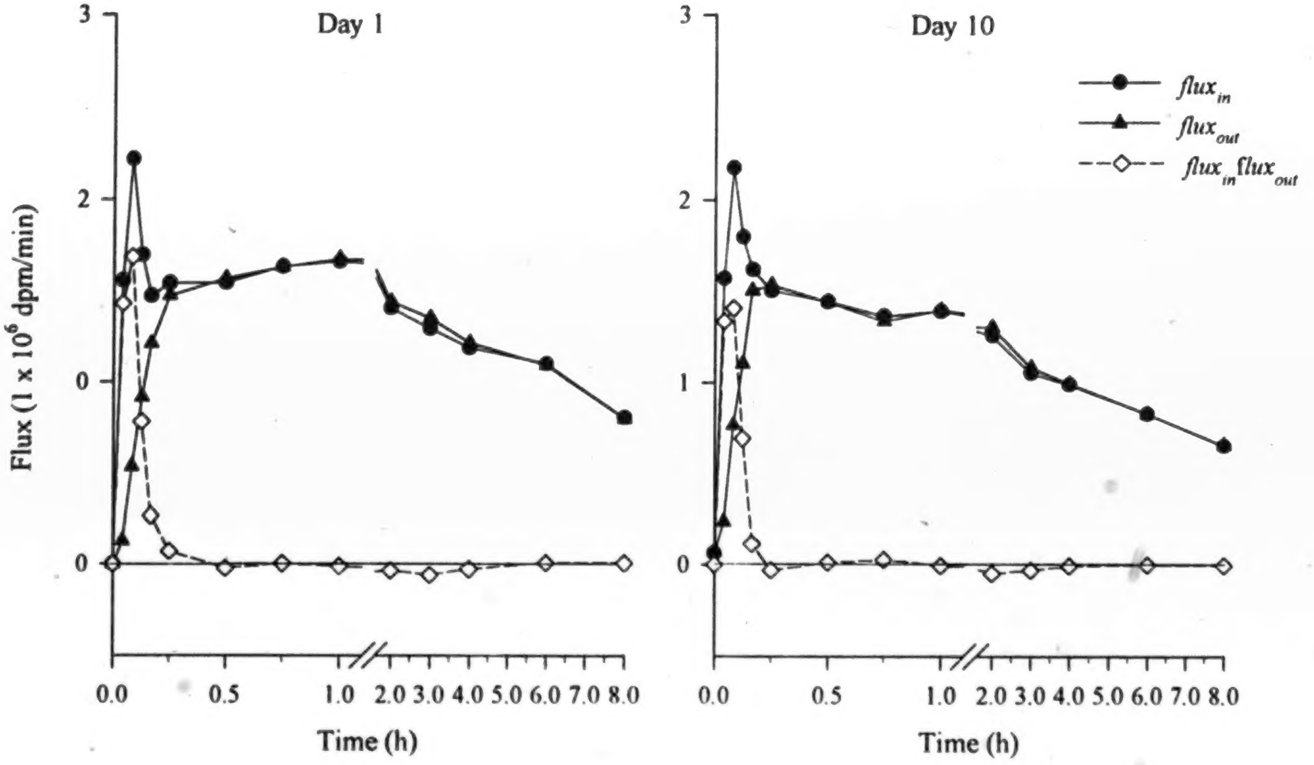

Figure 3.7 Time courses of hepatic tissue uptake after a single i.v. dose of LD was infused over 5 min on day 1 and on day 10 in instrumented dogs. Data points are expressed as mean values (n = 4). Error bars are omitted for the sake of clarity. Amount of net uptake of LD and its metabolic products on each treatment day are estimated from the area under the ($flux_{in}$ - $flux_{out}$) curve. Early sampling time profiles (0 - 1 h) are expanded to reveal a rapid attainment of equilibrium in the hepatic tissue uptake process.

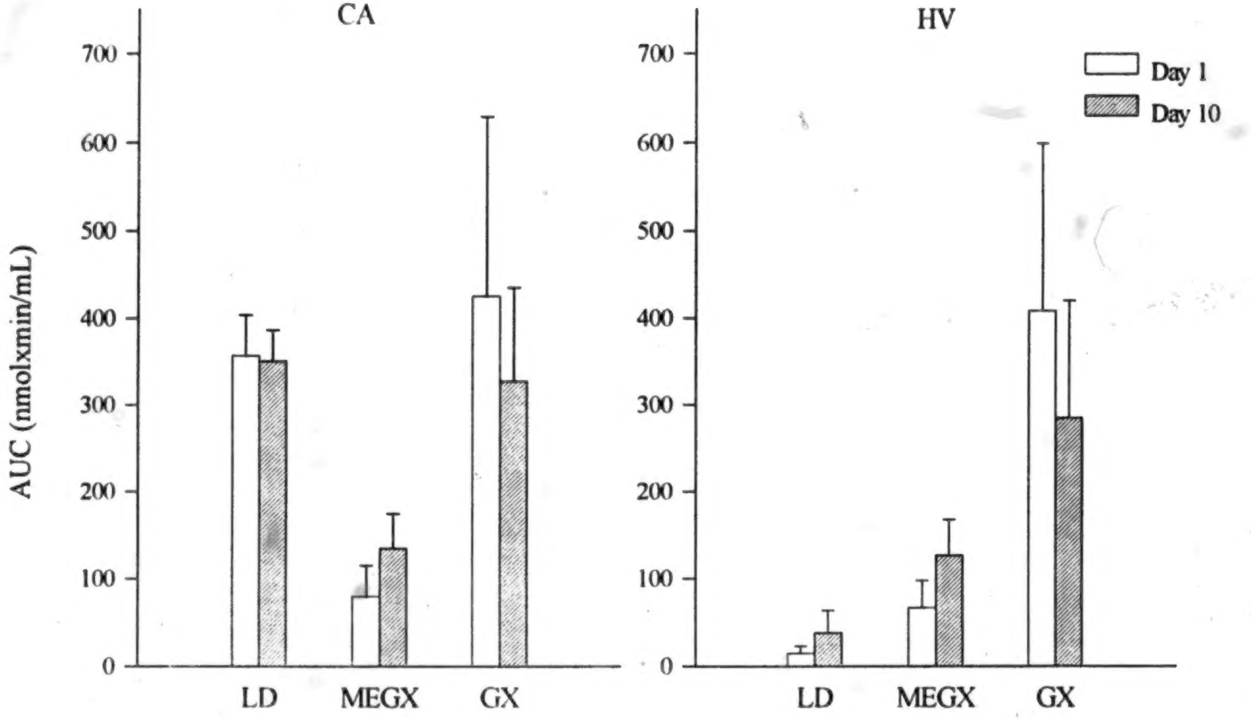

Figure 3.8 Mean AUC values of LD and its metabolites in systemic circulation (CA) and at the outlet of the liver (HV) after a single i.v. dose (2 mg/kg) administration of LD on day 1 (open bars) and on day 10 (shaded bars) to instrumented dogs. Error bars are SD in each group (n = 4). *p* values for all pairwise comparison are reported in the results section.

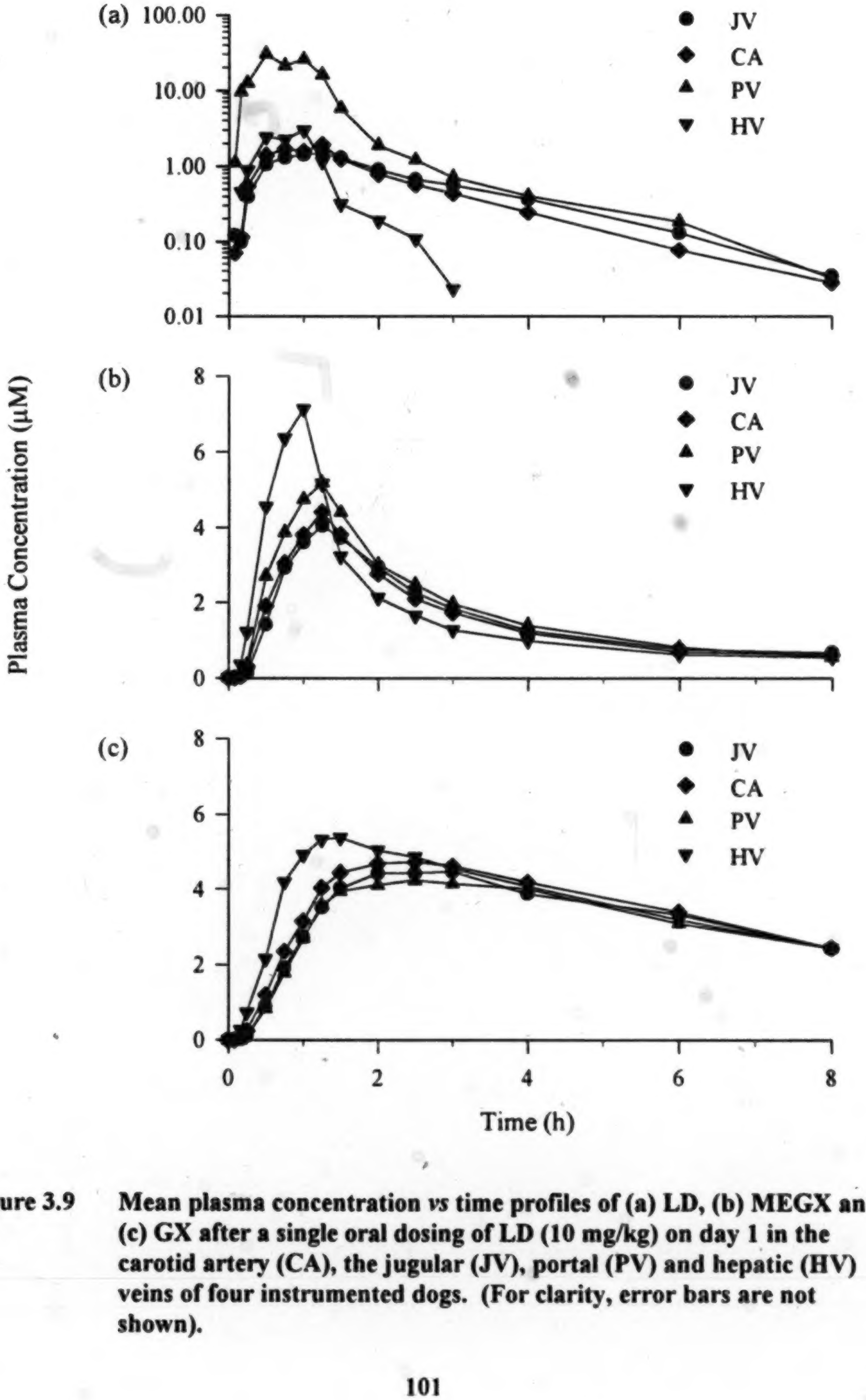

Figure 3.9 Mean plasma concentration *vs* time profiles of (a) LD, (b) MEGX and (c) GX after a single oral dosing of LD (10 mg/kg) on day 1 in the carotid artery (CA), the jugular (JV), portal (PV) and hepatic (HV) veins of four instrumented dogs. (For clarity, error bars are not shown).

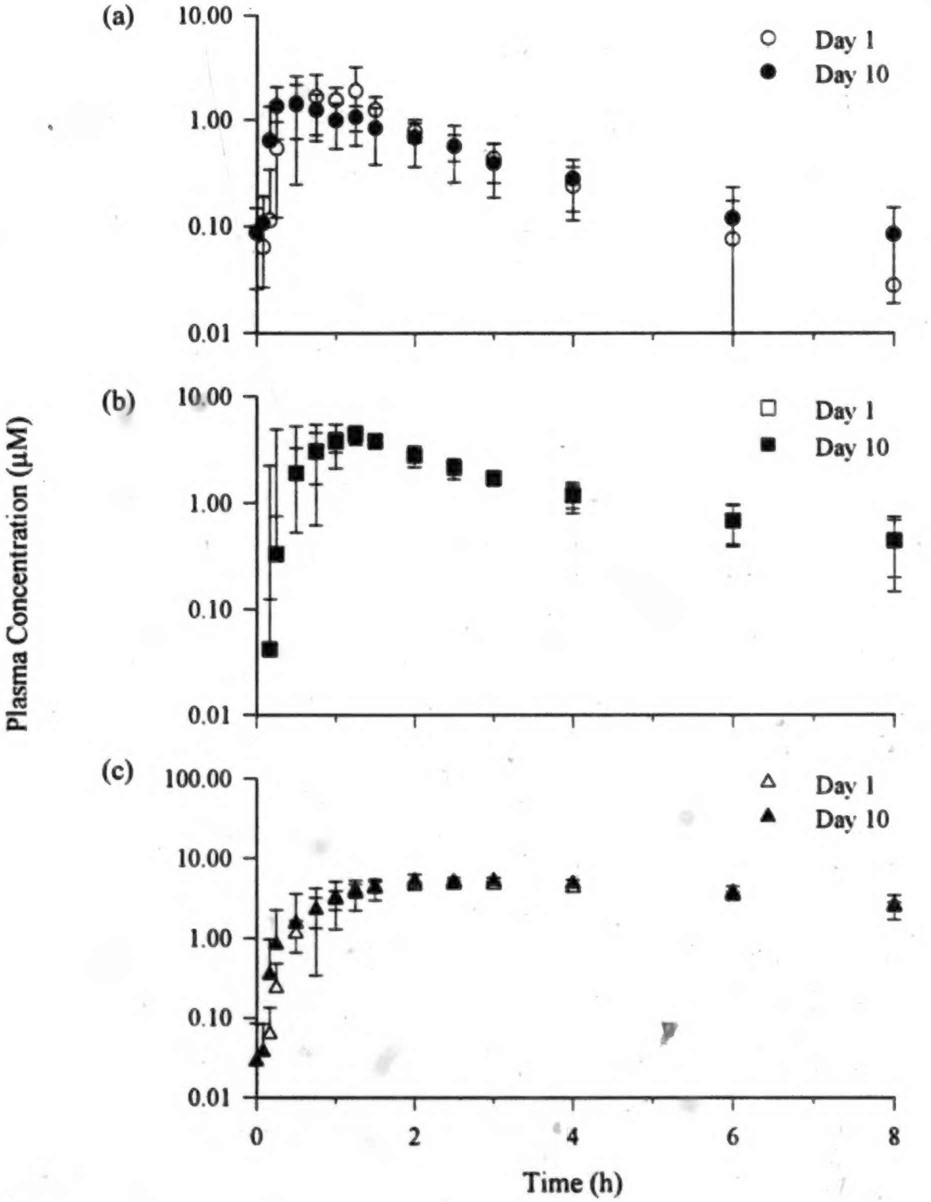

Figure 3.10 Mean (± SD) plasma concentration *vs* time profiles in the carotid artery after a single oral LD dose (10 mg/kg) given on day 1 and day 10 in four instrumented dogs: (a) LD, (b) MEGX and (c) GX.

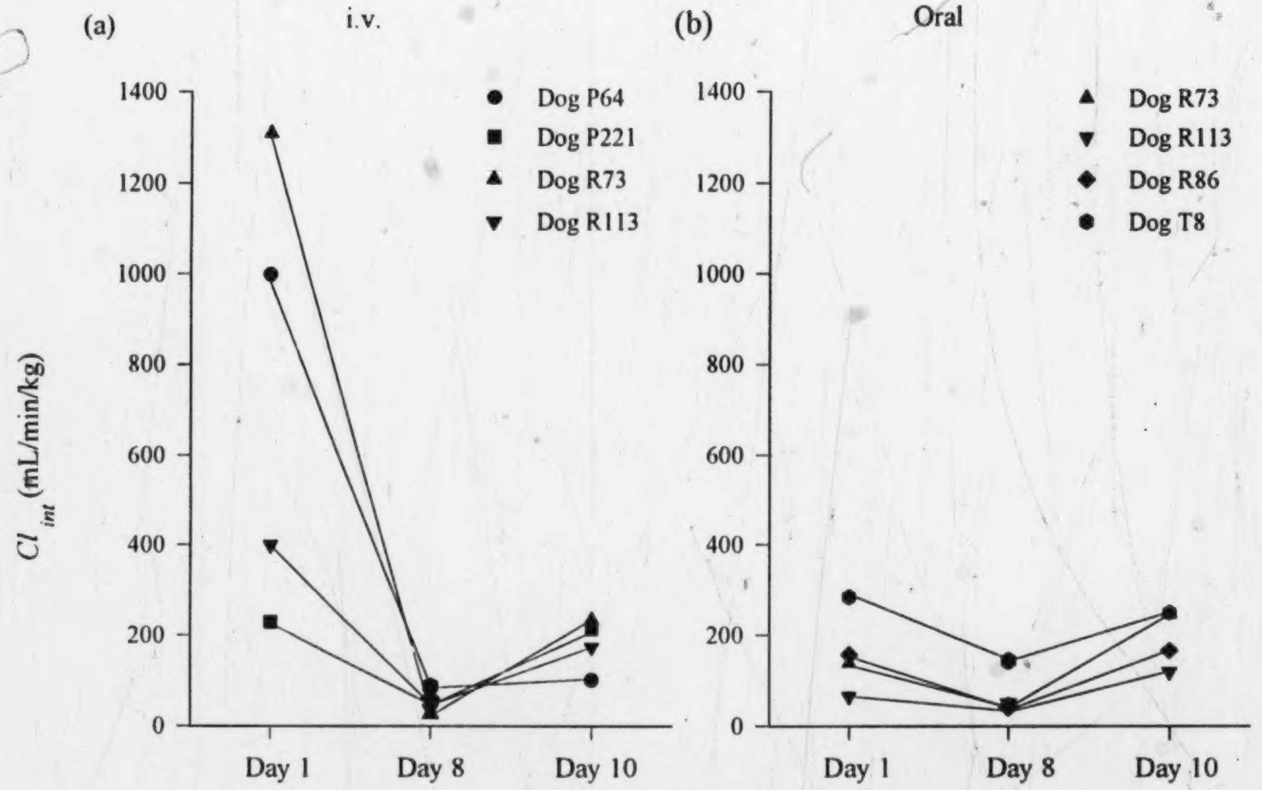

Figure 3.11 **A plot of hepatic intrinsic clearance in instrumented dogs after single i.v. (2 mg/kg) and oral (10 mg/kg) dose administration on day 1 and day 10 and at the end of a 12-h i.v. infusion (75 µg/min/kg) on day 8 (n=4 per group). Cl_{int} values were estimated using plasma concentration and hepatic plasma flow.**

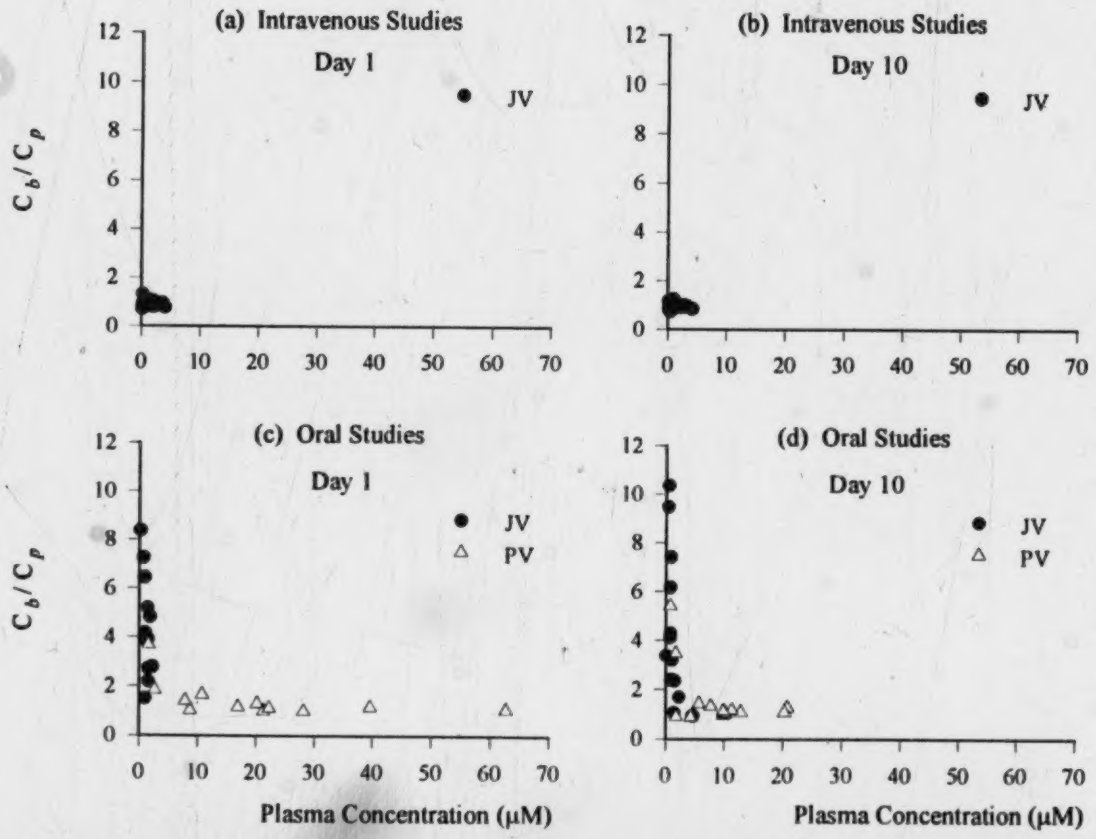

Figure 3.12 Plots of blood-to-plasma concentration ratio *vs* plasma concentration of LD in the jugular (JV) and portal (PV) veins after (a & b) i.v. (2 mg/kg) and (c &d) oral (10 mg/kg) administration of LD to instrumented dogs (n = 4 per group).

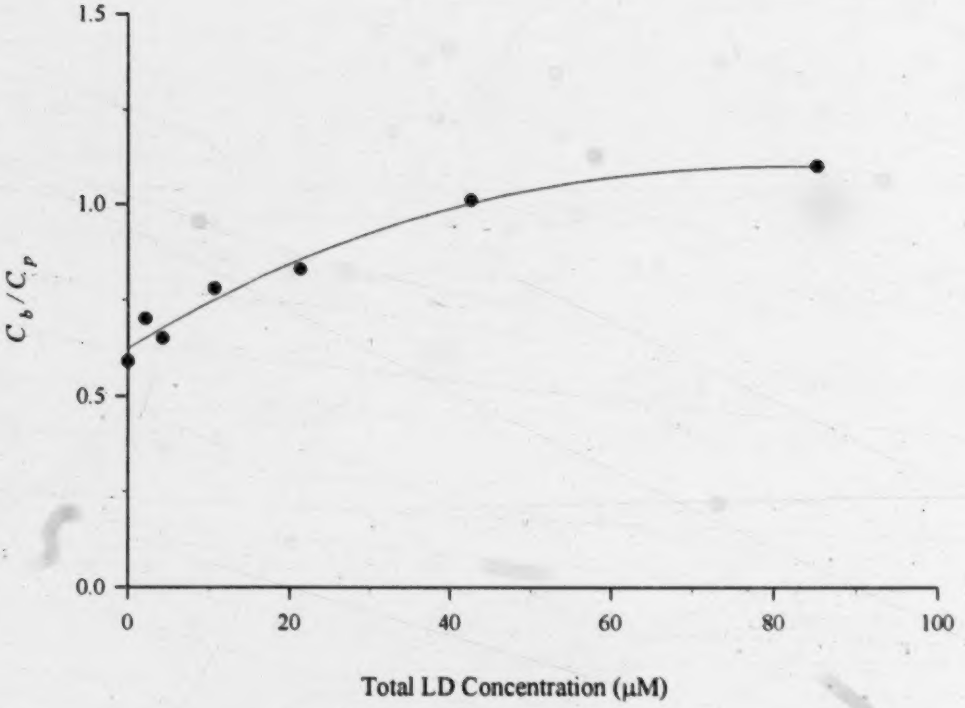

Figure 3.13 **Effect of increasing LD concentration on *in vitro* drug distribution in blank canine blood spiked with various amounts of LD.**

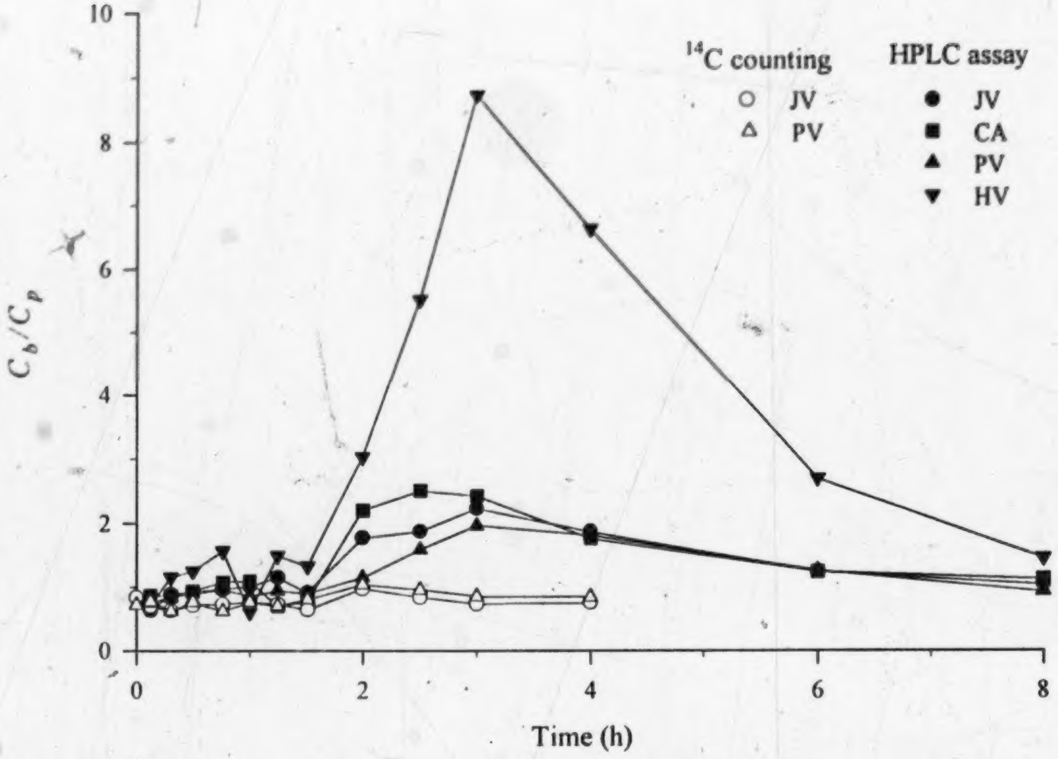

Figure 3.14 Time courses of LD blood-to-plasma concentration ratio in the carotid artery (CA) and the jugular (JV), portal (PV) and hepatic (HV) veins as determined by HPLC assay and in the jugular and portal veins by ^{14}C radioactivity method after a single oral dose (10 mg/kg) administration to dog R113.

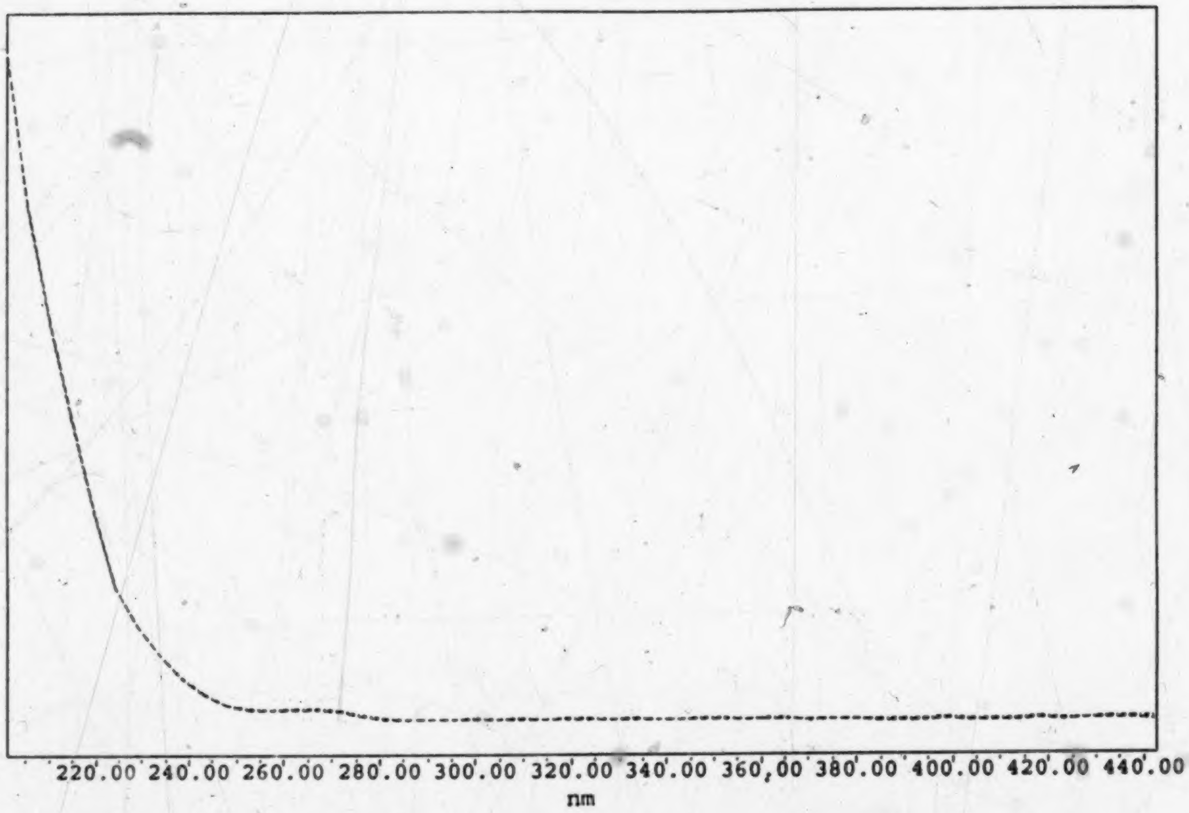

Figure 3.15 A typical diagram showing that UV spectrum (200 - 450 nm) of LD peak in a jugular venous blood sample (......) taken after a single oral dose of LD (10 mg/kg) is superimposable to that of authentic LD (----). These spectra are extracted at peak maxima.

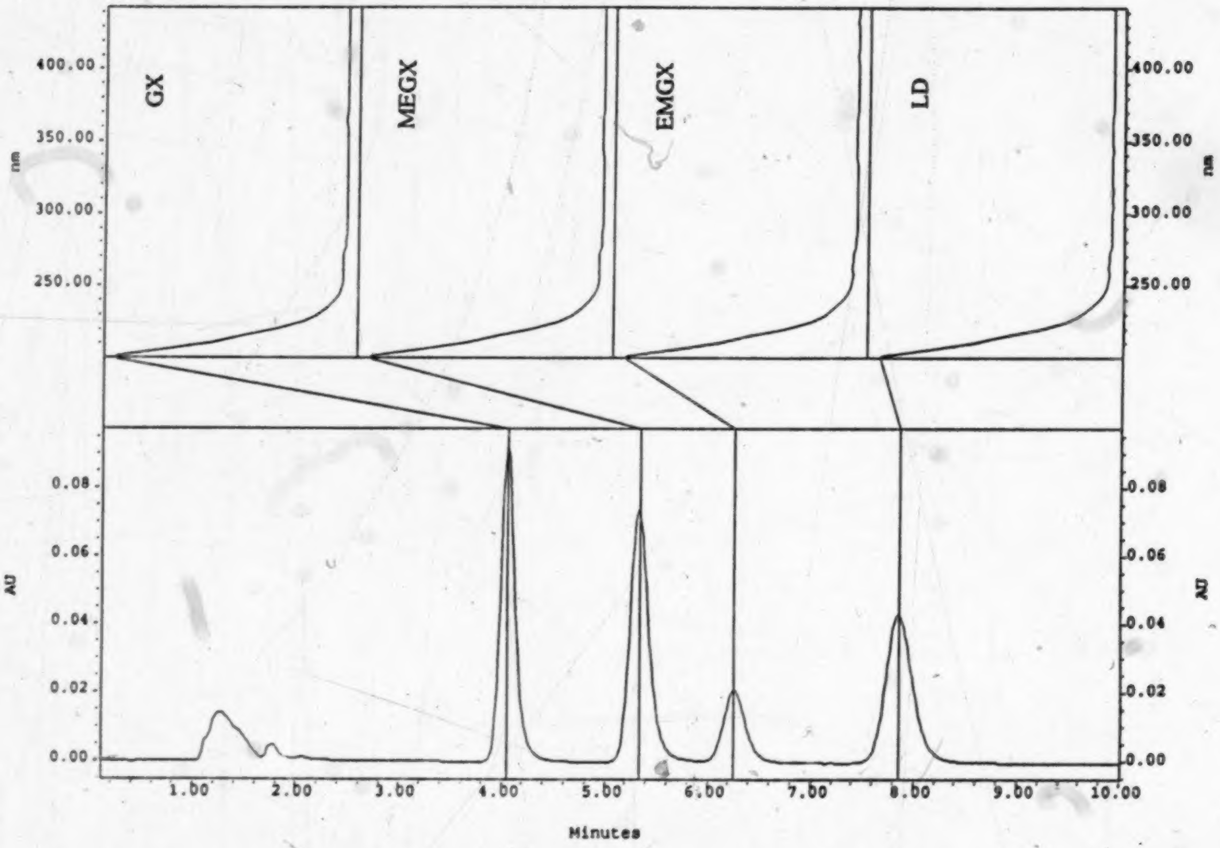

Figure 3.16 A typical chromatogram of blank plasma spiked with authentic LD, MEGX, GX and internal standard (EMGX) with their corresponding UV spectra shown in the upper panel.

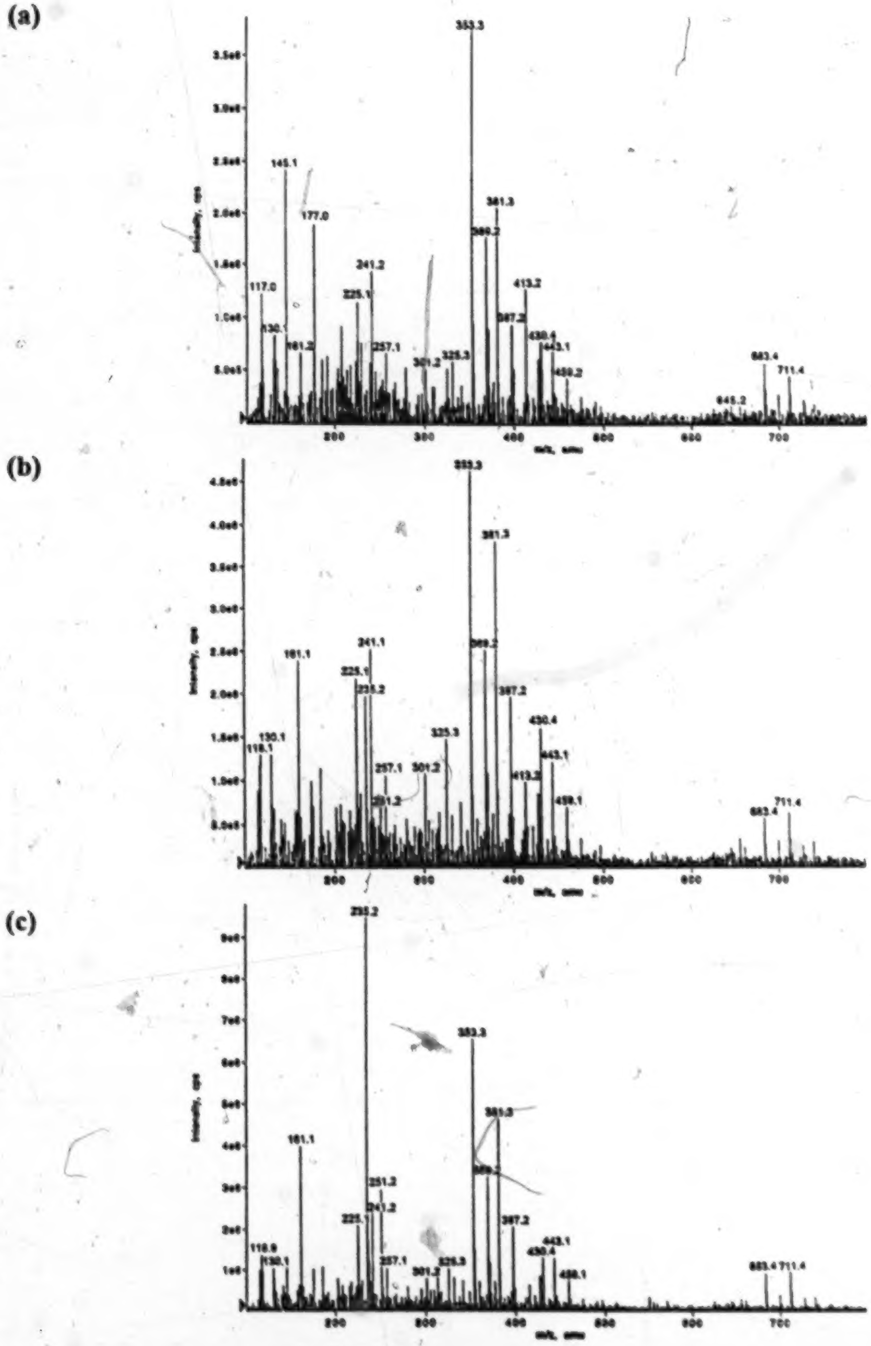

Figure 3.17 Representative mass spectra of (a) system control sample, (b) blank blood and (c) blood sample taken from the jugular vein at 60 min after administration of a single oral dose 10 mg/kg to dog T8.

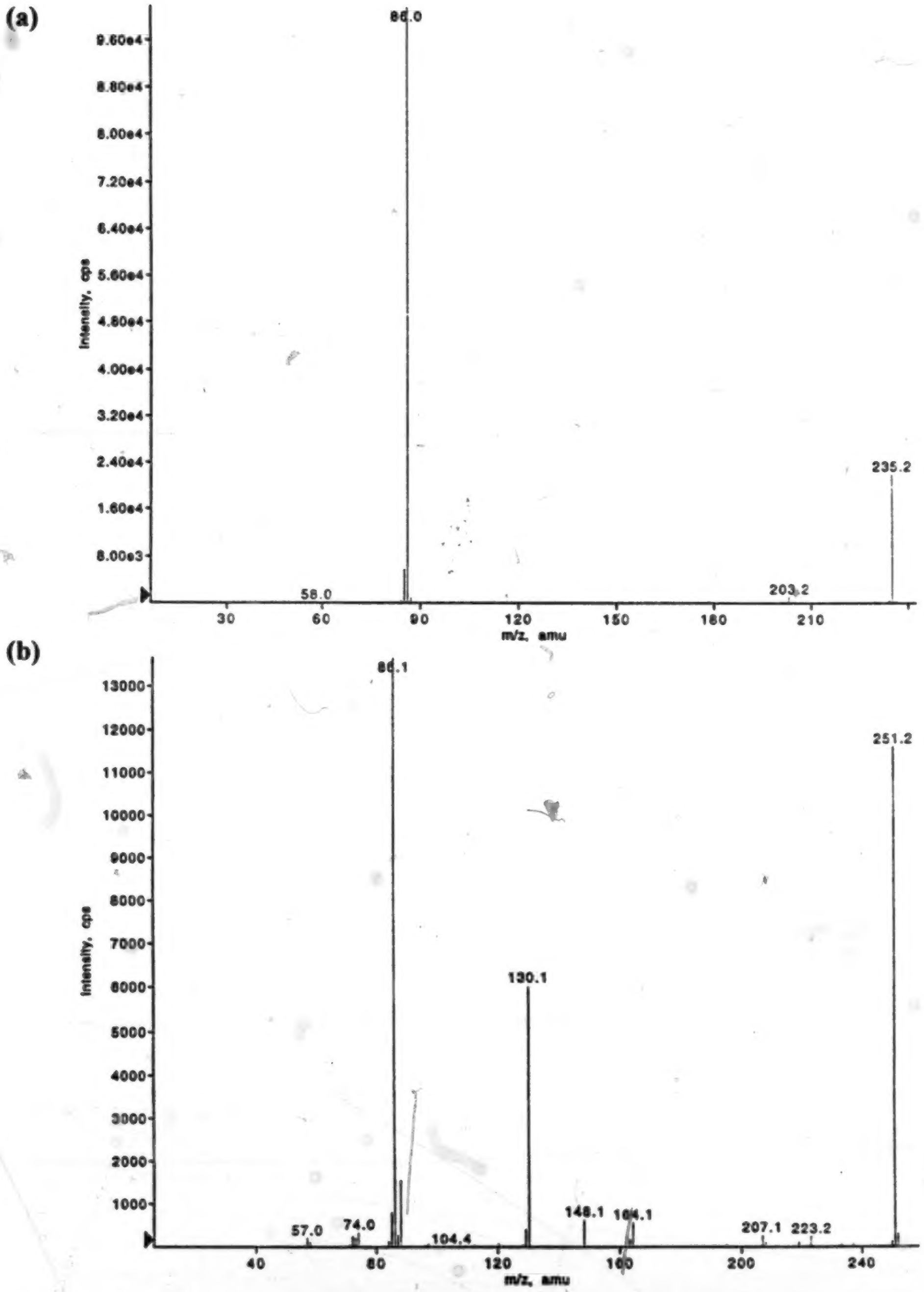

Figure 3.18 (a) Mass spectrum of authentic LD showing molecular ion ((MH^+)) of *m/z* 235 and its fragmentation ion of *m/z* 86. (b) The $(MH+16)^+$ ion (*m/z* 251) in Figure 3.16c was selected for fragmentation, which yields the diagnostic ion of *m/z* 86.

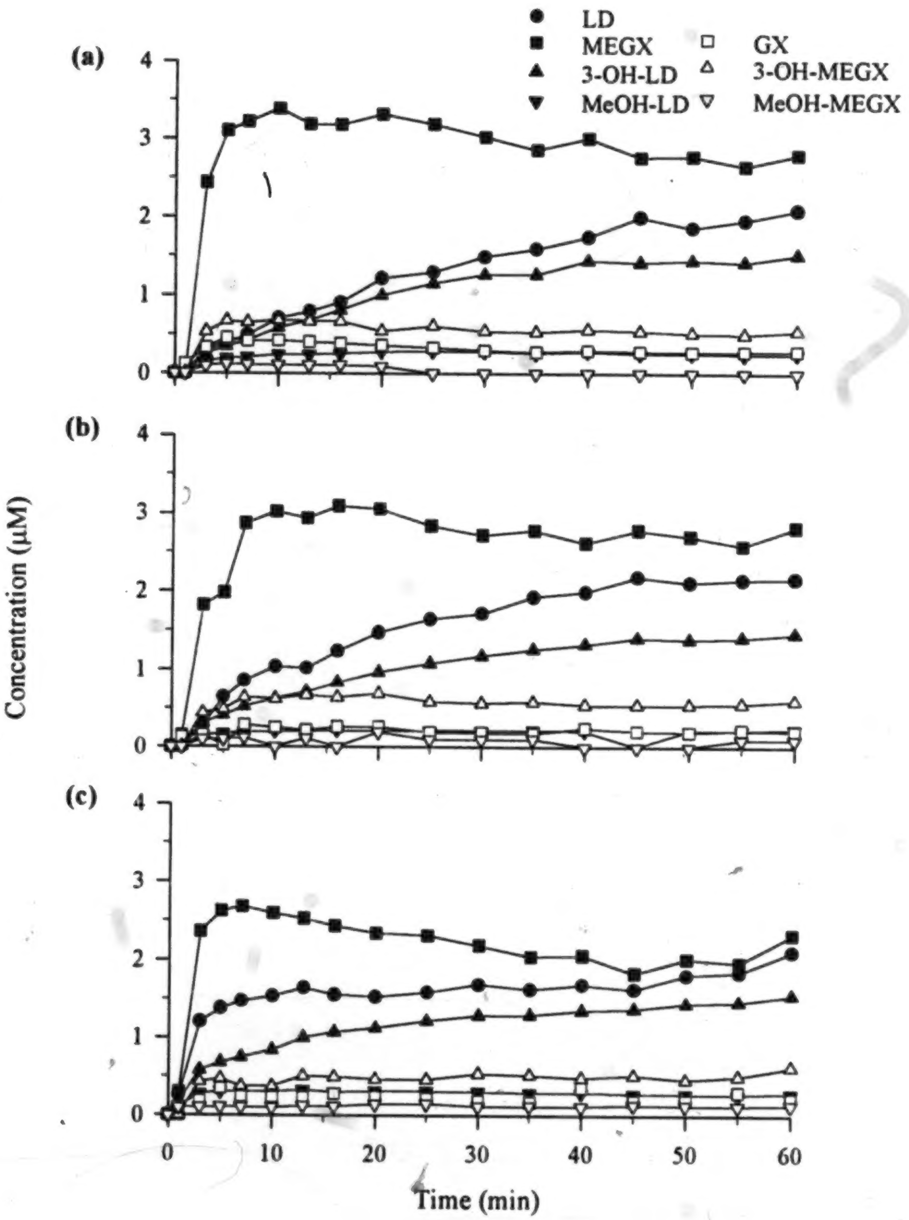

Figure 3.19 **Representative concentration *vs* time profiles of LD and its metabolites in the effluent of isolated perfused rat livers. (a) Diethyl ether anesthesia (C_{in} = 17.3 µM, T_{ss} = 45 min); (b) methoxyflurane anesthesia (C_{in} = 14.9 µM, T_{ss} = 30 min); and (c) sodium pentobarbital anesthesia (C_{in} = 15.2 µM, T_{ss} = 30 min).**

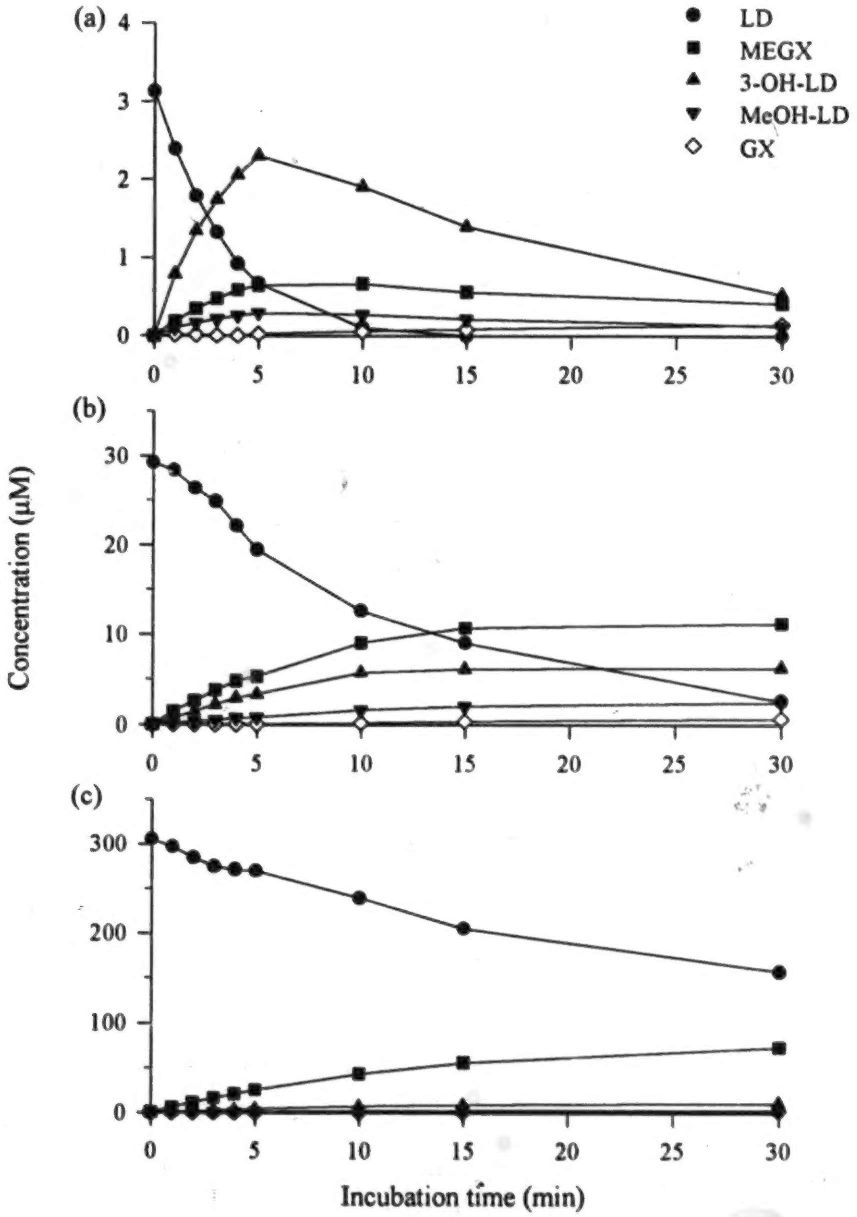

Figure 3.20 **Time courses of *in vitro* LD metabolism in rat liver microsomes. The disappearance of LD and formation of its metabolites during incubation at substrate concentrations of (a) 3 µM, (b) 30 µM and (c) 300 µM are plotted against incubation time. Each data point represents mean value of two separate determinations.**

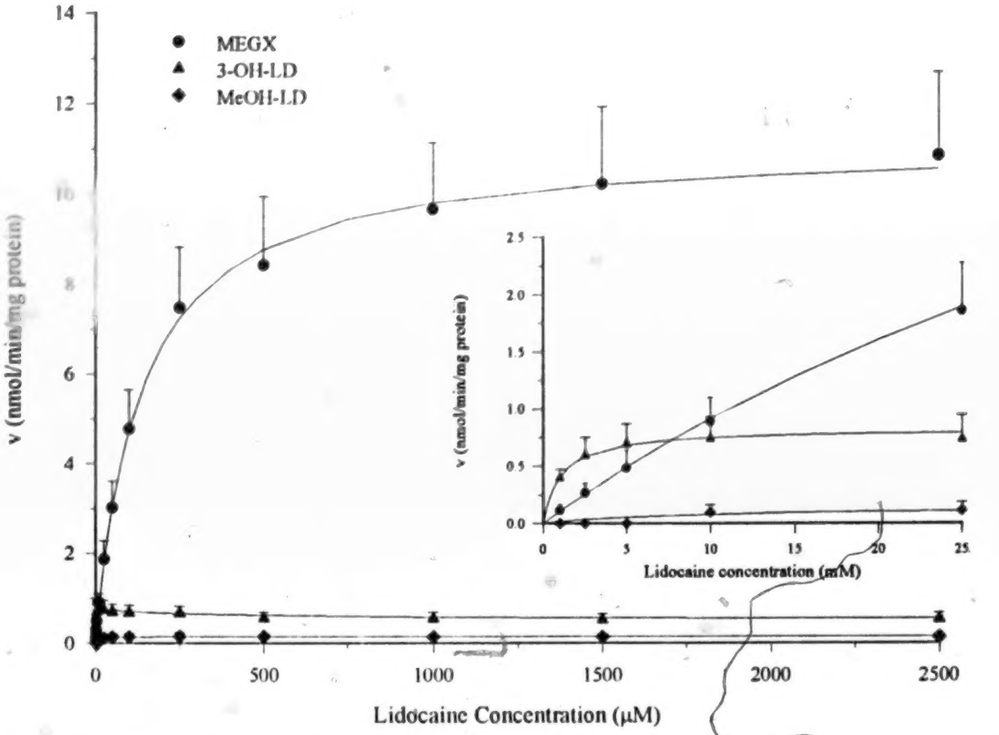

Figure 3.21 Effect of substrate concentration on the rates of N-dealkylation, 3-hydroxylation and arylmethyl hydroxylation of LD. LD (1 - 2500 μM) was incubated in the presence of NAPDH 1mM and rat liver microsomal protein 0.5 mg/mL in the final mixture. Inset shows rate of metabolite formation at low substrate concentrations (1 - 25 μM). Data represent mean (± SD) values for the control group (n = 5). Results for LD pretreated group are similarly described by Michaelis-Menten equation. The K_m and V_{max} values for each metabolic pathway for both control and LD pretreated groups are shown in Table 3.12.

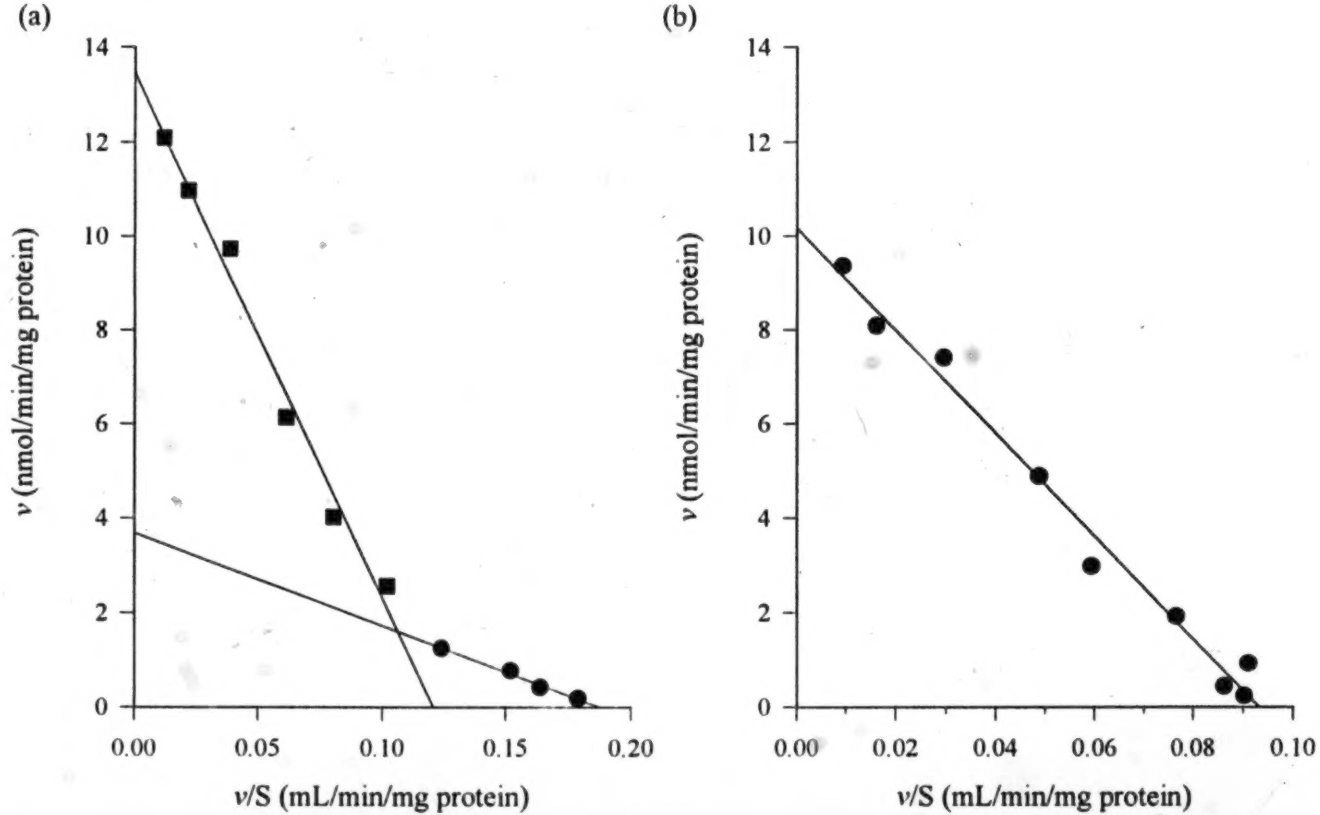

Figure 3.22 **Representative Eadie-Hofstee plots of MEGX formation showing heterogeneity of N-dealkylase activities in rat liver microsomes. N-dealkylation of LD is catalyzed by two enzymes in some rat liver microsomes (as indicated by biphasic slope in panel a) and by one enzyme in other rat liver microsomes (linear slope in panel b). Data presented in the graph are obtained from two individual rat liver microsomal preparations in the control group.**

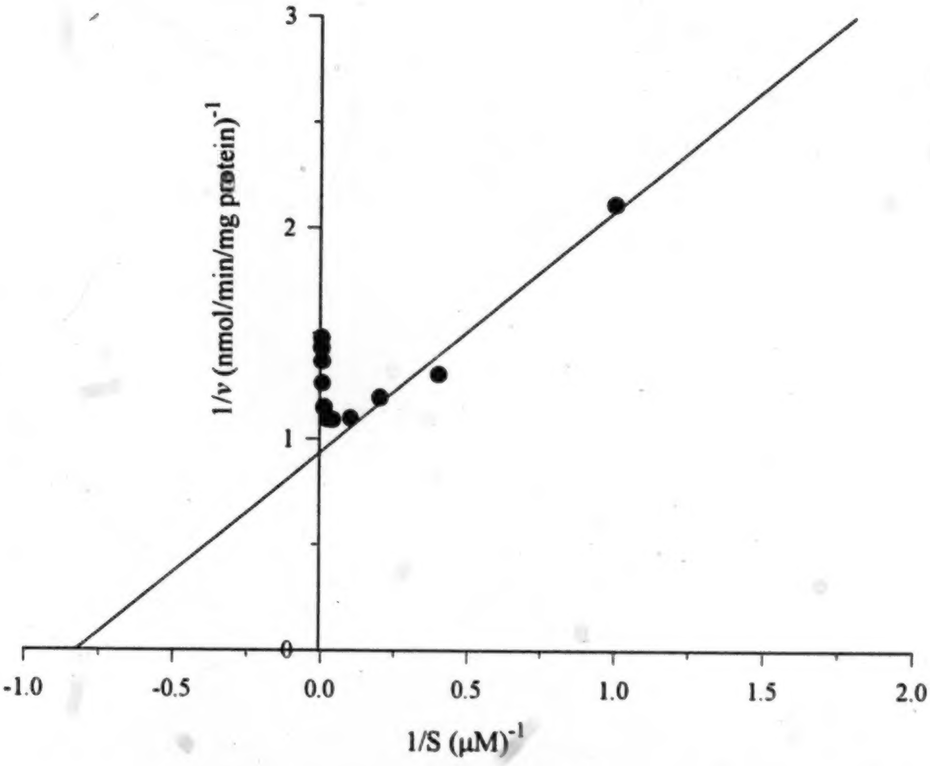

Figure 3.23 Deviation of 3-OH-LD formation rate (ν) from linearity. The upward turn in the Lineweaver-Burk plot as LD concentration increases (that is as 1/S approaches zero) is indicative of high substrate inhibition. Representative data obtained from one rat liver microsome of the control group is shown here and Michaelis-Menten plot of this set of data is shown in Figure 3.24a. The same nonlinearity in enzyme kinetics is observed consistently in all microsomes for both control and LD pretreated groups.

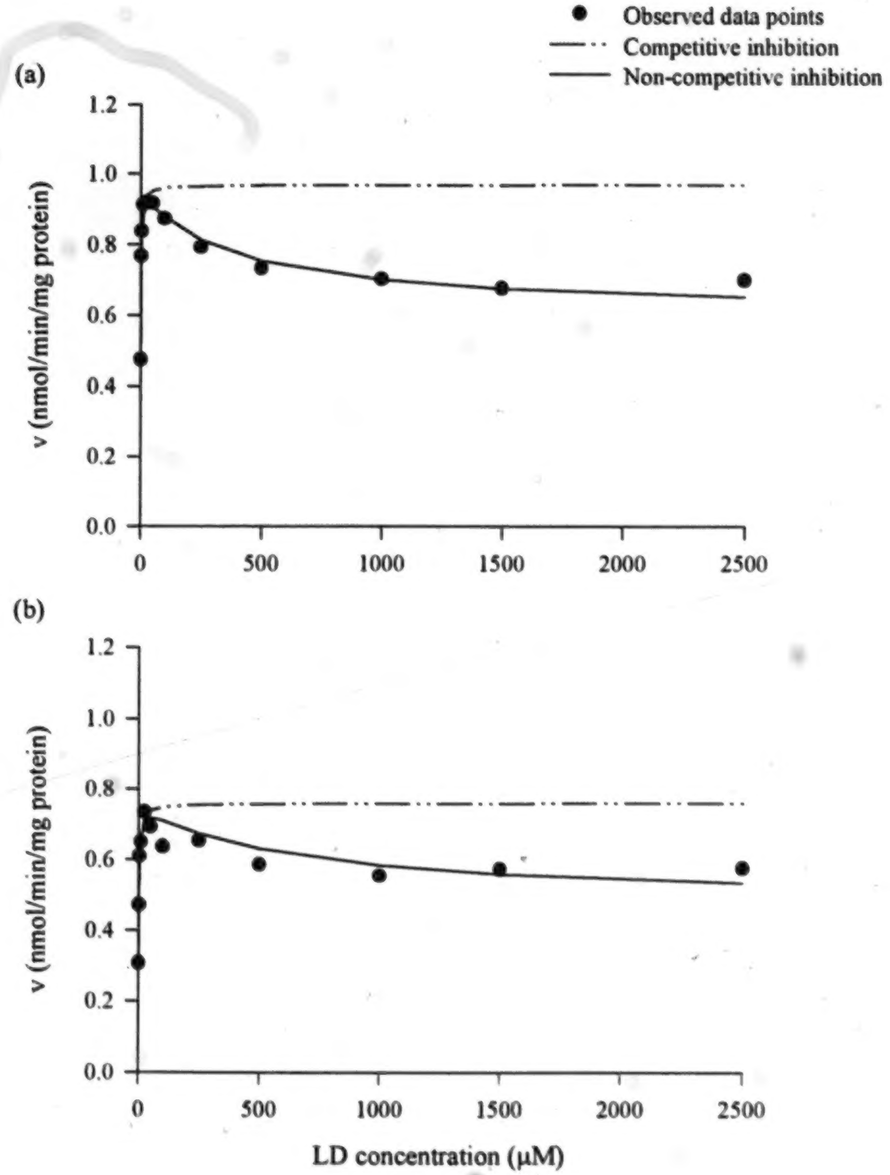

Figure 3.24 **Michaelis-Menten plots of concentration dependency of formation rate of 3-OH-LD when rat liver microsomes were incubated with various substrate concentrations (1-2500 μM). Computer simulation curves are generated assuming product inhibition by MEGX formed during incubation studies. Representative plots from the control group (panel a) and from LD pretreatment group (panel b) are shown.**

4. DISCUSSION

4.1 Evaluation of chronic instrumented dogs for pharmacokinetic studies of lidocaine

Our first objective is to assess the suitability of the chronically instrumented dog as an animal model for *in vivo* studies of LD disposition kinetics. Our data obtained in non-instrumented dogs (Table 3.1) were comparable to previously published data by other investigators — $t_{½}$, 45 - 91 min (59,138,239); Cl_p, 30 - 40 mL/min/kg (59,138,239); and V_{dss}, 2.18 L/kg (138). Mean values of these kinetic parameters (Table 3.1) were also in close agreement with those found in man (80 - 108 min; 10 - 17 mL/min/kg; and 0.6 - 2.0 L/kg respectively) (30), suggesting that dogs and humans share similar kinetics characteristics of LD. The higher clearance found in the dog when normalized to body weight could probably be related to a much greater hepatic blood flow per unit body weight in smaller species than in man (234).

Surgical instrumentation probably did not compromise the liver's ability to remove LD in our instrumented dogs. In the present study, no significant differences in the mean values of disposition kinetic parameters of LD could be detected between non-instrumented dogs and instrumented dogs (data obtained on day 1) (Table 3.1). In addition, liver function tests taken from instrumented dogs were within normal ranges. However, no definite conclusion could be drawn based on these data alone, since plasma clearance may not serve as a sensitive indicator of changes in Cl_{int} for highly extracted drugs when given intravenously (Table 3.3). Further supporting evidence is provided from studies using compounds which are almost completely removed by the liver and have a low to medium hepatic extraction ratio, such as ICG (159) and mibefradil (189). A lack of change in disposition kinetics of these two compounds after surgical implantation of catheters and flow probes is consistent with our postulation that liver functions are not compromised by surgical instrumentation.

In all dog studies, pharmacokinetic parameters were computed based on carotid artery plasma concentration profiles, rather than jugular venous data. The reason is a sampling-site related over-estimation of AUC. In our dogs, a jugular vein catheter is inserted *via* the right external jugular vein into superior vena cava with the tip being placed at the junction of the left and right external jugular vein. This location is in close proximity (a few centimeters) to the right and left axillary branches where the cephalic veins enter systemic bloodstream. When LD is given as a continuous infusion *via* the cephalic vein, insufficient mixing of the drug solution with blood could result in an erroneously high plasma LD levels and an underestimation of Cl_{sys}. We have observed an arterial-venous difference ($C_{JV} > C_{CA}$) as great as two-fold during a 12-h infusion. This difference was minimized when more complete mixing was allowed by changing the site of drug administration to a vein in the hind leg (n = 3; data not shown). Another pitfall is that blood collected from the jugular vein catheter is drained from the anterior part of the body where usually little elimination occurs. Drug concentrations measured at this site would be different from those obtained from posterior vena cava where blood emerging from eliminating organs such as liver and kidneys is well mixed with blood from non-eliminating tissues. This could also lead to an over-estimation of AUC values by up to 50% in our i.v. and oral dog studies. In a preliminary study, when the jugular vein catheter is placed inside the right atrium of a dog such that well mixed blood from the whole body could be sampled, the discrepancy between the arterial and venous plasma levels disappeared. Therefore, caution is needed to avoid erroneous conclusion of significant lung elimination of LD in our dogs.

4.2 Intravenous studies in dogs

Our second objective is to evaluate the effects of continuous LD infusion on hepatic blood flow, plasma protein binding, hepatic tissue uptake and metabolic activities and, in turn, the implications that these alterations have on the time-dependency reported in the literature (63,67,85,95,116,147-150). Biliary excretion is not considered because this process is negligible for LD (51). Any residual effects that might persist after cessation of infusion were assessed by pairwise comparison between the identical dose administrations on day 1 (baseline values) and day 10. With this approach, each dog serves as its own control.

Based on conventional kinetic parameters, there was no apparent evidence of a time-dependent changes in LD kinetics. Cl_H remained constant throughout the 12 h period of LD infusion and a steady state was attained in our dogs (Table 3.2). However, there is a trend that LD is capable of inducing an elevation in hepatic hemodynamics and causing a marked reduction in the intrinsic ability of the liver to remove drug with time of infusion when drug concentration or dose are invariant; a time-dependent phenomenon

(16). Due to the small sample size (n = 4) and the large variability, no statistically significant difference could be detected.

4.2.1 Hepatic blood flow

By the use of ultrasonic transit time flow probes, we have confirmed that hepatic blood flow is increased, but not decreased, during a 12-h LD infusion. The alterations in hepatic blood flow rates are clearly drug-related, but not due to diurnal variation. Evidence was provided by a preliminary study in which normal saline solution was infused at the same flow rate for 12 h to instrumented dogs (n = 2). Q_{HA}, Q_{PV} and Q_H were found to be stable throughout the whole time period. The increase in hepatic arterial and total hepatic blood flows is shared by other species including rhesus monkey (70) and man (155). These changes in hepatic blood flows are associated with a reduction in splanchnic vasculature resistance due to a local vasodilatation effect of LD. Increased cardiac output due to drug action at the central nervous system at higher plasma levels could partly contribute to the stimulatory effect of LD on splanchnic hemodynamics (155). Although we do not know whether LD evoked a change in cardiac output in our dogs, it seems to exert similar effects on the canine cardiovascular system (161). We observed an average of 26% increase in mean Q_H values at mean steady state plasma level of 10.3 μM in our dogs. This is consistent with Wiklund's findings of an increase in total hepatic blood flow by 37% at plasma concentration of 10.2 μM in man (155). An increase in Q_H alone should in theory lead to a corresponding increase in Cl_H and a lower than predicted steady state plasma level for a highly cleared drug such as LD (equation 2.12). Thus, it is unlikely that

LD-induced changes in hepatic blood flow rate during infusion could explain the time-dependent reduction in LD clearance reported in the literature.

4.2.2 Hepatic intrinsic clearance

Despite a lack of change in Cl_H during infusion, our data clearly demonstrated that the intrinsic ability of the liver to remove LD was greatly impaired in our dogs. This is indicated by a progressive drop in Cl_{int} and E_H values and a corresponding increase in F_H values. At the end of the 12-h infusion, the estimated Cl_{int} values were 3 - 9% of the corresponding values at on day 1. A similar time-dependent phenomenon in E_H and Cl_{int} was observed in a dog study by LeLorier *et al.* (152). At the end of a 24-h LD infusion, E_H and estimated Cl_{int} were significantly reduced to 32% and to 15% of the 90-min infusion group respectively (152).

4.2.2.1 Plasma protein binding

Perturbation in drug binding to plasma proteins is an unlikely cause of the reduction in Cl_{int} values following single dose administration on day 1 and day 10. Cl_{int} were estimated based on total (free and bound) LD concentration. Estimation of intrinsic clearance of free drug is confounded by nonlinear plasma protein binding of LD as its plasma level was declining with time after a single i.v. dose injection. Nonetheless, free fraction values measured in plasma samples matched for total LD concentration were similar on day 1 and day 10 (Figure 3.6). No significant difference could be detected for the slopes of the least-square regression lines ($p = 0.285$). Hence, the reduction in Cl_{int} of total drug reflects a true impairment in the intrinsic ability of the liver to remove free drug. This coincides with other investigators' viewpoint that factors other than an enhancement in LD plasma protein binding caused by an increased AAG levels would be held responsible for time-dependent reduction in LD clearance (63,123,150,151).

4.2.2.2 Hepatic tissue binding

Irreversible binding in the liver has been proposed to be responsible for time-related changes in hepatic clearance of LD (110,136). Using isolated rat hepatocytes and ^{14}C-labeled LD, Chen *et al.* (172) found that hepatic tissue binding is a capacity-limited process. At low LD concentration (0.3 μM) in the media, 31% of radioactivity was irreversibly bound in the cellular debris whereas 56% was readily displaced from binding sites (172). Our data provide some evidence of both reversible and irreversible binding. LD and its metabolites are strongly retained in the liver, as denoted by a net uptake of approximately 56.5 or 43.9 nmol/g liver on day 1 and day 10 respectively. Most of the amounts of LD and its metabolites retained in the liver could eventually be displaced from the binding sites with approximately 12.4 nmol/g liver irreversibly bound in dog livers. This value was in close approximation with that observed previously in isolated perfused rat liver (approximately 6.9 nmol LD/g liver) by Saville (197), with the consideration of species difference. Saville (197) found that of the total amount of ^{14}C-labeled material bound to liver tissue, only 2.9 ± 0.9% was bound to liver proteins. Restricted by the present experimental setup, it was impossible to deduce whether the binding sites were proteins or other cellular components. Nevertheless, the difference of 12.4 nmol/g liver represents a decrease of ~25% in the extent of hepatic uptake process. However, the extent of reduction in Cl_{int} values on day 10 (~79% on average) was far greater. Thus, hepatic tissue binding could not be the sole explanation for time-dependent reduction in Cl_{int} of LD.

4.2.2.3 Hepatic metabolism

The elevation in plasma MEGX levels on day 10 despite the fact that the same dose of LD was administered provides evidence that metabolic activities are probably altered after a course of LD infusion. This agrees with the findings of Barchowsky *et al.* (83), who reported a significant increase in the ratio of MEGX to LD plasma concentration at the end of prolonged LD infusion (36 - 72 h). Two possibilities could occur — either the rate of elimination of MEGX was reduced or the rate of its formation was enhanced. A substantial reduction in the mean AUC values of ratio of GX to MEGX suggested that N-dealkylation of MEGX might be inhibited. However, the N-dealkylation process is a minor pathway of MEGX elimination (107). Other important pathways such as amide hydrolysis might also be inhibited. On the other hand, it is unlikely that N-dealkylation of LD to MEGX was enhanced. This is supported by a marked reduction in mean Cl_{int} values and an increase in AUC values of LD in the hepatic vein in all dogs on day 10; both indicate that LD elimination was actually impaired. The fact that Cl_{int} values of LD remained low on day 10, even though LD and its metabolites were present in negligible quantities before drug administration, indicated that mechanism(s) other than product inhibition might also be responsible. Nevertheless, the metabolic capacity for LD transformation was large, as reflected by a mean Cl_{int} value being ~55-fold higher than that of Q_H (day 1, Table 3.3). Despite the loss of enzyme activities that might be incurred by LD infusion, Cl_{int} values were still several times greater than Q_H (day 10, Table 3.3). This suggests that the rate limiting step of LD elimination was in the rate of drug delivery and, consequently, alterations in enzymatic activities were not obvious from plasma concentration profiles of LD in the carotid artery.

4.2.2.4 Cumulative exposure

Although the exact mechanism responsible for the impairment of the hepatic elimination activity is unknown, it is unlikely to be a concentration-dependent process since Cl_{int} was altered despite similar drug concentration profiles on day 1 and day 10. On the other hand, the impairment elicited by LD infusion did not fully revert to normal 36 h after the termination of infusion; Cl_{int} values on day 10 were 9 - 75% of day 1 values. The fact that a previous exposure to a high dose treatment would attenuate metabolic clearance during subsequent drug administration seems to agree with the postulation of enzyme inactivation (240) and has been applied to explain the underestimation of LD and propranolol steady state levels when infusion rate is switched from a high to low rate (190,241). Propranolol is capable of forming a metabolic intermediate which is irreversibly bound to enzymes both *in vivo* and *in vitro* (242,243), resulting in inhibition of propranolol metabolism and interactions with other drugs. After pretreatment of rats with labeled propranolol, time course of bound radioactivity showed a decline phase with a half-life of 45 h (243). It is conceivable that low level of metabolic capacity would persist even after the discontinuation of drug administration. *In vitro* irreversible binding of LD or its metabolites to hepatocellular components has been demonstrated in rat liver microsomes (242,244,245). Similar observations were found with rat and dog hepatic microsomes in preliminary studies in our laboratory (data not shown). ^{14}C-labeled material (that is, LD or its metabolic intermediates) was retained in microsomal pellet despite an exhaustive extraction procedure with methanol and ether (243). *In vivo* tight binding could be implicated by the reduction in the net amount of ^{14}C radioactivity retained in hepatic tissue following single i.v. LD injection after a 12-h infusion.

Gray and his colleagues (173,240) have developed pharmacokinetic methods for analyzing time-dependent kinetics of drugs which undergo enzyme inactivation. For LD, a partial enzyme inactivation has been linked to N-dealkylation pathway and the overall enzyme activity is exponentially dependent on the cumulative extent of contact of the enzyme with the drug. The latter is a function of both time and dosing rate of an infusion. An inverse relationship between Cl_{int}, an indicator of overall metabolic activity, and cumulative dose (dosing rate × infusion time) is illustrated in Figure 4.1. The dependency of metabolic activities on cumulative exposure of hepatic enzymes to LD could be applied to explain the apparent contradictory findings between our study and that of LeLorier *et al.*. For instance, the use of a high loading dose (20 mg/kg) and a high infusion rate (140 µg/min/kg) of LD allows LeLorier *et al.* (152) to achieve a significant reduction in hepatic intrinsic clearance to a similar level as in our dogs within a shorter time period (90 min in their study as oppose to 6 h in our study). When cumulative exposure increased as infusion continued for 24 h in the LeLorier *et al.* (152) study, Cl_{int} was reduced to 15 - 24 mL/min/kg and LD became a low extraction drug (0.26). It was at this point that LeLorier *et al.* (152) found that total body clearance was reduced to half and $t_{½}$ was doubled. The reason that we did not observe a change in Cl_H at the end of a 12-h infusion is probably due to an insufficient cumulative exposure of our dogs to LD.

4.2.3 Implication

In this study, the dosage regimens in both the 5-min and the 12-h infusion studies were chosen to achieve plasma levels that are within the therapeutic window in a human clinical situation. One may argue that the dog is not a good model since a time-dependent reduction in LD clearance was not obvious and the mean E_H value obtained on day 1 was much higher in our experimental dogs (0.97 ± 0.018) than has been reported for human (0.6 - 0.8). However, our findings point out that a loss of Cl_{int} induced by LD infusion might be masked in subjects with a high E_H. Besides, potential drug interactions might occur with drugs, which are extensively biotransformed *via* the impaired metabolic pathways, even though LD is completely cleared from the body.

4.3 Oral studies in dogs

For drugs which exihibit significant hepatic first-pass effect, oral dosage is usually much larger than the size of i.v. dose in order to achieve similar drug concentrations in systemic circulation. Therefore, following single oral dose, the cumulative extent of contact of hepatic enzymes to drug might be sufficiently great such that intrinsic ability of the liver to remove drug is significantly impaired. Our third objective is to explore the effect of oral administration on time-dependent kinetics of a drug. As illustrated in Figure 4.2, our data show that a single oral dose of LD (day 1) causes a marked reduction in Cl_{int} to a level similar to that obtained during i.v. infusion when equivalent cumulative hepatic influx is achieved. This confirms that impairment of drug elimination is not solely related to time, but primarily to the cumulative exposure of hepatic enzymes to drug. Contrary to the large intersubject variability observed on day 1 during the i.v. studies, Cl_{int} values among individual dogs were in close agreement with each other (Figure 3.11). In addition, mean Cl_{int} values of LD and AUCs of MEGX were similar upon repeated oral dosing on days 1 and 10. These findings suggest that metabolic activities responsible for their elimination might have been compromised after the first oral dose. Therefore, it is possible that nonlinear kinetics of LD would not be apparent if a multiple oral dosing regimen were to be given instead of i.v. infusion.

4.4 Nonlinear blood-to-plasma ratio

A time- and sampling site-dependency of C_b/C_p for LD was observed following oral administration, as oppose to a constant value of approximately 0.9 following a single i.v. dose injection. The latter value agrees well with values of 0.8 to 0.9 reported in the literature (21,61,62,80,83,93,94). However, no information about C_b/C_p values attained upon oral administration of LD is available. To our knowledge, there is no documentation about nonlinear behavior of LD distribution in blood in the literature. Our fourth objective is to investigate if the phenomenon is due to an artifact which arises during experiment and to verify the identity of LD peak measured by HPLC assay.

We have found that changes in C_b/C_p following a single oral dose of LD could not be explained by artifacts arising during sample collection and analysis procedures. Reasons are: 1) Although there were some differences in lag time between blood sampling and centrifugation, we have shown that post-sampling redistribution of LD in blood did not occur even when blood samples were allowed to stand at room temperature for up to 24 h. 2) All blood and plasma samples taken after each dose administration were extracted, together with standard samples freshly prepared every time, according to the same extraction procedures for both i.v. and oral samples. 3) Standard curve prepared using plasma and blood as biological media gives similar peak responses with less than 10% deviation (data not shown).

The discrepancy between HPLC and ^{14}C radioactivity measurements of C_b/C_p ratio (Figure 3.14) seems to suggest that the unusually large C_b/C_p values after oral dosing is of *in vivo* origin. One possible explanation is that the formation of a metabolite which becomes significant due to first-pass metabolism when drug is administered orally and that this metabolite preferentially distributes inside red blood cells. For instance, about 5% of a single dose of chlorpromazine, a phenothiazine with a tertiary amine, was recovered as N-hydroxynorchlorpromazine in erythrocytes but only as 0.5% of the dose in plasma in man. This metabolite was retained in erythrocytes thirteen days after dose administration when the drug and other metabolites were cleared from plasma (246). It is possible that N-dealkylated metabolites (MEGX and GX) undergoes metabolic N-oxidation at the basic nitrogen yielding hydroxylamines, which are reactive nucleophiles and are capable of strong binding to red blood cell components as nitroso derivatives (247). However, our results from mass spectrometry analysis did not support this postulation, since molecular ions of these hydroxylamines (*m/z* 223, 195) were not detected in blood samples.

On the other hand, the presence of a prominent $(MH+16)^+$ ion (*m/z* 251) suggests the addition of an oxygen atom to the parent drug. Enzymatic monooxygenation could potentially take place at various sites of a LD molecule. Metabolic C-oxidation can take place at aromatic ring and arylmethyl group; however, these metabolites could be readily separated by our HPLC method. Mather and Thomas (20) have proposed that N-hydroxylation of xylidide nitrogen may occur to a significant extent, as evident by a 10 - 20% urinary recoveries of a dose as amide-hydroxy metabolites of LD and MEGX. However, the importance of this pathway is refuted by Nelson *et al.* (248) who concluded from a detailed evaluation that these metabolites represented only negligible amounts of a LD dose. Another likely location is the basic nitrogen of the glycine moiety. N-oxidation of tertiary amines is mediated by two enzyme systems: flavin-containing monooxygenase and CYP, both present in liver microsomes (249-251). Although *in vitro* LD N-oxide formation in rat liver microsomes has been reported (104), no *in vivo* data are available in the literature. Even if LD N-oxide is formed in an intact animal, it is not readily detected in systemic circulation due to its rapid elimination by renal excretion (252) and by metabolic reduction; the latter of which is partly mediated by CYP (250,253-255) in liver microsomal fraction, N-oxide reductase in mitochrondria (256) and aldehyde oxidase in liver cytosol (257). Non-enzymatic formation of N-oxide due to interactions of LD with chemical reagents during our sample extraction procedures is unlikely. Moreover, this metabolite will be more polar than the parent compound and would be expected to elute closer to solvent front under reversed-phase HPLC condition. Thus, N-oxidation of LD could not explain the high C_b/C_p ratio in our dog samples. It is possible that *m/z* 251 ion might be generated during mass spectrometry analysis, as suggested by the occurrence of several clusters of ions which differ by 16 mass unit. Nevertheless, it could be inferred from the close agreement between the ratio of m/z 235 ion abundance in blood sample to that in plasma and C_b/C_p determined by HPLC method that LD blood concentration determined by our HPLC method is real.

Drug concentration inside red blood cells is then computed using whole blood and plasma concentration profiles obtained in section *3.4.2*, according to equation 2.13. As shown in Figure 4.3, time course of LD in whole blood parallels that in red blood cells whereas LD elimination from plasma occurs more rapidly. This observation is common to all four blood vessels, although only the profiles in the portal and hepatic veins are shown for illustration. Apparently, there is a slow release of LD from erythrocytes into plasma. There are *in vitro* evidence in the literature that LD is rapidly distributed into erythrocytes (< 30s) and uptake is not saturable at concentration less than 600 μM (92). Inside the cell, approximately 15% of LD is incorporated in the inner lipid layer of cell membrane and 61% exists as free form in cytoplasm; the remaining 24% is unexplained (258). Most of the intracellular LD are removable when LD-loaded erythrocytes were dialyzed against drug-free buffer solution (92). However, there is a trend towards increased association of drug molecules with erythrocytes as total drug concentration decreases (80,92), suggesting some kind of drug adsorption or binding in erythrocytes. Although changes in plasma protein binding due to an elevated AAG level (83) or saturation of plasma protein binding sites (80) could shift the equilibrium of drug distribution in blood, the resultant changes in C_b/C_p values are usually modest (0.7 to 1.2) (80,92). Besides, no correlation between C_b/C_p values and free fractions in our dog plasma samples could be made. The reason for the unexpectedly high accumulation of LD in erythrocytes only after oral, but not i.v., administration is not understood.

4.4.1 Implications of nonlinear drug distribution in blood on pharmacokinetic analysis

In pharmacokinetics, it is generally assumed that distribution equilibrium of a drug between erythrocytes and plasma is instantaneous. There is, however, ample evidence in the literature that this assumption may not hold true. The role of red blood cell binding in first-pass effect, hepatic and renal clearance of low and high extraction ratio drugs has been investigated for drugs such as acetazolamide (8,259), methazolamide (260), chlorthalidone (7), hydrochlorothiazide (261), doxorubicin (10), propranolol (262), cyclosporin A (9) and tacrolimus (263). When drug efflux from erythrocytes into plasma (in terms of a few minutes) is much slower than mean transit time of blood through eliminating organs (a few seconds), erythrocytes may act as a barrier to drug elimination. In this case, it may be more appropriate to regard free drug concentration in plasma as the true driving force for drug elimination (261), whereas erythrocytes may be viewed as a tissue compartment (7). The use of whole blood concentration and blood flow would lead to an under-estimation of true hepatic intrinsic clearance. The degree of discrepancy between kinetic parameters computed using blood and plasma data depends on fractional efflux of drug from erythrocytes during each passage of blood through the liver and on concentration-dependent binding to erythrocytic components (263). In a preliminary study, we have compared kinetic parameters of LD calculated based on blood and plasma data, assuming that no drug efflux occurs during each hepatic transit. The greatest difference is observed for Cl_{int}; estimated value based on plasma data is 1.9-fold greater than when blood data is used. Deviations in estimated values of E_H, F_H and Cl_H based on plasma data are +37%, -57% and -18% of those based on blood data respectively. Due to the nonlinear behavior of C_b/C_p after oral LD administration (Figures 3.12 and 3.14), pharmacokinetic parameters were computed using plasma concentrations and hepatic plasma flow to allow qualitative comparison between oral and i.v. data. Characterization of red blood cell binding process and equilibration rate of LD between red blood cells and plasma would help to understand the role of this nonlinear behavior on LD pharmacokinetics.

4.5 Effects of anesthetic regimens on lidocaine metabolism

In this study, we aim to evaluate potential residual effects of a brief exposure to diethyl ether, methoxyflurane and sodium pentobarbital anesthesia on the rate and extent of LD metabolism in subsequent isolated rat liver perfusion and microsomal studies. The inclusion of a control group using euthanasia methods such as decapitation and cervical dislocation is not feasible, because re-establishment of oxygen and energy supply to hepatocytes could not be achieved instantly and the viability of livers so prepared would be severely compromised.

Consistent with previously reported findings (144), the time for LD to reach steady state is much delayed than that predicted based on the mean residence time of the perfusate in the liver (3 - 5 min) (173). The existence of the characteristic "hump" in MEGX level is also obvious in the diethyl ether group (Figure 3.19a). These phenomena are not unique to rat livers which were exposed to ether anesthesia prior to their excision, since these profiles are reproducible in the methoxyflurane and pentobarbital groups (Figures 3.19b and c). A lack of difference in mean T_{ss} values among the three treatment groups implies that the extent of LD binding to liver proteins and tissues is not influenced by previous exposure to anesthetic agents.

Our findings strongly suggest that the overall ability of the isolated rat liver to eliminate LD is not differentially impaired by acute exposure to anesthetic agents, as indicated by comparable mean values of C_{out} at steady state, E_H, Cl_H, and Cl_{int} among the three treatment groups (Table 3.9). Moreover, these values agree with data reported by Tam *et al.* (144,192) and Ke *et al.* (264) who included diethyl ether anesthesia in their protocols and with the findings of Zaman *et al.* (265-267) who used methoxyflurane.

Steady-state recovery values (expressed as percentage of dose) reveal that, of all the oxidative pathways in the metabolism of LD, only aryl methyl hydroxylation shows a tendency to be selectively elevated by pentobarbital anesthesia (Table 3.10). In rat, aryl methyl hydroxylation of LD is catalyzed by CYP2B2 (107), an isozyme which is inducible by phenobarbital. Although it is not known how quickly the induction effect occurs, a 4.2-fold increase in synthesis of CYP enzymes was observed 6 hr after a single dose of phenobarbital (268). It is conceivable that CYP2B2 activity could be induced during short term exposure to pentobarbital. While enzyme induction by pentobarbital is likely, however, the result would have to be interpreted with caution because MeOH-MEGX levels are close to or below the quantitation limit of the HPLC assay.

By contrast, there is no differential influence of diethyl ether, methoxyflurane and sodium pentobarbital anesthesia on N-dealkylation and 3-hydroxylation of LD (Table 3.10). Hence, CYP2C11 (102,107) and CYP2D (108), the major isozymes catalyzing N-dealkylation and 3-hydroxylation of LD respectively in the rat, are not affected. Formation of MEGX in rat is also mediated by CYP2B1 and CYP1A2; the latter isozyme also catalyzes the formation of 3-OH-LD (102,107). Recently, Liu *et al.* (210) have demonstrated that acute diethyl ether anesthesia reduces total CYP contents and CYP1A and CYP2B activities in rat. However, since the relative contribution of CYP1A2 and 2B1 to LD metabolism in uninduced rat livers is unknown, it is not possible to deduce from these data whether these activities are altered by diethyl ether or not.

It is unlikely that brief exposure to the three anesthetic agents during liver harvest has any residual effects on conjugation reactions of LD metabolites (Table 3.10). According to the findings of Watkins and Klaassen (213), acute exposure to diethyl ether, methoxyflurane and sodium pentobarbital anesthesia causes a depletion of hepatic UDP-glucuronic acid content by 30 - 95%. If these anesthetic agents were to have residual effects on glucuronidation, then the amount of 3-OH-LD glucuronide formed would be significantly different among the three treatment groups.

At steady state, there remains approximately 30 - 40% of LD dose unaccounted for in all the treatment groups. This may be attributed to the possible existence of unknown metabolic pathways (144). If, however, there were any alterations in the activities of enzymes involved in these metabolic pathways, it would have been reflected in the levels of unchanged LD and/or its known metabolites.

4.6 Effect of pretreatment on lidocaine metabolism

LD is extensively metabolized by rat liver microsomes. Consistent with the literature (105,109,144), our data show that 3-hydroxylation pathway has the highest affinity and is readily saturable at low LD concentrations (< 5 μM). Our values of K_m (1.04 ± 0.16 μM) and V_{max} (0.83 ± 0.23 nmol/min/mg protein) are in close agreement with those reported by Suzuki *et al.* (1.78 ± 0.20 μM and 0.30 ± 0.04 nmol/min/mg protein respectively) (109) and by Kawai *et al.* (1.65 ± 0.03 μM and 0.29 ± 0.05 nmol/min/mg protein respectively) (105), despite the use of a different strain (Wistar rat). As LD concentrations increase, N-dealkylation pathway predominates and is not saturable at therapeutic concentrations. Most literature reported a single-enzyme system for MEGX kinetics; for instance, a mean K_m value of approximately 250 μM and mean V_{max} value of about 15 nmol/min/mg protein were reported by Nyberg *et al.* in male Sprague Dawley rats (113), 595 μM and 9.80 nmol/min/mg protein respectively in male Wistar rats by Suzuki *et al.* (109) and 245 μM and 21.7 nmol/min/mg protein respectively in Dark Agouti rats by Suzuki *et al.* (269). A single-component N-dealkylase is present in half of our rat liver microsomes, but, in the other half, there are two enzymes responsible for MEGX formation (Table 3.12). The latter agrees with Kawai *et al.* (105) who found that at least two enzymes were contributing to N-dealkylation of LD (K_{m1}: 34.4 μM and V_{max1}:

0.52 ± 0.33 nmol/min/mg protein *vs* K_{m2}: 736 μM and V_{max2}: 10.0 nmol/min/mg protein respectively). Hydroxylation at the arylmethyl carbon is a minor metabolic pathway of LD, since it has the lowest metabolic capacity. In contrast to our results, Suzuki *et al.* (269) found that there are at least two enzymes involved in this metabolic step. At substrate concentrations below 25 μM, the sum of formation rates of MEGX, 3-OH-LD and MeOH-LD is within ± 20% of the disappearance rate of LD. At higher substrate concentrations, it is difficult to obtain accurate measurement of substrate disappearance rate. An estimate of hepatic intrinsic clearance, calculated by summing V_{max}/K_m of the three pathways and multiplying by a scaling factor of microsomal protein content (mg per g liver) and liver weight for each rat, gives mean values of 155 ± 16 mL/min for the control group and 155 ± 62 mL/min for LD pretreatment group. These values are lower than the mean value of 295 ± 132 mL/min in the methoxyflurane group in the single-pass isolated rat liver perfusion studies (Table 3.9).

Previous studies using isolated rat livers showed that partial enzyme inactivation of N-dealkylase activities may contribute to time-dependent kinetics of LD. This is evident by a characteristic "hump" in MEGX level; that initial formation rate of MEGX was faster and slowly declined to a non-zero plateau level as enzyme inactivation, which is a slow process, is completed. Enzyme inactivation probably involves the generation of a reactive metabolic intermediate which subsequently forms tight binding to enzymes. In preliminary studies, we have demonstrated that incubation of rat liver microsomes with ^{14}C-labeled LD resulted in irreversible binding of ^{14}C-labeled material to microsomal proteins. This irreversible binding requires metabolic activation for generation of reactive intermediates, was evident by a marked diminution of binding when CYP activity was abolished in the absence of NADPH and oxygen, by heat denaturation of microsomal proteins and by inhibition by SKF-525A.

In this project, we attempted to identify particular metabolic pathway(s) and the CYP isozymes which are involved in enzyme inactivation and to quantify the change in enzyme kinetic parameters of each of LD metabolic pathways. The pretreatment protocol of Saville (197) was followed. If enzyme inactivation occurs, we would expect a reduction in enzyme kinetics in LD pretreated group. By contrast, K_m and V_{max} values determined in the present study were not different among rat liver microsomes isolated from control and LD-pretreated rats.

There are several possible explanations for the lack of drug pretreatment effect on metabolic activities. First, it is probable that a single dose of 10 mg/kg is not sufficient to generate substantial amounts of metabolic intermediate complexes with CYP isozymes. However, evidence in the literature has shown that single dose injection of tertiary amine compounds, which are capable of forming CYP complexes *in vitro*, is effective *in vivo*. For instance, approximately 30% of total CYP was complexed *in vivo* following a single dose of triacetyloleandomycin (186,270). In preliminary studies, we found that multiple dosing of LD (10 mg/kg) with 5 doses given every 12 h intravenously or intraperitoneally did not cause any significant changes in K_m and V_{max} as compared to single dose pretreatment by the corresponding route of administration (data not shown). In addition, Saville *et al.* (173) were able to demonstrate that, following the same pretreatment protocol, the characteristic MEGX hump disappeared and T_{ss} was significantly reduced to about 7 min during subsequent isolated rat liver perfusion studies. Therefore, pretreatment of rats with a single i.v. dose of LD seems to be effective in eliminating enzyme activities that are affected by complex formation.

Second, it is possible that significant regeneration of CYP isozymes occurs during the 24 h period between dosing and sacrifice of animals. Generally speaking, turnover of heme prosthetic group of CYP is faster than that of apoprotein moiety. In normal (uninduced) rats, the turnover half-lives of CYP heme and apoprotein moieties range from 7 to 19 h and 10 to 20 h respectively (271,272). The fate of complexed enzymes might be different; as evident by the fact that CYP metabolic-intermediate complexes persist in the liver for up to 15 days following *in vivo* pretreatment of macrolide antibiotics for three days (184). In another study, 31% of total CYP remains as complexed form 24 h after single treatment of rats with erythralosamine (186). Further support is provided by kinetic analysis done by Saville (197), who estimated that metabolic activities of CYP were impaired for about 35 days following single dose pretreatment of LD. The estimated half life for enzyme turnover was 25 days, as computed based on the rate of enzyme regeneration of 0.026 day^{-1}. Hence, recoveries of metabolic activities due to enzyme regeneration could not explain the lack of difference in enzyme kinetic parameters in our control and pretreatment groups.

Another possible reason is a lack of metabolic intermediate complex formation *in vivo* or destruction of the complex during microsomal preparation. For certain tertiary amines such as SKF 525A (273), imipramine (182,274), amitriptyline (182,274), propoxyphene (275), orphenadrine (180,181) and triacetyloleandomycin (185,186,270), formation of metabolic intermediate complexes occur *in vivo* when animals are treated with these agents. These complexes are sufficiently stable to survive various procedures during microsomal preparation and could subsequently be measured *in vitro*. On the other hand, metabolic intermediate complex formation from amphetamine derivatives such as norbenzphetamine has been demonstrated in isolated perfused rat livers (275). However, no such complex could be detected in hepatic microsomes prepared from rats following *in vivo* pretreatment with these compounds (275). The author explained this discrepancy by a lack of *in vivo* formation of complex, although this is not proven.

LD is similar to amphetamine compounds in that effects of *in vivo* pretreatment of rats with LD could not be demonstrated in subsequent *in vitro* studies using liver microsomes. Rather than a lack of *in vivo* formation, restoration of enzyme activities due to dissociation of the metabolic intermediate complex during microsomal preparation procedures is a plausible explanation for the lack of difference in enzyme kinetics between control and LD-pretreated liver microsomes. Saville *et al.* (173) have shown that *in vivo* pretreatment of rats with a single dose of LD was capable of inducing a change in enzyme activities and that this effect persisted during a subsequent *in vitro* isolated liver perfusion study. Their findings of a monotonic rise of MEGX level and a quick attainment of steady state of LD in isolated livers are consistent with the hypothesis of enzyme inactivation. The fact that formation of metabolic intermediate complex, if any, following *in vivo* pretreatment with LD could be demonstrated *in vitro* in isolated intact organ but not in microsomal fractions suggests that binding of metabolic intermediate to enzyme is not irreversible. Although different anesthetic agents were employed in the study by Saville *et* *al.* (173) and in the present study (diethyl ether and methoxyflurane anesthesia respectively), it is an unlikely explanation since we have shown that these two agents do not have differential influence on LD metabolism.

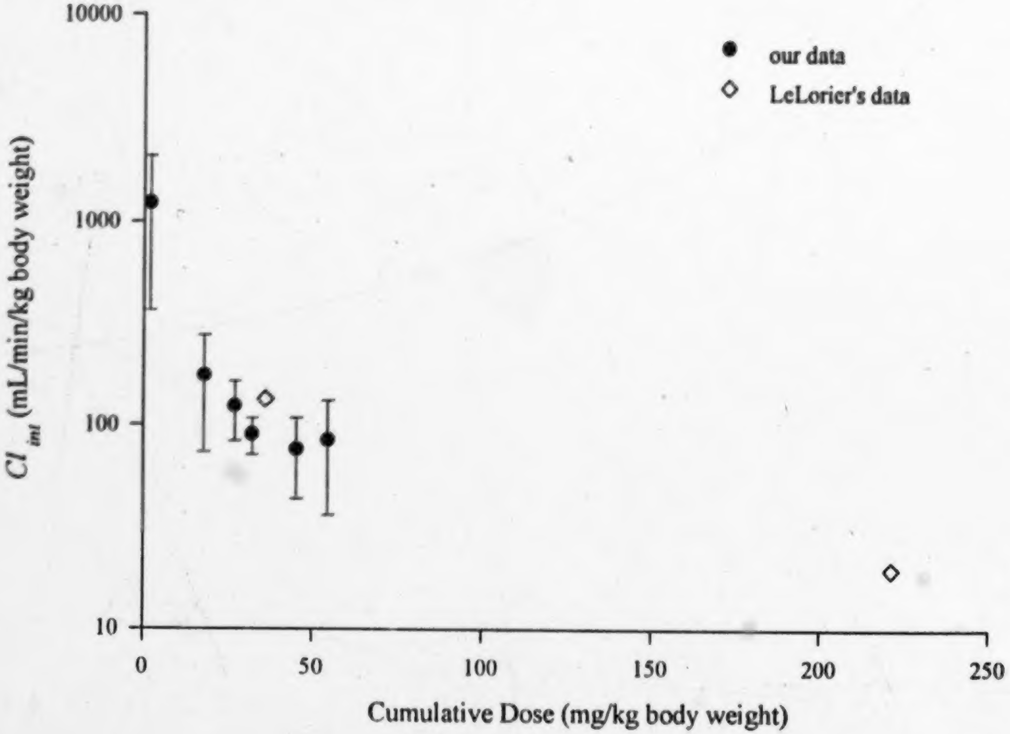

Figure 4.1 Effect of increasing cumulative dose (calculated by: infusion rate×hours of infusion) on hepatic intrinsic clearance. Cl_{int} values after the 5-min infusion of LD (2 mg/kg, day 1) and at various time points of the 12-h i.v. infusion in our instrumented dogs (n = 4) were plotted against cumulative dose. Mean Cl_{int} values estimated from the study reported by LeLorier *et al.* (152) for both the 90-min infusion and 24-h infusion groups were plotted for comparison with our findings.

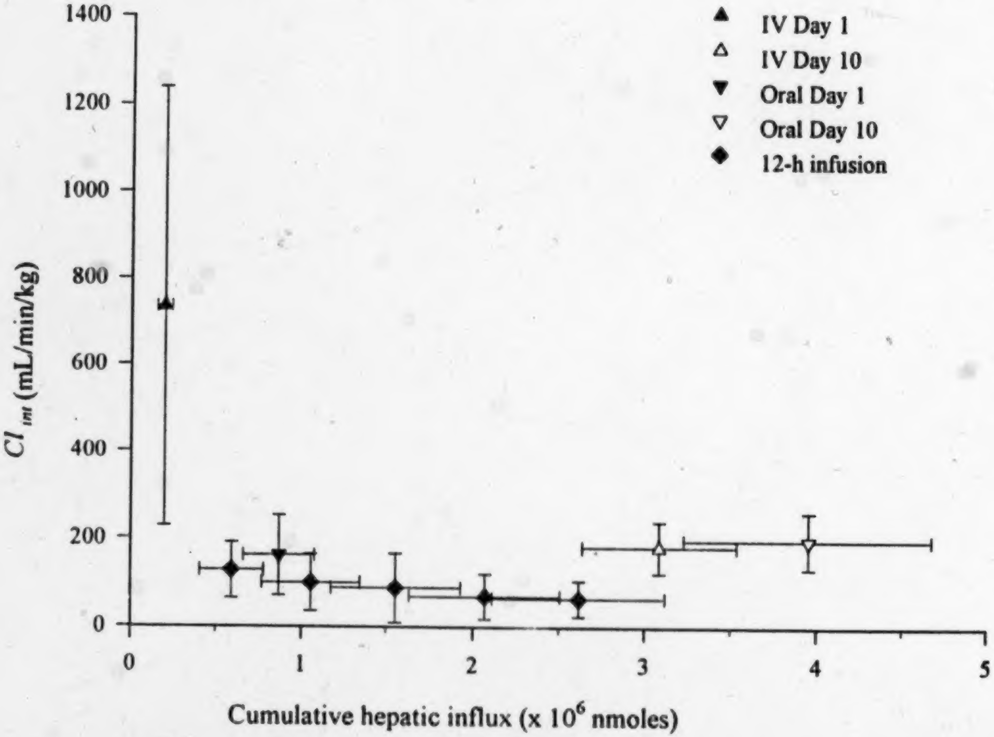

Figure 4.2 A plot of hepatic intrinsic clearance vs cumulative hepatic influx in instrumented dogs after LD administration (i.v. single dose 2 mg/kg; oral single dose 10 mg/kg and a 12-h i.v. infusion 75 μg/min/kg) (n=4 per group). Cl_{int} and cumulative flux were calculated using plasma concentration and hepatic plasma flow.

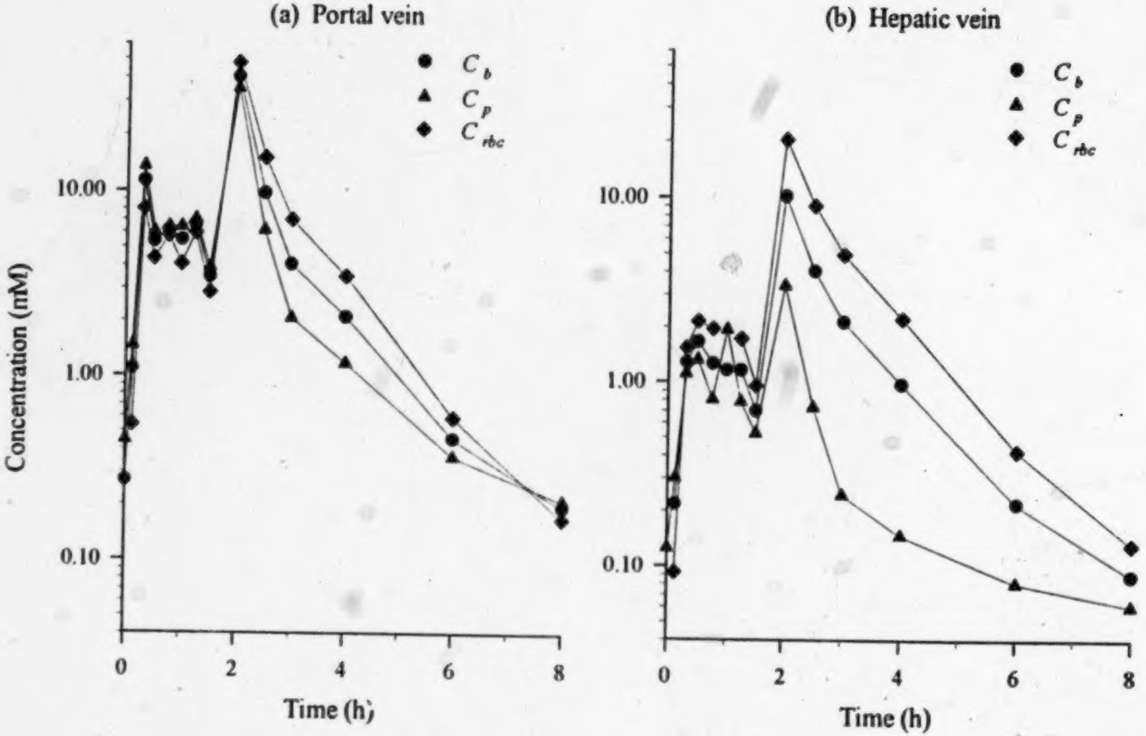

Figure 4.3 **Time courses of LD concentration in blood (C_b), plasma (C_p) and red blood cells (C_{rbc}) in (a) portal vein and (b) hepatic vein after a single oral dose (10 mg/kg) administration to one dog.**

5. SUMMARY AND CONCLUSIONS

Time-dependent kinetics of LD have been observed in humans who received a long-term i.v. infusion (> 12 h). Plasma LD concentrations continued to rise long after the predicted time to reach steady state based on single i.v. bolus data. Half-life was doubled as a result of a reduction in LD clearance. The current project was undertaken to evaluate alterations in hepatic blood flow, plasma protein binding, hepatic tissue uptake and metabolic activities as potential mechanisms responsible for the time-effect. These processes were assessed in an intact, conscious animal using chronically instrumented dog model.

During a constant rate i.v. infusion, a steady state has been reached as indicated by a constant plasma level of LD during 4 to 12 h (Figure 3.2). Interestingly, there was a trend of an elevation in total hepatic blood flow which lasted during a course of infusion (Figure 3.4). Although a rise in the hepatic blood flow would, in theory, lead to an increase in LD elimination, Cl_H remained constant at the infusion regimen we have employed (Table 3.2). This could be explained by a gradual decline in E_H, which was associated with a concentration-independent reduction in Cl_{int} of LD as infusion continued (Table 3.2). This alteration of Cl_{int} persisted even after the cessation of an infusion (Table 3.3). Moreover, the reduction in Cl_{int} of total drug reflects a true impairment in the intrinsic ability of the liver to remove free drug, as supported by a lack of change in the free fraction of LD (Figure 3.6). LD-induced alterations in hepatic tissue binding and in enzyme activities are implicated from a reduction in the net hepatic uptake of ^{14}C-labeled material and a change in MEGX profile respectively in our study. The site(s) of inhibition in the metabolic pathway remain unclear. However, saturable metabolism and competitive inhibition by metabolite(s) are unlikely mechanisms. Rather, the progressive decline in Cl_{int} during a course of LD infusion is dependent on the cumulative exposure of hepatic enzymes to the drug. This is in accordance with our hypothesis that time-dependent kinetics of LD could be partly attributed to enzyme inactivation. Both time and dosing rate of an infusion are important determinants of cumulative exposure to LD and, thereby, the extent of reduction in metabolic intrinsic clearance. Time-dependent reduction in LD clearance could not be demonstrated in our infusion studies could be explained by an insufficient cumulative hepatic influx which is incurred by a short infusion period and a low dosing rate. Oral administration of a large single dose is effective in causing a marked impairment of hepatic elimination of LD comparable to that obtained during infusion at a time when similar cumulative exposure was achieved (Figure 4.2).

During our oral studies, we found that LD distribution in blood was nonlinear. This was unexpected based on our *in vitro* findings and a close-to-unity value of C_b/C_p obtained in blood samples following i.v. administration. We have verified that the LD peak measured by our HPLC method was pure and no co-eluting substance could be detected. Time courses of drug concentrations in plasma and in erythrocytes suggested that drug efflux from erythrocytes was not instantaneous. The mechanism(s) underlying this phenomenon is(are) not understood.

Previous findings from our laboratory (173) have demonstrated evidence of time-dependent changes in N-dealkylase activities using isolated perfused rat livers and that the time-effect disappeared after pretreatment of the animals with single dose of LD (10 mg/kg). We attempted to further investigate the site of metabolic impairment and quantify the extent of reduction in enzyme activities using rat liver microsomes.

The use of anesthetic agents is inevitable during surgical isolation of the liver for harvesting liver microsomes. It is well known that various anesthetic agents influence many important physiological processes such as systemic and regional hemodynamics and metabolic activities of the liver. Since different anesthetic agents were used in previous work and in the present project in our laboratory and by other investigators, we have examined this factor using single-pass isolated liver perfusion system. Our results indicate that the use of diethyl ether, methoxyflurane and sodium pentobarbital anesthesia in isolated liver perfusion studies did not have differential residual effects on N-dealkylation and aromatic ring hydroxylation, indicating that CYP2C11, CYP1A2, CYP2B1 and CYP2D activities were probably unaffected. Similarly, glucuronidation and sulfation of LD and its metabolites were not altered by brief exposure to these anesthetic agents. However, the use of sodium pentobarbital may selectively alter CYP2B2-catalyzed metabolic pathways such as LD aryl methyl hydroxylation. Since this pathway plays a minor role in LD elimination, the overall rate and extent of LD clearance by the isolated rat livers did not differ significantly among diethyl ether, methoxyflurane and sodium pentobarbital groups.

To explain for the time-effect observed in previous studies using single-pass isolated liver perfusion system (173), the formation of a reactive metabolic intermediate and its involvement in tight binding to CYP enzymes has been implicated. However, enzyme kinetics studies using liver microsomes prepared from saline control and LD pretreated rats failed to reveal any difference in K_m and V_{max} for N-dealkylation, aromatic ring hydroxylation and aryl methyl hydroxylation of LD. A possible explanation is restoration of enzyme activities as a result of dissociation of the metabolic intermediate complex, if it is formed *in vivo*, during microsomal preparation using ultracentrifugation.

In summary, a time-dependent reduction in hepatic intrinsic clearance of LD has been observed in instrumented dogs. Changes in MEGX plasma profile provides *in vivo* evidence of changes in metabolic activities of the liver. Conversely, alterations in plasma protein binding and hepatic tissue binding probably play a minor role. On the other hand, drug-induced changes in hepatic blood flow could not explain the time-dependent phenomenon, since it is elevated, rather than reduced, during a course of drug infusion.

6. REFERENCES

1. D. S. Riggs. Linear vs. nonlinear operators. In *Control theory and physiological feedback mechanisms*, Robert E. Krieger Publishing Company, New York, 1976, pp. 23-27.

2. T. M. Ludden. Nonlinear pharmacokinetics: clinical implications. *Clin. Pharmacokinet.* **20**:429-446 (1991).

3. D. Jung, J. R. Powell, P. Walson, and D. Perrier. Effect of dose on phenytoin absorption. *Clin. Pharmacol. Ther.* **28**:479-485 (1980).

4. B. G. Reigner, W. Couet, J.-P. Guedes, J.-B. Fourtillan, and T. N. Tozer. Saturable rate of cefatrizine absorption after oral administration to humans. *J. Pharmacokinet. Biopharm.* **18**:17-34 (1990).

5. D. G. Shand, S. C. Hammill, L. Aanonsen, and E. L. C. Pritchett. Reduced verapamil clearance during long-term oral administration. *Clin. Pharmacol. Ther.* **30**:701-703 (1981).

6. L. Gram, H. Flachs, A. Würtz-Jorgensen, J. Parnas, and B. Andersen. Sodium valproate, relationship between serum levels and therapeutic effect: a controlled study. In S. I. Johannessen, P. L. Morselli, C. E. Pippenger, A. Richens, D. Schmidt, and H. Meinardi (eds.), *Antiepileptic therapy: advances in drug monitoring*, Raven Press, New York, 1980, pp. 247-252.

7. H. L. J. Fleuren and J. M. van Rossum. Nonlinear relationship between plasma and red blood cell pharmacokinetics of chlorthalidone in man. *J. Pharmacokinet. Biopharm.* **5**:359-375 (1977).

8. S. M. Wallace, V. P. Shah, and S. Riegelman. GLC analysis of acetazolamide in blood, plasma and saliva following oral administration to normal subjects. *J. Pharm. Sci.* **66**:527-530 (1977).

9. B. Legg and M. Rowland. Saturable binding of cyclosporin A to erythrocytes: estimation of binding parameters in renal transplant patients and implications for bioavailability assessment. *Pharm. Res.* **5**:80-85 (1988).

10. H.-J. Lee and W. L. Chiou. Erythrocytes as barriers for drug elimination in the isolated rat liver. I. Doxorubicin. *Pharm. Res.* **6**:833-839 (1989).

11. G. Levy. Pharmacokinetics of salicylate elimination in man. *J. Pharm. Sci.* **54**:959-967 (1965).

12. S. C. Tsao, T. H. Dickinson, and D. R. Abernethy. Metabolite inhibition of parent drug biotransformation: studies of diltiazem. *Drug Metab. Dispos.* **18:**180-182 (1990).

13. L. Bertilsson, B. Höjer, G. Tybring, J. Osterloh, and A. Rane. Autoinduction of carbamazepine metabolism in children examined by a stable isotope technique. *Clin. Pharmacol. Ther.* **27:**83-88 (1980).

14. R. E. Galinsky and G. Levy. Dose- and time-dependent elimination of acetaminophen in rats: pharmacokinetic implications of cosubstrate depletion. *J. Pharmacol. Exp. Ther.* **219:**14-20 (1981).

15. J. H. Lin. Dose-dependent pharmacokinetics: experimental observations and theoretical considerations. *Biopharm. Drug Dispos.* **15:**1-31 (1994).

16. R. H. Levy. Time-dependent pharmacokinetics. *Pharmacol. Ther.* **17:**383-397 (1982).

17. A. Reinberg and M. H. Smolensky. Circadian changes of drug disposition in man. *Clin. Pharmacokinet.* **7:**401-420 (1982).

18. A. Richens. Liver enzyme induction by antiepileptic drugs: its clinical significance. In A. Richens and F. P. Woodford (eds.), *Anticonvulsant drugs and enzyme induction,* Associated Scientific Publishers, Amsterdam, 1976, pp. 3-12.

19. J. Trap-Jensen, J. P. Clausen, I. Noer, O. A. Larsen, A. R. Krogsgaard, and N. J. Christensen. The effects of beta-adrenoceptor blockers on cardiac output, liver blood flow and skeletal muscle blood flow in hypertensive patients. *Acta Physiol. Scand.* **30 (Suppl. 44):**27 (1976).

20. L. E. Mather and J. Thomas. Metabolism of lidocaine in man. *Life Sci.* **11:**915-919 (1972).

21. L. E. Mather and G. T. Tucker. Pharmacokinetics and biotransformation of local anesthetics. *International Anesthesiology Clinics* **16:**23-51 (1978).

22. K. A. Collinsworth, S. M. Kalman, and D. C. Harrison. The clinical pharmacology of lidocaine as an antiarrhythmic drug. *Circulation* **50:**1217-1230 (1974).

23. N. Löfgren. Studies on local anesthetics: Xylocaine, a new synthetic drug. Stockholm, Ivar Haeggstroms. (1948).

24. L. M. Hondeghem and R. D. Miller. Local Anesthetics. In B. G. Katzung (ed.), *Basic and clinical pharmacology,* 3rd ed., Appleton & Lange, Los Altos, 1987, pp. 289-294.

25. J. M. Ritchie and N. M. Greene. Local anesthetics. In A. G. Gilman, L. S. Goodman, T. W. Rall, and F. Murad (eds.), *Goodman and Gilman's: The pharmacological basis of therapeutics,* 7th ed., Macmillan Publishing Company, Toronto, 1985, pp. 302-321.

26. W. Likoff. Cardiac arrhythmias complicating surgery. *Am. J. Cardiol.* **3**:427-429 (1959).

27. W. A. Weiss. Intravenous use of lidocaine for ventricular arrhythmias. *Anesth. Analg.* **39**:369-381 (1960).

28. In C. M. E. Krogh (ed.), *Compendium of Pharmaceuticals and Specialties,* 29th ed., Canadian Pharmaceutical Association, Ottawa, 1994, pp. 1450-1468.

29. D. P. Zipes. Management of cardiac arrhythmias. In E. Braunwald (ed.), *Heart Disease: A textbook of cardiovascular medicine,* 2nd ed., WB Saunders, Philadelphia, 1984, pp. 653-656.

30. N. L. Benowitz and W. Meister. Clinical pharmacokinetics of lignocaine. *Clin. Pharmacokinet.* **3**:177-201 (1978).

31. P. E. J. Nolan and M. D. Otto. Lidocaine. In J. E. Murphy (ed.), *Clinical pharmacokinetics,* ASHP, Bethesda, 1993, pp. 115-144.

32. J. T. Bigger and B. F. Hoffman. Antiarrhythmic drugs. In A. G. Gilman, L. S. Goodman, T. W. Rall, and F. Murad (eds.), *Goodman and Gilman's: The pharmacological basis of therapeutics,* 2nd ed., Macmillan Publishing Company, Toronto, 1985, pp. 748-783.

33. J. A. Pieper and J. H. Rodman. Lidocaine. In W. E. Evans, J. J. Schentag, and W. J. Jusko (eds.), *Applied pharmacokinetics: Principles of therapeutic drug monitoring,* 2nd ed., Applied Therapeutics, Inc. Spokane, 1986, pp. 639-681.

34. F. F. Foldes, R. Molloy, P. G. McNall, and L. R. Koukal. Comparison of toxicity of intravenously given local anesthetic agents in man. *JAMA* **172**:1493-1498 (1960).

35. A. W. Rademaker, J. Kellen, Y. K. Tam, and D. G. Wyse. Character of adverse effects of prophylactic lidocaine in the coronary care unit. *Clin. Pharmacol. Ther.* **40**:71-80 (1986).

36. R. Gianelly, J. O. von der Groeben, A. P. Spivack, and D. C. Harrison. Effect of lidocaine on ventricular arrhythmias in patients with coronary heart disease. *New Engl. J. Med.* **277:**1215-1219 (1967).

37. D. E. Jewitt, Y. Kishon, and M. Thomas. Lignocaine in the management of arrhythmias after acute myocardial infarction. *Lancet* **1:**266-270 (1968).

38. H. J. Pfeifer, D. J. Greenblatt, and J. Koch-Weser. Clinical use and toxicity of intravenous lidocaine. *Am. Heart J.* **92:**168-173 (1976).

39. E. Grenadier, G. Alpan, S. Keidar, and A. Palant. Respiratory and cardiac arrest after the administration of lidocaine into the central venous system. *Eur. J. Cardiol.* **2:**235-237 (1981).

40. D. E. Manyari-Ortega and F. J. Brennan. Lidocaine-induced cardiac asystole. *Chest* **74:**227-229 (1978).

41. G. R. Strichartz and J. M. Ritchie. The action of local anesthetics on ion channels of excitable tissues. In G. R. Strichartz (ed.), *Local anesthetics,* Vol. 81, Springer-Verlag, New York, 1987, pp. 21-52.

42. B. Hillie. Theories of anesthesia: general perturbations verus specific receptors. *Prog. Anesthesiol.* **2:**1-6 (1980).

43. T. Narahashi and D. T. Frazier. Site of action and active form of local anesthetics. *Neurosci. Res.* **4:**65-99 (1971).

44. G. R. Strichartz. Current concepts of the mechanism of action of local anesthetics. *J. Dent. Res.* **60:**1460-1467 (1981).

45. A. M. Shanes. Electrochemical aspects of physiological and pharmacological action in excitable cells. *Pharmacol. Rev.* **10:**59-273 (1958).

46. M. R. Rosen, C. Merker, and C. E. Pippenger. The effects of lidocaine on the canine ECG and electrophysiologic properties of Purkinje fibers. *Am. Heart J.* **91:**191-202 (1976).

47. M. R. Rosen, B. F. Hoffman, and A. L. Wit. Electrophysiology and pharmacology of cardiac arrhythmias. V. Cardiac antiarrhythmic effects of lidocaine. *Am. Heart J.* **89:**526-536 (1975).

48. J. Kupersmith, E. M. Antman, and B. F. Hoffman. *In vivo* electrophysiological effects of lidocaine in canine acute myocardial infarction. *Circ. Res.* **36:**84-91 (1975).

49. L. M. Hondeghem. Effects of lidocaine, phenytoin and quinidine on the ischemic canine myocardium. *J. Electrocardiol.* **9:**203-209 (1976).

50. R. N. Boyes, D. B. Scott, P. J. Jebson, M. J. Godman, and D. G. Julian. Pharmacokinetics of lidocaine in man. *Clin. Pharmacol. Ther.* **12:**105-116 (1971).

51. J. B. Keenaghan and R. N. Boyes. The tissue distribution, metabolism and excretion of lidocaine in rats, guinea pigs, dogs and man. *J. Pharmacol. Exp. Ther.* **180:**454-463 (1972).

52. P. N. Bennett, L. J. Aarons, M. R. Bending, J. A. Steiner, and M. Rowland. Pharmacokinetics of lidocaine and its deethylated metabolite: dose and time dependency studies in man. *J. Pharmacokinet. Biopharm.* **10:**265-281 (1982).

53. D. B. Scott, P. J. Jebson, M. J. Godman, and D. G. Julian. Oral lignocaine. *Lancet* **1:**93 (1970).

54. P.-M. Huet, J. LeLorier, G. Pomier, and D. Marleau. Bioavailability of lidocaine in normal volunteers and cirrhotic patients. *Gastroenterology* **75:**969 (1978).

55. S. Nattel, G. Gagné, and M. Pineau. The pharmacokinetics of lignocaine and β-adrenoceptor antagonists in patients with acute myocardial infarction. *Clin. Pharmacokinet.* **13:**293-316 (1987).

56. L. S. Cohen, J. E. Rosenthal, D. W. Horner, J. M. Atkins, O. A. Matthews, and S. J. Sarnoff. Plasma levels of lidocaine after intramuscular administration. *Am. J. Cardiol.* **29:**520-523 (1972).

57. V. Bernstein, M. Bernstein, J. Griffiths, and D. I. Peretz. Lidocaine intramuscularly in acute myocardial infarction. *JAMA* **219:**1027-1031 (1972).

58. M. L. Schwartz, M. B. Meyer, B. G. Covino, P. K. Narang, V. Sethi, A. J. Schwartz, and P. Kamp. Antiarrhythmic effectiveness of intramuscular lidocaine: influence of different injection sites. *J. Clin. Pharmacol.* **14:**77-83 (1974).

59. J. R. Wilcke, L. E. Davis, C. A. Neff-Davis, and G. D. Koritz. Pharmacokinetics of lidocaine and its active metabolites in dogs. *J. Vet. Pharmacol. Ther.* **6:**49-58 (1983).

60. S. Nattel, R. L. Rinkenberger, L. L. Lehrman, and D. P. Zipes. Therapeutic blood lidocaine concentrations after local anesthesia for cardiac electrophysiologic studies. *New Engl. J. Med.* **301:**418-420 (1979).

61. G. T. Tucker and L. E. Mather. Pharmacology of local anaesthetic agents. Pharmacokinetics of local anaesthetic agents. *Br. J. Anaesth.* **47 suppl:**213-224 (1975).

62. M. Rowland, P. D. Thomson, A. Guichard, and K. L. Melmon. Disposition kinetics of lidocaine in normal subjects. *Ann. N. Y. Acad. Sci.* **179:**383-398 (1971).

63. L. A. Bauer, T. Brown, M. Gibaldi, L. Hudson, S. Nelson, V. Raisys, and J. P. Shea. Influence of long-term infusions on lidocaine kinetics. *Clin. Pharmacol. Ther.* **31:**433-437 (1982).

64. R. N. Boyes and J. B. Keenaghan. Some aspects of the metabolism and distribution of lidocaine in rats, dogs, and man. In D. B. Scott and D. G. Julian (eds.), *Lidocaine in the treatment of ventricular arrhythmias*, E. & S. Livingstone, Edinburgh, 1971, pp. 140-151.

65. P. D. Thomson, M. Rowland, and K. L. Melmon. The influence of heart failure, liver disease, and renal failure on the disposition of lidocaine in man. *Am. Heart J.* **82:**417-421 (1971).

66. P. D. Thomson, K. L. Melmon, J. A. Richardson, K. Cohn, W. Steinbrunn, R. Cudihee, and M. Rowland. Lidocaine pharmacokinetics in advanced heart failure, liver disease, and renal failure in humans. *Ann. Intern. Med.* **78:**499-508 (1973).

67. R. L. Nation, E. J. Triggs, and M. Selig. Lignocaine kinetics in cardiac patients and aged subjects. *Br. J. Clin. Pharmacol.* **4:**439-448 (1977).

68. G. T. Tucker and R. A. Boas. Pharmacokinetic aspects of intravenous regional anesthesia. *Anesthesiology* **34:**538-549 (1971).

69. A. G. L. Burm, A. G. De Boer, J. W. van Kleef, N. P. E. Vermeulen, L. G. J. De Leede, J. Spierdijk, and D. D. Breimer. Pharmacokinetics of lidocaine and bupivacaine and stable isotope labelled analogues: a study in healthy volunteers. *Biopharm. Drug Dispos.* **9:**85-95 (1988).

70. N. Benowitz, R. P. Forsyth, K. L. Melmon, and M. Rowland. Lidocaine disposition kinetics in monkey and man. I. Prediction by a perfusion model. *Clin. Pharmacol. Ther.* **16:**87-98 (1974).

71. K. Ahmad and F. Medzihradsky. Distribution of lidocaine in blood and tissues after single doses and steady infusion. *Res. Commun. Chem. Pathol. Pharmacol.* **2:**813-828 (1971).

72. J. Katz. The distribution of ^{14}C-labelled lidocaine injected intravenously in the rat. *Anesthesiology* **29:**249-253 (1968).

73. J. B. Löfström. Tissue distribution of local anesthetics with special reference to the lung. *International Anesthesiology Clinics* **16:**53-71 (1978).

74. B. Åkerman, A. Åström, S. Ross, and A. Telc. Studies on the absorption, distribution and metabolism of labelled prilocaine and lidocaine in some animal species. *Acta Pharmacol. Toxicol.* **24:**389-403 (1966).

75. L. Jorfeldt, D. H. Lewis, J. B. Löfström, and C. Post. Lung uptake of lidocaine in healthy volunteers. *Acta Anaesthesiol. Scand.* **23:**567-574 (1979).

76. M. Stanton-Hicks, T. M. Murphy, J. J. Bonica, P. U. Berges, L. E. Mather, and G. T. Tucker. Effects of peridural block: V. Properties, circulatory effects, and blood levels of etidocaine and lidocaine. *Anesthesiology* **42:**398-407 (1975).

77. C. Post and K. Eriksdotter-Behm. Dependence of lung uptake of lidocaine *in vivo* on blood pH. *Acta Pharmacol. Toxicol.* **51:**136-140 (1982).

78. Å. Bertler, D. H. Lewis, J. B. Löfström, and C. Post. *In vivo* lung uptake of lidocaine in pigs. *Acta Anaesthesiol. Scand.* **22:**530-536 (1978).

79. C. Post, R. G. G. Andersson, Å. Ryrfeldt, and E. Nilsson. Transport and binding of lidocaine by lung slices and perfused lung of rats. *Acta Pharmacol. Toxicol.* **43:**156-163 (1978).

80. G. T. Tucker, R. N. Boyes, P. O. Bridenbaugh, and D. C. Moore. Binding of anilide-type local anesthetics in human plasma: I. Relationships between binding, physicochemical properties, and anesthetic activity. *Anesthesiology* **33:**287-303 (1970).

81. P. J. McNamara, R. L. Slaughter, J. A. Pieper, M. G. Wyman, and D. Lalka. Factors influencing the serum free fraction of lidocaine in man. *Clin. Pharmacol. Ther.* **27:**271 (1980).

82. P. A. Routledge, A. Barchowsky, T. D. Bjornsson, B. B. Kitchell, and D. G. Shand. Lidocaine plasma protein binding. *Clin. Pharmacol. Ther.* **27:**347-351 (1980).

83. A. Barchowsky, D. G. Shand, W. W. Stargel, G. S. Wagner, and P. A. Routledge. On the role of α_1-acid glycoprotein in lignocaine accumulation following myocardial infarction. *Br. J. Clin. Pharmacol.* **13:**411-415 (1982).

84. P. A. Routledge, W. W. Stargel, A. L. Finn, A. Barchowsky, and D. G. Shand. Lignocaine disposition in blood in epilepsy. *Br. J. Clin. Pharmacol.* **12:**663-666 (1981).

85. P. A. Routledge, D. G. Shand, A. Barchowsky, G. Wagner, and W. W. Stargel. Relationship between α_1-acid glycoprotein and lidocaine disposition in myocardial infarction. *Clin. Pharmacol. Ther.* **30:**154-157 (1981).

86. D. L. Goolkasian, R. L. Slaughter, D. J. Edwards, and D. Lalka. Displacement of lidocaine from serum alpha-1-acid glycoprotein. Binding sites to basic drugs. *Eur. J. Clin. Pharmacol.* **25:**413-417 (1983).

87. E. Krauss, C. F. Polnaszek, D. A. Scheeler, H. B. Halsall, J. H. Eckfeldt, and J. L. Holtzman. Interaction between human serum albumin and alpha-1-acid glycoprotein in the binding of lidocaine to purified protein fractions and sera. *J. Pharmacol. Exp. Ther.* **239:**754-759 (1986).

88. D. G. Shand. Alpha-1-acid glycoprotein and plasma lidocaine binding. *Clin. Pharmacokinet.* **9:**27-31 (1984).

89. E. A. Krauss, C. F. Polnaszek, Y. Yost, J. H. Eckfeldt, and J. L. Holtzman. The binding parameters of lidocaine to serum proteins. *Fed. Proc.* **41:**1557 (1982).

90. J. L. Holtzman. The study of drug-protein interactions by spin labeling. In M. M. Reidenberg and S. Erill (eds.), *Drug-protein binding,* Vol. 6, Praeger Publishers, Toronto, 1986, pp. 46-69.

91. D. E. Drayer, B. Lorenzo, S. Werns, and M. M. Reidenberg. Plasma levels, protein binding and elimination data of lidocaine and active metabolites in cardiac patients of various ages. *Clin. Pharmacol. Ther.* **34:**14-22 (1983).

92. E. Nishiguchi, J. Sindo, and N. Hamasaki. Requirement of cytoplasmic components for lidocaine-induced shape change in human erythrocytes. *Biochimica. Biophysica. Acta* **1176:**95-105 (1993).

93. B. G. Covino and H. G. Vassallo. Local anesthetics: Mechanisms of action and clinical use. In R. J. Kitz and M. B. Laver (eds.), *The scientific basis of clinical anesthesia,* Grune & Stratton, New York, 1976.

94. R. P. Remmel, A. K. Copa, and D. M. Angaran. The effects of hemodilution, pH, and protamine on lidocaine plasma protein binding and red blood-cell uptake *in vitro*. *Pharm. Res.* **8:**127-130 (1991).

95. N. D. S. Bax, G. T. Tucker, and H. F. Woods. Lignocaine and indocyanine green kinetics in patients following myocardial infarction. *Br. J. Clin. Pharmacol.* **10:**353-361 (1980).

96. D. Lalka, C. V. Manion, A. Berlin, D. T. Baer, B. Dodd, and M. B. Meyer. Dose dependent pharmacokinetics of lidocaine in volunteers. *Clin. Pharmacol. Ther.* **19:**110 (1976).

97. S. D. Nelson, W. A. Garland, G. D. Breck, and W. F. Trager. Quantification of lidocaine and several metabolites utilizing chemical-ionization mass spectrometry and stable isotope labeling. *J. Pharm. Sci.* **66:**1180-1190 (1977).

98. A. H. Beckett, R. N. Boyes, and P. J. Appleton. The metabolism and excretion of lignocaine in man. *J. Pharm. Pharmacol.* **18:**S76-S81 (1966).

99. Y. K. Tam, S. R. Tawfik, J. Ke, R. T. Coutts, M. R. Gray, and D. G. Wyse. High-performance liquid chromatography of lidocaine and nine of its metabolites in human and urine. *J. Chromatogr. Biomed. Appl.* **423:**199-206 (1987).

100. R. E. Stenson, R. T. Constantino, and D. C. Harrison. Interrelationships of hepatic blood flow, cardiac output and blood levels of lidocaine in man. *Circulation* **43:**205-211 (1971).

101. M. J. Bargetzi, T. Aoyama, F. J. Gonzalez, and U. A. Meyer. Lidocaine metabolism in human liver microsomes by cytochrome P450IIIA4. *Clin. Pharmacol. Ther.* **46:**521-527 (1989).

102. S. Imaoka, K. Enomoto, Y. Oda, A. Asada, M. Fujimori, T. Shimada, S. Fujita, F. P. Guengerich, and Y. Funae. Lidocaine metabolism by human cytochrome P-450s purified from hepatic microsomes: comparison of those with rat hepatic cytochrome P-450s. *J. Pharmacol. Exp. Ther.* **255:**1385-1391 (1990).

103. G. Hollunger. On the metabolism of lidocaine. I. The properties of the enzyme system responsible for the oxidative metabolism of lidocaine. *Acta Pharmacol. Toxicol.* **17:**356-364 (1960).

104. L. H. Patterson, G. Hall, B. S. Nijjar, P. K. Khatra, and D. A. Cowan. In-vitro metabolism of lignocaine to its N-oxide. *J. Pharm. Pharmacol.* **38:**326-327 (1986).

105. R. Kawai, S. Fujita, and T. Suzuki. Simultaneous quantitation of lidocaine and its four metabolites by high-performance liquid chromatography: application to studies on *in vitro* and *in vivo* metabolism of lidocaine in rats. *J. Pharm. Sci.* **74:**1219-1224 (1985).

106. Y. Masubuchi, S. Umeda, S. Igarashi, S. Fujita, S. Narimatsu, and T. Suzuki. Participation of the CYP2D subfamily in lidocaine 3-hydroxylation and formation of a reactive metabolite covalently bound to liver microsomal protein in rats. *Biochem. Pharmacol.* **46:**1867-1869 (1993).

107. Y. Oda, S. Imaoka, Y. Nakahira, A. Asada, M. Fujimori, S. Fujita, and Y. Funae. Metabolism of lidocaine by purified rat liver microsomal cytochrome P 450 isozymes. *Biochem. Pharmacol.* **38:**4439-4444 (1989).

108. Y. Masubuchi, S. Umeda, M. Chiba, S. Fujita, and T. Suzuki. Selective 3-hydroxylation deficiency of lidocaine and its metabolite in Dark Agouti rats. *Biochem. Pharmacol.* **42:**693-695 (1991).

109. T. Suzuki, S. Fujita, and R. Kawai. Precursor-metabolite interaction in the metabolism of lidocaine. *J. Pharm. Sci.* **73:**136-138 (1984).

110. C. von Bahr, I. Hedlund, B. Karlén, D. Bäckström, and H. Grasdalen. Evidence for two catalytically different binding sites of liver microsomal cytochrome P-450: importance for species and sex differences in oxidation pattern of lidocaine. *Acta Pharmacol. Toxicol.* **41:**39-48 (1977).

111. S. Fujita, J. Tatsuno, R. Kawai, H. Kitagawa, T. Suzuki, and K. Kitani. Age associated alteration of lidocaine metabolism is position selective. *Biochem. Biophys. Res. Commun.* **126:**117-122 (1985).

112. R. T. Coutts, G. A. Torok-Both, L. V. Chu, Y. K. Tam, and F. M. Pasutto. *In vivo* metabolism of lidocaine in the rat. Isolation of urinary metabolites as pentafluorobenzoyl derivatives and their identification by combined gas chromatography-mass spectrometry. *J. Chromatogr. Biomed. Appl.* **421:**267-280 (1987).

113. G. Nyberg, B. Karlén, I. Hedlund, R. Grundin, and C. von Bahr. Extraction and metabolism of lidocaine in rat liver. *Acta Pharmacol. Toxicol.* **40:**337-346 (1977).

114. G. Hollunger. On the metabolism of lidocaine. II. The biotransformation of lidocaine. *Acta Pharmacol. Toxicol.* **17:**365-373 (1960).

115. K. K. Adjepon-Yamoah and L. F. Prescott. Lignocaine metabolism in man. *Br. J. Pharmacol.* **47:**672P-673P (1973).

116. L. F. Prescott, K. K. Adjepon-Yamoah, and R. G. Talbot. Impaired lignocaine metabolism in patients with myocardial infarction and cardiac failure. *Br. Med. J.* **1:**939-941 (1976).

117. J. M. Strong, M. Parker, and A. J. Atkinson. Identification of glycinexylidide in patients treated with intravenous lidocaine. *Clin. Pharmacol. Ther.* **14**:67-72 (1973).

118. H. Halkin, P. Meffin, K. L. Melmon, and M. Rowland. Influence of congestive heart faliure on blood levels of lidocaine and its active monodeethylated metabolite. *Clin. Pharmacol. Ther.* **17**:669-676 (1975).

119. K. A. Collinsworth, J. M. Strong, A. J. Atkinson, and R. A. Winkle. Pharmacokinetics and metabolism of lidocaine in patients with renal failure. *Clin. Pharmacol. Ther.* **18**:59-64 (1975).

120. P. K. Narang, W. G. Crouthamel, N. H. Carliner, and M. L. Fisher. Lidocaine and its active metabolites. *Clin. Pharmacol. Ther.* **24**:654-662 (1978).

121. J. M. Strong, D. E. Mayfield, A. J. Atkinson, B. C. Burris, F. Raymon, and L. T. Webster. Pharmacological activity, metabolism, and pharmacokinetics of glycinexylidide. *Clin. Pharmacol. Ther.* **17**:184-194 (1975).

122. R. G. Burney, C. A. DiFazio, M. J. Peach, K. A. Petrie, and M. J. Silvester. Anti-arrhythmic effects of lidocaine metabolites. *Am. Heart J.* **88**:765-769 (1974).

123. A. H. Thomson, H. L. Elliott, A. W. Kelman, P. A. Meredith, and B. Whiting. The pharmacokinetics and pharmacodynamics of lignocaine and MEGX in healthy subjects. *J. Pharmacokinet. Biopharm.* **15**:101-115 (1987).

124. R. N. Boyes. A review of the metabolism of amide local anaesthetic agents. *Br. J. Anaesth.* **47 suppl**:225-230 (1975).

125. F. P. Guengerich. Human cytochrome P450 enzymes. In P. R. Ortiz de Montellano (ed.), *Cytochrome P450: structure, mechanism, and biochemistry*, 2nd ed., Plenum Press, New York, 1995, pp. 473-536.

126. I. De Waziers, P. H. Cugnenc, C. S. Yang, J.-P. Leroux, and P. H. Beaune. Cytochrome P450 isoenzymes,epoxide hydrolase and glutathione transferases in rat and human hepatic and extrahepatic tissues. *J. Pharmacol. Exp. Ther.* **253**:387-394 (1990).

127. S. A. Wrighton and J. C. Stevens. The human hepatic cytochromes P450 involved in drug metabolism. *Crit. Rev. Toxicol.* **22**:1-21 (1992).

128. D. A. Smith and B. C. Jones. Speculations on the substrate structure-activity relationship (SSAR) of cytochrome P450 enzymes. *Biochem. Pharmacol.* **44**:2089-2098 (1992).

129. D. A. Smith. Species differences in metabolism and pharmacokinetics: Are we close to an understanding? *Drug Metab. Rev.* **23:**355-373 (1991).

130. G. I. Murray, T. S. Barnes, H. F. Sewell, S. W. B. Ewen, W. T. Melvin, and M. D. Burke. The immunochemical localisation and distribution of cytochrome P450 in normal hepatic and extrahepatic tissues with a monoclonal antibody to human cytochrome P450. *Br. J. Clin. Pharmacol.* **25:**465-475 (1988).

131. D. R. Krishna and U. Klotz. Extrahepatic metabolism of drugs in humans. *Clin. Pharmacokinet.* **26:**144-160 (1994).

132. P. B. Watkins, S. A. Wrighton, E. G. Schuetz, D. T. Molowa, and P. S. Guzelian. Identification of glucocorticoid cytochrome P-450 in the intestinal mucosa of rats and man. *J. Clin. Invest.* **80:**1029-1036 (1987).

133. W. H. M. Peters and P. G. Kremers. Cytochromes P-450 in the intestinal mucosa of man. *Biochem. Pharmacol.* **38:**1535-1538 (1989).

134. J. C. Kolars, W. M. Awni, R. M. Merion, and P. B. Watkins. First-pass metabolism of cyclosporin by the gut. *Lancet* **338:**1488-1490 (1991).

135. H. R. Ochs, D. J. Greenblatt, W. Eikelkraut, C. Bakker, R. Gobel, and N. Hahn. Hepatic *vs.* gastrointestinal extraction of oral midazolam adn flurazepam. *J. Pharmacol. Exp. Ther.* **243:**852-856 (1987).

136. M. S. Lennard, G. T. Tucker, and H. F. Woods. Time-dependent kinetics of lignocaine in the isolated perfused rat liver. *J. Pharmacokinet. Biopharm.* **11:**165-182 (1983).

137. C. M. Hunt, W. R. Westerkam, and G. M. Stave. Effect of age and gender on the activity of human hepatic CYP3A. *Biochem. Pharmacol.* **44:**275-283 (1992).

138. R. N. Boyes, H. J. Adams, and B. R. Duce. Oral absorption and disposition kinetics of lidocaine hydrochloride in dogs. *J. Pharmacol. Exp. Ther.* **174:**1-8 (1970).

139. A. F. De Rick, F. M. Belpaire, C. Dello, and M. G. Bogaert. Influence of enhanced alpha-1-acid glycoprotein concentration on protein binding, pharmacokinetics and antiarrhythmic effect of lidocaine in the dog. *J. Pharmacol. Exp. Ther.* **241:**289-293 (1987).

140. R. W. Sallie, J. M. Tredger, and R. Williams. Extrahepatic production of the lignocaine metabolite monoethylglycinexylidide (MEGX). *Biopharm. Drug Dispos.* **13:**555-558 (1992).

141. K.-T. Lê, H. Maurice, and P. du Souich. First-pass metabolism of lidocaine in the anesthetized rabbit: contribution of the small intestine. *Drug Metab. Dispos.* **24:**711-716 (1996).

142. K. Tanaka, Y. Oda, A. Asada, M. Fujimori, and Y. Funae. Metabolism of lidocaine by rat pulmonary cytochrome P450. *Biochem. Pharmacol.* **47:**1061-1066 (1994).

143. K. S. Pang, J. A. Terrell, S. D. Nelson, K. F. Feuer, M.-J. Clements, and L. Endrenyi. An enzyme-distributed system for lidocaine metabolism in the perfused rat liver preparation. *J. Pharmacokinet. Biopharm.* **14:**107-130 (1986).

144. Y. K. Tam, M. Yau, R. Berzins, P. R. Montgomery, and M. Gray. Mechanisms of lidocaine kinetics in the isolated perfused rat liver. I. Effects of continuous infusion. *Drug Metab. Dispos.* **15:**12-16 (1987).

145. F. G. McMahon and L. A. Woods. Further studies on the metabolism of lidocaine in the dog. *J. Pharmacol. Exp. Ther.* **103:**354 (1951).

146. Y. K. Tam, J. Ke, R. T. Coutts, D. G. Wyse, and M. R. Gray. Quantification of three lidocaine metabolites and their conjugates. *Pharm. Res.* **7:**504-507 (1990).

147. J. LeLorier, D. Grenon, Y. Latour, G. Caillé, G. Dumont, A. Brosseau, and A. Solignac. Pharmacokinetics of lidocaine after prolonged intravenous infusions in uncomplicated myocardial infarction. *Ann. Intern. Med.* **87:**700-702 (1977).

148. D. S. Fredrick and R. B. Boersma. Lidocaine infusions: effect of duration and method of discontinuation on recurrence of arrhythmias and pharmacokinetic variables. *Am. J. Hosp. Pharm.* **36:**778-781 (1979).

149. P. A. Routledge, W. W. Stargel, G. S. Wagner, and D. G. Shand. Increased alpha-1-acid glycoprotein and lidocaine disposition in myocardial infarction. *Ann. Intern. Med.* **93:**701-704 (1980).

150. H. R. Ochs, G. Carstens, and D. J. Greenblatt. Reduction in lidocaine clearance during continuous infusion and by coadministration of propranolol. *New Engl. J. Med.* **303:**373-377 (1980).

151. A. H. Thomson, A. W. Kelman, P. J. de Vane, W. S. Hillis, and B. Whiting. Changes in lignocaine disposition during long-term infusion in patients with acute ventricular arrhythmias. *Ther. Drug. Monit.* **9:**283-291 (1987).

152. J. LeLorier, R. Moisan, J. Gagné, and G. Caillé. Effect of the duration of infusion on the disposition of lidocaine in dogs. *J. Pharmacol. Exp. Ther.* **203:**507-511 (1977).

153. M. R. Blair. Cardiovascular pharmacology of local anaesthetics. *Br. J. Anaesth.* **47**:247-252 (1975).

154. I. Yoneda, M. Nishizawa, K. T. Benson, T. L. Chaffee, and H. Goto. Attenuation of arterial baroreflex control of renal sympathetic nerve activity during lidocaine infusion in alpha-chloralose-anesthesized dogs. *Acta Anaesthesiol. Scand.* **38**:70-74 (1994).

155. L. Wiklund. Human hepatic blood flow and its relation to systemic circulation during intravenous infusion of lidocaine. *Acta Anaesthesiol. Scand.* **21**:148-160 (1977).

156. L. Gariépy, P. Larose, B. Bailey, and P. du Souich. Effect of lignocaine on arginine-vasopressin plasma levels: baseline or induced by frusemide. *Br. J. Pharmacol.* **106**:470-475 (1992).

157. C. Skak and S. Keiding. Methodological problems in the use of indocyanine green to estimate hepatic blood flow and ICG clearance in man. *Liver* **7**:155-162 (1987).

158. M. J. A. P. Daemen, H. H. W. Thijssen, H. van Essen, H. T. M. Vervoort-Peters, F. W. Prinzen, H. A. J. Struyker, and J. F. M. Smits. Liver blood flow measurement in the rat. *J. Pharmacol. Methods* **21**:287-297 (1989).

159. A. Skerjanec, D. W. O'Brien, and Y. K. Tam. Hepatic blood flow measurements and indocyanine green kinetics in a chronic dog model. *Pharm. Res.* **11**:1511-1515 (1994).

160. J. H. Thomsen, W. Terry, R. R. Stenlund, S. Querimit, and G. G. Rowe. The effects of lidocaine on systemic and coronary hemodynamics. *Arch. Int. Pharmacodyn. Ther.* **194**:83-92 (1971).

161. F. F. Kao and U. H. Jalar. The central action of lignocaine and its effect on cardiac output. *Br. J. Pharmacol.* **14**:522-526 (1959).

162. R. T. Constantino, S. E. Crockett, and J. S. Vasko. Cardiovascular effects of lidocaine. *Ann. Thor. Surg.* **8**:425-436 (1969).

163. J. J. Bonica, P. U. Berges, and K.-I. Morikawa. Circulatory effects of peridural block: I. Effects of level of analgesia and dose of lidocaine. *Anesthesiology* **33**:619-626 (1970).

164. Y. F. Huang, R. N. Upton, A. J. Rutten, and W. B. Runciman. I.V. bolus administration of subconvulsive doses of lignocaine to conscious sheep: effects on circulatory function. *Br. J. Anaesth.* **69**:368-374 (1992).

165. M. Manz, R. Mletzko, W. Jung, and B. Lüderitz. Electrophysiological and haemodynamic effects of lidocaine and ajmaline in the management of sustained ventricular tachycardia. *Eur. Heart J.* **13**:1123-1128 (1992).

166. M. A. Martin, N. D. S. Bax, G. T. Tucker, and J. W. Ward. Disopyramide and lignocaine: a comparison of cardiac effects using echocardiography. *Br. J. Clin. Pharmacol.* **10**:237-244 (1980).

167. J. M. H. Kremer, J. Wilting, and L. H. M. Janssen. Drug binding to human alpha-1-acid glycoprotein in health and disease. *Pharmacol. Rev.* **40**:1-47 (1988).

168. R. F. Davies, L. M. Dubé, N. Mousseau, I. McGilveray, and D. S. Beanlands. Perioperative variability of binding of lidocaine, quinidine, and propranolol after cardiac operations. *J. Thor. Cardiovasc. Surg.* **96**:634-641 (1988).

169. A. Agostoni, C. Vergani, R. Stabilini, B. Marasini, R. Arcidiacono, A. Sbaffi, and P. C. Binaghi. Immunochemical quantitation of acute phase reactive proteins in myocardial infarction. *Am. Heart J.* **80**:313-318 (1970).

170. B. G. Johansson, C. O. Kindmark, E. Y. Trell, and F. A. Wollheim. Sequential changes of plasma proteins after myocardial infarction. *Scand. J. Clin. Lab. Invest.* **29**:117-126 (1972).

171. P. A. Routledge. The plasma protein binding of basic drugs. *Br. J. Clin. Pharmacol.* **22**:499-506 (1986).

172. C.-P. Chen, V. T. Vu, and S. D. Cohen. Lidocaine uptake in isolated rat hepatocytes and effects of *dl*-propranolol. *Toxicol. Appl. Pharmacol.* **55**:162-168 (1980).

173. B. A. Saville, M. R. Gray, and Y. K. Tam. Evidence for lidocaine-induced enzyme inactivation. *J. Pharm. Sci.* **78**:1003-1008 (1989).

174. M. D. Hussain, Y. K. Tam, M. R. Gray, and R. T. Coutts. Mechanisms of time-dependent kinetics of diltiazem in the isolated perfused rat liver. *Drug Metab. Dispos.* **22**:36-42 (1994).

175. B. A. Saville and M. R. Gray. The metabolism of lidocaine in the liver:steady-state and dynamic modelling. *Can. J. Chem. Eng.* **64**:617-624 (1986).

176. M. R. Gray, B. A. Saville, and Y. K. Tam. Mechanisms of lidocaine kinetics in the isolated perfused rat liver. III. Evaluation of liver models for time-dependent behavior. *Drug Metab. Dispos.* **15:**22-26 (1987).

177. Y. Masubuchi, J. Araki, S. Narimatsu, and T. Suzuki. Metabolic activation of lidocaine and covalent binding to rat liver microsomal protein. *Biochem. Pharmacol.* **43:**2551-2557 (1992).

178. A. Bast, A. J. Valk, and H. Timmerman. Cytochrome P-450 metabolic-intermediate complex formation with a series of diphenhydramine analogues. *Agents & Actions* **30:**161-165 (1990).

179. A. Bast, E. M. Savenije-Chapel, and J. Noordhoek. Relationship between molecular structure and cytochrome P450-metabolic intermediate complex formation, studied with orphenadrine analogues. *J. Pharm. Sci.* **73:**953-956 (1984).

180. A. Bast and J. Noordhoek. Spectral interaction of orphenadrine and its metabolites with oxidized and reduced hepatic microsomal cytochrome P-450 in the rat. *Biochem. Pharmacol.* **31:**2745-2753 (1982).

181. G. F. Reidy, I. Mehta, and M. Murray. Inhibition of oxidative drug metabolism by orphenadrine: *in vitro* and *in vivo* evidence for isozyme-specific complexation of cytochrome P-450 and inhibition kinetics. *Mol. Pharmacol.* **35:**736-743 (1989).

182. M. Murray and S. L. Field. Inhibition and metabolite complexation of rat hepatic microsomal cytochrome P450 by tricyclic antidepressants. *Biochem. Pharmacol.* **43:**2065-2071 (1992).

183. D. Larrey, M. Tinel, and D. Pessayre. Formation of inactive cytochrome P-450 Fe(II)-metabolite complexes with several erythromycin derivatives but not with josamycin and midecamycin in rats. *Biochem. Pharmacol.* **32:**1487-1493 (1983).

184. M. R. Franklin. Cytochrome P450 metabolic intermediate complexes from macrolide antibiotics and related compounds. In J. N. Abelson and M. I. Simon (eds.), *Methods in enzymology,* Vol. 206, Academic Press, Inc. Toronto, 1991, pp. 559-573.

185. D. Pessayre, V. Descatoire, M. Konstantinova-Mitcheva, J.-C. Wandscheer, B. Cobert, R. Level, J.-P. Benhamou, M. Jaouen, and D. Mansuy. Self-induction by triacetyloleandomycin of its own transformation into a metabolite forming a stable 456 nm-absorbing complex with cytochrome P-450. *Biochem. Pharmacol.* **30:**553-558 (1981).

186. M. Delaforge, M. Jaouen, and D. Mansuy. Dual effects of macrolide antibiotics on rat liver cytochrome P-450. Induction and formation of metabolite-complexes: a structure-activity relationship. *Biochem. Pharmacol.* **32**:2309-2318 (1983).

187. A. Bast, E. M. Savenjie-Chapel, F. A. A. van Kemenade, L. W. C. Scheefhals, and J. Noordhoek. Effect of multiple administration of orphenadrine or mono-N-desmethylorphenadrine on cytochrome P-450 catalyzed reactions in the rat. *Arch. Toxicol.* **54**:131-137 (1983).

188. H. A. Semple, Y. K. Tam, and D. W. O'Brien. Physiological modelling of the hepatic interaction between food and hydralazine in the conscious dog. *Pharm. Res.* **7**:S223 (1990).

189. A. Skerjanec, S. Tawfik, and Y. K. Tam. Mechanisms of dose and time dependent kinetics of mibefradil in chronically instrumented dogs. *J. Pharmacol. Exp. Ther.* **278**:817-825 (1996).

190. N. Vicuna, D. Lalka, S. R. Burrow, A. J. McLean, P. du Souich, and J. L. McNay. Dose-dependent pharmacokinetics behavior of lidocaine in the conscious dog. *Res. Commun. Chem. Pathol. Pharmacol.* **22**:485-491 (1978).

191. D. E. Coyle and D. D. Denson. Protein binding of lidocaine in canine serum and plasma: effects of an acidic pH and the technique of study. *Biopharm. Drug Dispos.* **5**:399-404 (1984).

192. B. A. Saville, M. R. Gray, and Y. K. Tam. Mechanisms of lidocaine kinetics in the isolated perfused rat liver. II. Kinetics of steady state elimination. *Drug Metab. Dispos.* **15**:17-21 (1987).

193. K. S. Pang. Liver perfusion studies in drug metabolism and drug toxicity. In J. R. Mitchell and M. G. Horning (eds.), *Drug metabolism and drug toxicity*, Raven Press, New York, 1984, pp. 331-352.

194. G. J. Gores, L. J. Kost, and N. F. LaRusso. The isolated perfused rat liver: conceptual and practical considerations. *Hepatology* **6**:511-517 (1986).

195. D. L. Schmucker and J. C. Curtis. A correlated study of the fine structure and physiology of the perfused rat liver. *Lab. Invest.* **30**:201-212 (1974).

196. D. L. Bloxam. Condition and performance of the rat liver perfused with Kreb's-ringer solution, with particular reference to amino acid metabolism. In I. Bartosek, A. Guaitani, and L. L. Miller (eds.), *Isolated liver perfusion and its applications*, Raven Press, New York, 1973, pp. 147-153.

197. B. A. Saville. Hepatic transport and metabolism of lidocaine. Ph.D. Thesis, University of Alberta, 1989, pp. 89-100.

198. S. I. Gelman. Disturbances in hepatic blood flow during anesthesia and surgery. *Arch. Surg.* **111**:881-883 (1976).

199. S. I. Gelman. The effect of enteral oxygen administration on the hepatic circulation during halothane anaesthesia: experimental investigations. *Br. J. Anaesth.* **47**:1253-1259 (1975).

200. L. L. Priano, D. L. Traber, and R. D. Wilson. Barbiturate anesthesia: an abnormal physiologic situation. *J. Pharmacol. Exp. Ther.* **165**:126-135 (1969).

201. R. L. Hughes, D. Campbell, and W. Fitch. Effects of enflurane and halothane on liver blood flow and oxygen consumption in the greyhound. *Br. J. Anaesth.* **52**:1079-1086 (1980).

202. F. Olmsted and I. H. Page. Hemodynamic changes in dogs caused by sodium pentobarbital anesthesia. *Am. J. Physiol.* **210**:817-820 (1966).

203. R. H. Cox. Influence of pentobarbital anesthesia on cardiovascular function in trained dogs. *Am. J. Physiol.* **223**:651-659 (1972).

204. D. G. Vidt, A. Bredemeyer, E. Sapirstein, and L. A. Sapirstein. Effect of ether anesthesia on the cardiac output, blood pressure, and distribution of blood flow in the Albino rat. *Circ. Res.* **7**:759-764 (1959).

205. C. B. Nash, F. Davis, and R. A. Woodbury. Cardiovascular effects of anesthetic doses of pentobarbital sodium. *Am. J. Physiol.* **185**:107-112 (1956).

206. M. Gumbleton, P. J. Nicholls, and G. Taylor. Differential influence of laboratory anaesthetic regimens upon renal and hepatosplanchnic haemodynamics in the rat. *J. Pharm. Pharmacol.* **42**:693-697 (1990).

207. D. J. Edwards, D. Lalka, R. L. Slaughter, and J. M. Hassett. Differential effect of pentobarbital and chloralose in anesthetic doses on the serum protein binding of lidocaine in the dog. *J. Pharm. Sci.* **77**:466-467 (1988).

208. F. S. LaBella and G. Queen. General anesthetics inhibit cytochrome P450 monooxygenases and arachidonic acid metabolism. *Can. J. Physiol. Pharmacol.* **71**:48-53 (1992).

209. P. T. Liu, C. Ioannides, J. Shavila, A. M. Symons, and D. V. Parke. Effects of ether anaesthesia and fasting on various cytochromes P450 of rat liver and kidney. *Biochem. Pharmacol.* **45:**871-877 (1993).

210. P. T. Liu, P. A. Kentish, A. M. Symons, and D. V. Parke. The effects of ether anaesthesia on oxidative stress in rats — dose response. *Toxicology* **80:**37-49 (1993).

211. F. Baekeland and N. M. Greene. Effect of diethyl ether on tissue distribution and metabolism of pentobarbital in rats. *Anesthesiology* **19:**724-732 (1958).

212. W. Johannessen, G. Gadeholt, and J. Aarbakke. Effects of diethyl ether anaesthesia on the pharmacokinetics of antipyrine and paracetamol in the rat. *J. Pharm. Pharmacol.* **33:**365-368 (1981).

213. J. B. Watkins and C. D. Klaassen. Chemically-induced alteration of UDP-glucuronic acid concentration in rat liver. *Drug Metab. Dispos.* **11:**37-40 (1983).

214. B. R. Brown and A. M. Sagalyn. Hepatic microsomal enzyme induction by inhalation anesthetics: mechanism in the rat. *Anesthesiology* **40:**152-161 (1974).

215. B. R. Brown. Effects of inhalation anesthetics on hepatic glucuronide conjugation: a study of the rat *in vitro*. *Anesthesiology* **37:**483-488 (1972).

216. E. C. A. To and P. G. Wells. Biochemical changes associated with the potentiation of acetaminophen hepatotoxicity by brief anesthesia with diethyl ether. *Biochem. Pharmacol.* **35:**4139-4152 (1986).

217. E. J. Frink and B. R. Brown. The effects of halothane, enflurane and isoflurane on the hepatic intrinsic clearance of lidocaine and propranolol. *Anesthesiology* **69:**A454 (1988).

218. M. Gumbleton and L. Z. Benet. Drug metabolism and laboratory anesthetic protocols in the rat: examination of antipyrine pharmacokinetics. *Pharm. Res.* **8:**544-546 (1991).

219. Y. Tan, L. K. Keefer, and C. S. Yang. Inhibition of microsomal *N*-nitrosodimethylamine demethylase by diethyl ether and other anesthetics. *Biochem. Pharmacol.* **36:**1973-1978 (1987).

220. T. A. Maguire, J. G. Swanton, and D. J. Temple. *In situ* liver perfusion techniques: the significance of the anaesthetic procedure used. *Eur. J. Drug Metab. Pharmacokinet.* **13:**35-40 (1988).

221. A. V. Oppenheim and R. W. Schafer. Digital Signal Processing. Prentice Hall, Englewood Clifs, 1975.

222. D. W. O'Brien, H. A. Semple, G. D. Molnar, Y. Tam, R. T. Coutts, R. V. Rajotte, and J. Bayens-Simmonds. A chronic conscious dog model for direct transhepatic studies in normal and pancreatic islet cell transplanted dogs. *J. Pharmacol. Methods* **25**:157-170 (1991).

223. L. L. Miller. Technique of isolated rat liver perfusion. In I. Bartosek, A. Guaitani, and L. L. Miller (eds.), *Isolated liver perfusion and its applications,* Raven Press, New York, 1973, pp. 11-52.

224. T. Omura and R. Sato. The carbon monoxide-binding pigment of liver microsomes. I. Evidence for its hemoprotein nature. *J. Biol. Chem.* **239**:2370-2378 (1964).

225. M. M. Bradford. A rapid and sensitive method for the quantitation of microgram quantities of protein utilizing the principle of protein-dye binding. *Anal. Biochem.* **72**:248-254 (1976).

226. M. Gibaldi and D. Perrier. Noncompartmental analysis based on statistical moment theory. In *Pharmacokinetics,* 2nd ed., Marcel Dekker Inc., New York, 1982, pp. 409-417.

227. C. Ediss and Y. K. Tam. An interactive computer program for determining areas bounded by drug concentration curves using lagrange interpolation. *J. Pharmacol. Toxicol. Methods* **34**:165-168 (1995).

228. K. S. Pang and M. Rowland. Hepatic Clearance of drugs. II. Experimental evidence for acceptance of the "well-stirred" model over the "parallel tube" model using lidocaine in the perfused rat liver *in situ* preparation. *J. Pharmacokinet. Biopharm.* **5**:655-680 (1977).

229. G. K. Weiner and G. E. Stucker. WINNONLIN version 1.1. Scientific Consulting Inc., Apex, NC, 1996.

230. J. Stanislawski. ENZYMEKINETICS version 1.4. Trinity Software, 1993.

231. R. G. D. Steel and J. H. Torrie. Analysis of variance. II. Multiway classifications. In *Principles and procedures of statistics: a biometrical approach,* 2nd ed., McGraw Hill Inc. Toronto, 1980, pp. 195-238.

232. F. Handel, F. A. Luzzi, T. L. Wenger, A. Barchowsky, D. G. Shand, and H. C. Strauss. Lidocaine and its metabolites in canine plasma and myocardium. *J. Cardiovasc. Pharmacol.* **5**:44-50 (1983).

233. C. A. DiFazio and R. E. Brown. Lidocaine metabolism in normal and phenobarbital-pretreated dogs. *Anesthesiology* **36:**238-243 (1972).

234. B. Davies and T. Morris. Physiological parameters in laboratory animals and humans. *Pharm. Res.* **10:**1093-1095 (1993).

235. E. R. Smith, B. R. Duce, and R. N. Boyes. Antiarrhythmic effects in dogs of lidocaine administered orally and intravenously. *Am. Heart J.* **83:**365-372 (1972).

236. M. S. L. Yau. Kinetic characteristics of lidocaine during prolonged infusion-a study using isolated perfused rat liver. M.Sc. Thesis, University of Alberta, 1986, pp. 1-29.

237. E. Schmidt, F. W. Schmidt, J. Mohr, P. Otto, I. Vido, K. Wrogemann, and C. Herfarth. Liver morphology and enzyme release: further studies in the isolated perfused rat liver. In D. Keppler (ed.), *Pathogenesis and mechanisms of liver cell necrosis,* University Park Press, Baltimore, 1975, pp. 147-162.

238. J. E. Bell and E. T. Bell. Deviations from linear kinetics. In *Proteins and enzymes,* Prentice-Hall, Inc. Toronto, 1988, pp. 370-377.

239. R. A. Branch, D. G. Shand, G. R. Wilkinson, and A. S. Nies. The reduction of lidocaine clearance by dl-propranolol: an example of hemodynamic drug interaction. *J. Pharmacol. Exp. Ther.* **184:**515-519 (1973).

240. M. R. Gray and Y. K. Tam. Pharmacokinetics of drugs that inactivate metabolic enzymes. *J. Pharm. Sci.* **80:**121-127 (1991).

241. C. Weber, K. Stoeckel, and D. Lalka. Accumulation kinetics of propranolol in the rat: comparison of Michaelis-Menten-mediated clearance anc clearance changes consistent with the "altered enzyme hypothesis". *Pharm. Res.* **11:**420-425 (1994).

242. L. Shaw, M. S. Lennard, G. T. Tucker, N. D. S. Bax, and H. F. Woods. Irreversible binding and metabolism of propranolol by human liver microsomes-relationship to polymorphic oxidation. *Biochem. Pharmacol.* **36:**2283-2288 (1987).

243. D. W. Schneck and J. F. Pritchard. The inhibitory effect of propranolol pretreatment on its own metabolism in the rat. *J. Pharmacol. Exp. Ther.* **218:**575-581 (1981).

244. Y. Masubuchi, K. Suzuki, S. Fujita, and T. Suzuki. A possible mechanism of the impairment of hepatic microsomal monooxygenase activities after multiple administration of propranolol in rats. *Biochem. Pharmacol.* **43:**757-762 (1992).

245. Y. Masubuchi, S. Narimatsu, and T. Suzuki. Activation of propranolol and irreversible binding to rat liver microsomes: strain differences and effects of inhibitors. *Biochem. Pharmacol.* **43:**635-637 (1992).

246. A. H. Beckett and E. E. Essien. Chlorpromazine 'hydroxylamines' in red blood cells as major metabolites of chlorpromazine in man. *J. Pharm. Pharmacol.* **25:**188-189 (1973).

247. M. Kiese. The biochemical production of ferrihemoglobin-forming derivatives from aromatic amines, and mechanisms of ferrihemoglobin formation. *Pharmacol. Rev.* **18:**1091-1161 (1966).

248. S. D. Nelson, W. A. Garland, and W. F. Trager. Lack of evidence for the formation of N-hydroxyamide metabolites of lidocaine in man. *Res. Commun. Chem. Pathol. Pharmacol.* **8:**45-54 (1974).

249. J. R. Cashman, Z. Yang, L. Yang, and S. A. Wrighton. Stereo- and regioselective N- and S-oxidation of tertiary amines and sulfides in the presence of adult human liver microsomes. *Drug Metab. Dispos.* **21:**492-501 (1993).

250. J. Rose and N. Castagnoli. The metabolism of tertiary amines. *Med. Res. Rev.* **3:**73-88 (1983).

251. P. Hlavica and M. Lehnerer. Some aspects of the role of cytochrome P-450 isozymes in the N-oxidative transformation of secondary and tertiary amine compounds. *J. Biochem. Toxicol.* **10:**275-285 (1995).

252. M. H. Bickel. The pharmacology and biochemistry of N-oxides. *Pharmacol. Rev.* **21:**325-354 (1969).

253. M. Sugiura, K. Iwasaki, and R. Kato. Reduction of tertiary amine N-oxides by liver microsomal cytochrome P-450. *Mol. Pharmacol.* **12:**322-324 (1976).

254. R. Kato, K. Iwasaki, and H. Noguchi. Reduction of tertiary amine N-oxides by cytochrome P-450. Mechanism of the stimulatory effect of flavins and methyl viologen. *Mol. Pharmacol.* **14:**654-664 (1978).

255. K. Iwasaki, H. Noguchi, R. Kato, Y. Imai, and R. Sato. Reduction of tertiary amine N-oxide by purified cytochrome P-450. *Biochem. Biophys. Res. Commun.* **77:**1143-1149 (1977).

256. M. Sugiura and R. Kato. Reduction of tertiary amine N-oxides by rat liver mitochondria. *J. Pharmacol. Exp. Ther.* **200:**25-32 (1977).

257. S. Kitamura and K. Tatsumi. Reduction of tertiary amine N-oxides by liver preparations: function of aldehyde oxidase as a major N-oxide reductase. *Biochem. Biophys. Res. Commun.* **121**:749-754 (1984).

258. E. Scheufler, R. Vogelgesang, B. Wilffert, B. L. Pegram, J. B. Hunter, D. Wermelskirchen, and T. Peters. Uptake of catamphiphilic drugs into erythrocytes and muscular tissue correlates to membrane enrichment and to ^{45}Ca displacement from phosphatidylserine monolayers. *J. Pharmacol. Exp. Ther.* **252**:333-338 (1990).

259. S. M. Wallace and S. Riegelman. Uptake of acetazolamide by human erythrocytes *in vitro*. *J. Pharm. Sci.* **66**:729-731 (1977).

260. W. F. Bayne, F. T. Tao, G. Rogers, L. C. Chu, and F. Theeuwes. Time course and disposition of methazolamide in human plasma and red blood cells. *J. Pharm. Sci.* **75**:70-80 (1981).

261. T.-M. Chen, M. H. Abdelhameed, and W. L. Chiou. Erythrocytes as a total barrier for renal excretion of hydrochlorothiazide: slow influx and efflux across erythrocyte membranes. *J. Pharm. Sci.* **81**:212-218 (1992).

262. H. J. Lee and W. L. Chiou. Erythrocytes as barriers for drug elimination in the isolated rat liver. II. Propranolol. *Pharm. Res.* **6**:840-843 (1989).

263. W. Piekoszewski, F. S. Chow, and W. J. Jusko. Disposition of tacrolimus (FK 506) in rabbits: role of red blood cell binding in hepatic clearance. *Drug Metab. Dispos.* **21**:690-698 (1993).

264. J. Ke, Y. K. Tam, W. W. K. Koo, M. R. Gray, and R. T. Coutts. Effects of parenteral nutrition on hepatic elimination of lidocaine: a study using the isolated perfused rat liver. *J. Pharmacol. Exp. Ther.* **255**:351-356 (1990).

265. N. Zaman, Y. K. Tam, L. D. Jewell, and R. T. Coutts. Effects of taurine supplementation in parenteral nutrition-associated hepatosteatosis and lidocaine metabolism. A study usng isolated rat liver perfusion. *Drug Metab. Dispos.* **24**:534-541 (1996).

266. N. Zaman, Y. K. Tam, L. D. Jewell, and R. T. Coutts. Effects of light-exposed parenteral nutrition on hepatic function and lidocaine metabolism: a study using isolated rat liver perfusion. *Pediatr. Res.* **40**:280-287 (1996).

267. N. Zaman, Y. K. Tam, L. D. Jewell, and R. T. Coutts. Effects of cholestyramine and parenteral nutrition on hepatic metabolism of lidocaine: a study using isolated rat liver perfusion. *J. Parenter. Nutr.* **20**:349-356 (1996).

268. R. A. Colbert, E. Bresnick, W. Levin, D. E. Ryan, and P. E. Thomas. Synthesis of liver cytochrome P-450b in a cell-free protein synthesizing system. *Biochem. Biophys. Res. Commun.* **91**:886-891 (1979).

269. T. Suzuki, R. Ishida, S.-I. Matsui, Y. Masubuchi, and S. Narimatsu. Kinetic analysis of mutual metabolic inhibition of lidocaine and propranolol in rat liver microsomes. *Biochem. Pharmacol.* **45**:1528-1530 (1993).

270. M. Delaforge, M. Jaouen, and D. Mansuy. The cytochrome P-450 metabolite complex derived from troleandomycin: properties *in vitro* and stability *in vivo*. *Chem. Biol. Interact.* **51**:371-376 (1984).

271. M. A. Correia. Cytochrome P450 Turnover. In M. R. Waterman and E. F. Johnson (eds.), *Cytochrome P450,* Vol. 206, Academic Press, Inc. Toronto, 1991, pp. 315-324.

272. R. Gasser, H. P. Hauri, and U. A. Meyer. The turnover of cytochrome P450b. *FEBS letters.* **147**:239-242 (1982).

273. J. B. Schenkman, B. J. Wilson, and D. L. Cinti. Diethylaminoethyl 2,2-diphenylvalerate HCl (SKF 525-A) — *in vivo* and *in vitro* effects of metabolism by rat liver microsomes — formation of an oxygenated complex. *Biochem. Pharmacol.* **21**:2373-2383 (1972).

274. M. K. Buening and M. R. Franklin. The formation of complexes absorbing at 455 nm from cytochrome P-450 and metabolites of compounds related to SKF 525-A. *Drug Metab. Dispos.* **2**:386-390 (1974).

275. M. R. Franklin. Inhibition of mixed-function oxidations by substrates forming reduced cytochrome P-450 metabolic-intermediate complexes. *Pharmacol. Ther.* **A 2**:227-245 (1977).

276. M. Hirata, B. Lindeke, and S. Orrenius. Cytochrome P450 product complexes and glutathione consumption produced in isolated hepatocytes by norbenzphetamine and its N-oxidized cogeners. *Biochem. Pharmacol.* **28**:479-484 (1979).